Aus dem Experimental and Clinical Research Center und
Max-Delbrück-Centrum für Molekulare Medizin
der Medizinischen Fakultät Charité – Universitätsmedizin Berlin

DISSERTATION

Identifizierung neuer Substanzen für die zielgerichtete Behandlung der MACC1-vermittelten Metastasierung

Identification of novel compounds for targeted therapy of MACC1-driven metastasis

zur Erlangung des akademischen Grades
Doctor medicinae (Dr. med.)

vorgelegt der Medizinischen Fakultät
Charité – Universitätsmedizin Berlin

von

Shixian Yan

aus Shandong, China

Datum der Promotion: .....26.06.2022.....

Contents

List of figures and tables

List of abbreviations

ANOVA	Analysis of variance
APC	Adenomatous polyposis coli
AP2α	Adaptor protein 2α
BRAF	V-Raf murine sarcoma viral oncogene homolog B
CDC4	Cell division control protein 4
CIN	Chromosomal instability
CMV	Cytomegalovirus
CRC	Colorectal cancer
CTCs	Circulating tumor cells
DCC	Deleted in colorectal cancer
DKTK	German Cancer Consortium
DMSO	Dimethylsulfoxide
EC_{50}	Effective concentration 50
EGFR	Epidermal growth factor receptor
EMT	Epithelial-Mesenchymal Transition
EMBL	European Molecular Biology Laboratory
FBS	Fetal bovine serum
5-FU	5-fluorouracil
GI	Gastrointestinal tract
HGF	Hepatocyte growth factor
HIF	Hypoxia-inducible factor
HPV	Human papillomavirus
HRAS	Harvey rat sarcoma viral oncogene homolog
HRP	Horseradish peroxidase
HTS	High throughput-screenings
IC_{50}	Inhibiting concentration 50

JPS	Juvenile polyposis syndrome
KRAS	Kirsten rat sarcoma viral oncogene homolog
MACC1	Metastasis Associated in Colon Cancer 1
MAPK	Mitogen-activated protein kinase
MET	Mesenchymal-Epithelial Transition
MMR	Mismatch repair
MSI	Microsatellite instability
MSI	Microsatellite instability
MS	Microsatellites
NOD/SCID mice	Non-obese diabetic/severe combined immunodeficiency mice
NRAS	Neuroblastoma RAS viral oncogene homolog
PI3K	Phosphoinositide 3 kinases
qRT-PCR	Quantitative real-time polymerase chain reaction
SCF	SKP1-CUL1-F-box protein
SMAD4	Drosophila mothers against decapentaplegic homolog 4
SSRs	Simple sequence repeats
SH3	SRC Homology 3
S100A4	Calcium-binding protein A4
TGF-β	Transforming growth factor-beta
TP53	Tumor protein p53
WB	Western blot
WHO	World Health Organization
Wnt	Wingless and Int-1 (drosophila homolog)

I. Abstract

Background Colorectal cancer (CRC) is one of the leading causes of cancer-associated death worldwide. Metastasis of CRC is directly linked to patient survival and the main cause of global CRC mortality. Therefore, it is a clinical need to find novel anti-metastatic drugs. MACC1 (Metastasis Associated in Colon Cancer 1) is a causal key molecule for metastasis, driving tumor progression and metastasis formation. High MACC1 expression was found in many tumor entities and is prognostic for metastasis and poor survival. In order to provide a therapeutic option for patients diagnosed with high MACC1 expression, it is necessary to provide novel inhibitors of MACC1 gene expression.

Methods We aimed to target MACC1 expression using the independent pMACC1-luciferase reporter-based high-throughput screening (HTS), testing over 118,500 compounds from the largest academic library of Germany. The HTS was performed at the European Molecular Biology Laboratory (EMBL), Heidelberg, Germany. The most promising compounds were characterized in vitro using luciferase assay, qRT-PCR, Western Blot, Cell viability, Migration and Wound-healing assays. Additionally, commercially available derivatives were tested. The most promising candidate molecules were tested in vivo for their metastasis inhibitory effects.

Results From the HTS, we found novel compounds that act as potent MACC1 transcriptional inhibitors. We identified even more effective derivatives of the intially identified lead compounds. Furthermore, these compounds not only inhibited MACC1 expression and MACC1 associated functions in vitro, but also restricted MACC1-induced tumor progression and metastasis formation in a xenograft mouse model.

Conclusions We identified novel compounds for MACC1 inhibition that might be used for targeted therapy of MACC1-driven metastasis. These compounds need further development in order to optimize tolerability, bioavailability and effectivity, bring therapeutic value to colon cancer patients in the future.

II. Zusammenfassung

Hintergrund Darmkrebs (CRC) ist weltweit eine der häufigsten Ursachen für krebsbedingte Todesfälle. Die Metastasierung des CRC steht in direktem Zusammenhang mit dem Überleben der Patienten. Sie ist die Hauptursache für die weltweite CRC-Sterblichkeit, kann aber nur begrenzt vorhergesagt werden. Daher ist es ein klinisches Bedürfnis, neue antimetastatische Arzneimittel zu finden. MACC1 (Metastasis Associated in Colon Cancer 1) ist ein kausales Schlüsselmolekül, das Tumorprogression und Metastasierung fördert.Hohe MACC1-Expressionen wurden in vielen Tumoren gefunden und das ist prognostisch für Metastasen und schlechtes Überleben. Um Patienten mit hoher intratumoraler MACC1-Expression eine spezifische therapeutische Option anbieten zu können, ist es notwendig, neuartige Inhibitoren der MACC1-Genexpression zu entwickeln.

Methoden Die MACC1-Expression wurde mit Hilfe eines unabhängigen, auf dem pMACC1-Luziferase-Reporter basierenden Hochdurchsatz-Screenings (HTS) untersucht. In diesem HTS wurden über 118,500 Substanzen aus der größten akademischen Substanzbibliothek Deutschlands getestet. Das HTS wurde am Europäischen Laboratorium für Molekularbiologie (European Molecular Biology Laboratory EMBL, Heidelberg, Deutschland) durchgeführt. Die vielversprechendsten Verbindungen wurden in vitro mittels Luciferase-Assay, qRT-PCR, Western Blot, Zellvitalitäts-, Migrations- und Wundheilungstests charakterisiert. Zusätzlich wurden kommerziell erhältliche Derivate getestet. Die vielversprechendsten Kandidatenmoleküle wurden in vivo auf ihre Metastasen-inhibierende Wirkung getestet.

Ergebnisse Im Rahmen des HTS konnten wir neue Substanzen, die als potente MACC1-Transkriptionsinhibitoren wirken, identifizieren. Die Derivate der anfänglich identifizierten Leitsubstanz zeigten eine erhöhte Wirksamkeit. Darüber hinaus hemmten diese Verbindungen nicht nur die MACC1-Expression und MACC1-assoziierte Funktionen in vitro, sondern inhibierten auch die MACC1-induzierte Tumorprogression und Metastasenbildung in einem Xenotransplantat-Mausmodell.

Schlussfolgerungen Im Rahmen dieser Arbeit identifizierten wir neue Substanzen zur Hemmung der MACC1 Genexpression. Sie könnten in Zukunft für eine gezielte Therapie der MACC1-gesteuerten Metastasierung eingesetzt werden. Diese Substanzen müssen nun weiter entwickelt werden, um z.B. Verträglichkeit,

Bioverfügbarkeit und Wirksamkeit weiter zu optimieren. Diese optimierten Substanzen stellen eine neue Therapieoption das, die in Zukunft einen therapeutischen Nutzen für Darmkrebspatienten erzielen kann.

1. Introduction

1.1 Colorectal cancer (CRC) epidemiology

Cancer is not a single disease but a general term for a large group of diseases. When gene mutation occurs in cells, the growth of these abnormal cells is uncontrolled, gradually spreading out of their normal growth range, and beginning to invade nearby tissues and organs or transferring to a distant place, and they can occur in almost any organs or tissues of the body.

According to the World Health Organization (WHO), an estimated 9.6 million people died of cancer in 2018, the second leading cause of death globally. Among the many different types of cancer, CRC is the third most common cancer among men and the second in women [1]. CRC is the second leading cause of cancer mortality. Therefore, CRC is one of the main causes of cancer-related deaths in the world [2].

It is estimated that the number of new CRC cases for men and women of all ages in the world was 10.2% in 2018. There are many factors that affect the incidence of CRC, such as age, gender, eating habits, living environment and infections [3]. According to the literature, CRC has a higher incidence in Western countries, such as Europe, Canada, the United States. The countries with the lowest incidence are mainly distributed in South and Central Asia, Africa and South America [4,5]. The high incidence of CRC in Western countries may be related to the diet. The Western diet is characterized by a low intake of dietary fiber and excessive intake of meat, sugar, etc. [6,7]. Therefore, identification of the potential relationship between CRC development and dietary patterns may provide useful insights for the definition of dietary guidelines for CRC prevention. In addition, lack of physical exercise, smoking and drinking are also high-risk factors. Among them, smoking is the most important risk factor for cancer. In Germany, according to statistics from the German Centre for Cancer Registry Data, about 16% of cancer cases are attributed to smoking [8]. In low- and middle-income countries, infections such as hepatitis and human papillomavirus (HPV) also account for 25% of cancer cases [9,10].

According to estimates by the Global Cancer Observatory, the CRC mortality rate of men and women of all ages in 2018 accounted for 9.2% of all cancers in the world. In

developing countries, the five-year relative survival rate of CRC is lower than that of high-income countries: 28% and 60%, respectively [1–3]. This shows that economies are another factor affecting the 5-year survival rate of cancer and this issue is increasing. In 2017, about 26% of low-income countries provided pathological services in the diagnosis and treatment of diseases, while in high-income countries, this proportion could reach 90%. The lack of pathological examinations has led to the fact that about four-fifths of low- and middle-income countries do not have reliable data with which o formulate policies related to cancer treatment. This has made advanced cancer and difficultty in obtaining diagnosis and treatment become a common phenomenon. Early diagnosis and treatment directly affect the 5-year survival rate [4,5]. In Germany, about one in eight cancer patients suffer from CRC and the 5-year relative survival rate is approximately 62 % [9]. With the improvement of diagnosis and treatment technology, although the 5-year survival rate has improved significantly, there has been no improvement for patients after metastasis [6]. Therefore, it can be seen that the survival rate is highly dependent on the stage of the tumor. For example, the five-year survival rate of patients with early local tumors is 90%, but when regional lymph nodes or even distant metastases have formed, the 5-year survival rate drops to 10%. Therefore, the metastatic transmission of primary colon cancer accounts for 90% of all colon cancer deaths, which makes the formation of metastasis a key process in the treatment of CRC [7].

1.2 Tumorigenesis and progression of CRC

The occurrence of CRC is a very complicated process which is the result of many factors affecting each other. Researchers around the world are trying to find the exact mechanisms that cause tumor formation, progression, metastasis and responsiveness or resistance to tumor treatment. Therefore, two pathways have been established to understand the molecular origin of CRC (Fig. 1). One of the pathways involved is chromosomal instability (CIN) that leads to tumor progression, also known as the "classic" (adenoma-carcinoma sequence) or "traditional" pathway [8]. The other is the approach involving microsatellite instability (MSI), called the “mutator” pathway [9]. Among them, the gene mutation involved in the classical pathway is considered to be the key driving force to give cancer cells growth advantages and protect cancer cells in the initial stage of tumor formation and development [10]. In this classical pathway, the most common genomic mutations are the adenomatous polyposis coli (APC) gene,

Kirsten rat sarcoma viral oncogene homolog (KRAS), tumor suppressor p53 (TP53) gene, and deleted in colorectal cancer (DCC) gene [8,10]. The “mutator” pathway is caused by the lack of DNA mismatch repair (MMR), and it can't repair the errors in the process of duplicate DNA sequence replication. This pathway accounts for approximately 15%-20% of all CRCs [9,11].

The specific details of these two different pathways will be described in detail in the next section.

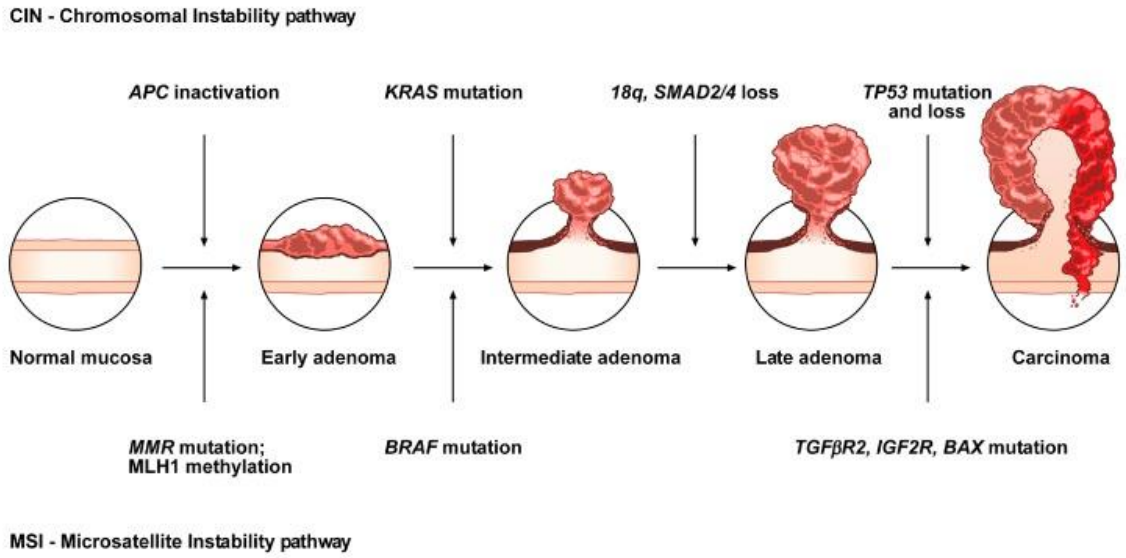

Fig. 1: Adenoma–carcinoma sequence model in CRC. This model briefly outlines the complex process of CRC transformation and illustrates the mutations and/or aberrations of several key genes related to cell growth control as well as CIN caused by dysfunctional cell division through methylation of certain gene promoters. This is followed by (in)-activation of the accumulation of these genes and mutations, leading to CIN or epigenetic silencing [12].

1.3 The adenoma-carcinoma sequence

The adenoma-carcinoma sequence has been one of the most important fundamental concepts in CRC in recent years. This pathway describes the process of gradual mutation and accumulation of genes related to cancer [13,14]. It mainly involves the mutations of tumor suppressor genes (e.g. APC, p53, DCC) and oncogenes (e.g. KRAS) [10,15]. Through this concept, we can not only understand the process of cancer occurrence and development of cancer more intuitively but also provide a variety of ideas for the prevention and treatment of CRC. As depicted in Figure. 1, we will next describe in detail the tumor formation process caused by mutations of these genes.

1.3.1 APC, β-Catenin and Wnt signaling

APC is one of the tumor suppressor genes and is located on human chromosomes 5q21–q22. Its deletion may lead to uncontrolled growth of cells, which in turn leads to tumors [16]. The protein produced by APC can promote the assembly or stability of multiple protein complexes (such as β-catenin disrupting complexes). By controlling the level of β-catenin, it is signaled by the classical Wnt (Wingless and Int-1) signaling pathway [17]. When APC is mutated, it interferes with the binding of its protein to β-catenin, leading to the continuous activation of the Wnt pathway [18,19]. This leads to uncontrolled cell growth and the development of invasive lesions (cancer) [20]. The APC gene is the most common and inactivated gene in the development of CRC, and mutation inactivation has been found in 60% of CRC patients [21]. At the same time, the inactivation of this gene is also the initial central link in the development of CRC tumors.

In addition, APC can also play a role by regulating the mitosis of cells. Loss of APC will lead to chromosome abnormality caused by CIN [22–24]. Consequently, mutations in the APC and WNT pathways are common mechanisms for progression from early CRC lesions to more advanced stages.

1.3.2 KRAS and MAPK signaling

KRAS is a murine sarcoma virus oncogene which encodes 21kD RAS protein, so it is also called the p21 gene [25]. The KRAS protein is part of the RAS/MAPK (mitogen-activated protein kinase) pathway. It can transmit signals from outside of the cell to the nucleus, indicating that the cell grows as well as proliferation, maturation and differentiation. The KRAS protein is a GTPase that can convert GTP to GDP. In this way, it uses protein dynamics to act as a signal on/off switch for molecules, which are controlled by GTP and GDP, respectively. To transmit a signal, the GTP molecule must be turned on by binding to it. When a protein binds to GDP, it does not transmit signals to the nucleus [26].

The KRAS gene has two states, which are wild type or mutated type. Under normal physiological conditions, when cells activate signaling pathways such as epidermal growth factor receptor (EGFR) after external stimulation, the KRAS signaling pathway is temporarily activated by phosphorylation of wild-type KRAS. The mutant-type KRAS protein can cause protein dysfunction, which is still activated in the absence of EGFR

activation signal stimulation, causing the MAPK signal cascade, promoting the continuous proliferation of cells, and causing tumors [27,28].

KRAS gene mutations occur early in the malignant transformation of the tumor, and can be detected in approximately 40% of CRC patients [29]. About 97% of KRAS gene mutations are caused by mutations in amino acid residues 12 or 13 [30,31]. Tumor patients with KRAS activating mutations usually have a poor prognosis and a much shorter survival time than those without KRAS activating mutations. Clinically, the efficacy of EGFR inhibitors can be predicted by detecting whether the KRAS gene (KRAS, p21) has activating mutations. Therefore, the detection of KRAS gene mutation is an important indicator for understanding the prognosis of cancers, and the therapeutic effect [32].

The BRAF gene (v-Raf murine sarcoma viral oncogene homolog B) is located at human chromosome 7 (7q34) and belongs to the RAF gene family. Its protein can affect cell growth, proliferation, differentiation, migration and apoptosis, and plays a role in regulating the RAS-RAF-MEK-ERK (MAPK/ERK) signaling pathway [33,34]. Therefore, the signal transduction of this signal pathway is essential for the normal development of cells. Among all the mutations of BRAF oncogene, the most important one is that the 600th amino acid residue of BRAF changes from valine residue (V) to glutamate residue (E), which is the V600E mutation. 8-14% of CRC patients exhibit BRAFV600E mutations, accounting for more than 95% of all BRAF mutation cases [35]. Under normal circumstances, BRAF protein has kinase activity only after being phosphorylated by RAS kinase. However, when the BRAF gene is mutated, the BRAF protein is always activated, and it then affects downstream signaling through the MAPK pathway, eventually leading to tumor formation.

1.3.3 CDC4, SMADs and TGF- β signaling

CDC4 (cell division control protein 4) is a substrate recognition component of the SCF (SKP1-CUL1-F-box protein) ubiquitin ligase complex. It can transfer ubiquitin to target proteins through the ubiquitin-proteasome pathway and causes its subsequent degradation [36]. CDC4 can be used as a regulator of the cell cycle and is essential for initiating the process of DNA replication and isolating the spindle to form mitosis [37]. Therefore, CDC4 plays a very important role in cell mitosis. When the gene is mutated,

it may affect the progress of the cell cycle through the overexpression of cyclin E, thereby causing the instability of CIN and leading to tumorigenesis [38].

SMAD4 (drosophila mothers against decapentaplegic homolog 4) is located on the human chromosome 18q21.2, and about 60% of CRCs show allele deletions at this site [39,40]. SMAD4 protein acts as a mediator between the extracellular growth factors of the transforming growth factor-beta (TGF-β) family and genes in the nucleus, and can directly transfer TGF-β signals from the cell membrane into the nucleus. When activated, SMAD is phosphorylated by specific receptors on the cell surface, transferring signals from the cell membrane to the nucleus and activating the transcription of target genes, thereby regulating the expression of different genes. Inhibitory SMADs block or attenuate TGF-β signals through negative feedback pathways. Therefore, the transcription of SMADs can be regulated by interacting with TGF-β [41].

The TGF-β superfamily plays an important role in regulating cell proliferation, differentiation, migration, and decay death. Therefore, after the structure of SMAD4 is changed, it is not be able to regulate the expression of genes related to cell growth, thereby causing uncontrolled cell growth and eventually leading to tumor formation [40,42]. SMAD4 has also been found to mutate in juvenile polyposis syndrome (JPS). JPS is characterized by hamartomatous polyps of the gastrointestinal tract (GI). These polyps increase the risk of CRC [43].

1.3.4 TP53

Tumor suppressor gene TP53 is located at human chromosome 17p13.1, which has the highest correlation with human tumors [44]. Among all malignant tumors, more than 50% of them will have mutations. The protein encoded by this gene is an important transcription factor which can regulate cell apoptosis, maintain genome stability and inhibit tumor angiogenesis [45]. The p53 protein can specifically bind to DNA. When DNA is damaged, it can keep the cell cycle at the G1/S regulatory point recognized by DNA damage, prevent DNA replication, and then repair the damage by activating DNA repair proteins. If not, it will lead to apoptosis. When a tumor needs new blood vessels to support its growth, p53 can affect angiogenesis by interfering with regulators of humor hypoxia, such as HIF1 and HIF2, and inhibiting the production of angiogenic promoting factors [46,47]. Therefore, p53 is described as "the guardian of genome".

The most common mutation of the p53 gene is a missense mutation. After the mutation, the spatial conformation of the p53 gene is changed, resulting in the loss of its normal function, and thereby losing its regulatory effect on cell growth, apoptosis and DNA repair. p53 mutations occur late in the adenomas-carcinoma sequence. Therefore, by predicting the frequency of p53 mutations, we can better understand the process of transition from pre-invasive disease to invasive disease (between 4%-26% of adenomas, 50% of invasive adenomas, and 50%-75% of CRCs) [8,13].

1.4 Microsatellite instability pathway

Microsatellites (MS) are short tandem repeats throughout the human genome. These sequences consist of repeating units of 1 to 6 base pairs in length [48]. The most common microsatellites are the dinucleotide repeats of nucleotides C and A [49]. Compared with normal cells, microsatellites in tumor cells change in length due to the insertion or deletion of repeat units, which is called microsatellite instability (MSI). High-frequency MSI (MSI-H) refers to the detection of MSI at more than 40% of the MS sites, while those below 40% are defined as MSI (MSI-L) [8,50].

MMR is a method that recognizes and repairs possible base mis-insertions, deletions, and mis-bindings during DNA replication and recombination, as well as repairing some forms of DNA damage, preventing gene mutations and maintaining the stability of the genome [51]. MSI is caused by MMR losing its own proofreading function (mismatch repair deficiency dMMR). The MMR system consists of at least 7 proteins, namely hMLH1, hMLH3, hMSH2, hMSH3, hMSH6, hPMS1 and hPMS2, which combine with specific partners to form functional heterodimers [8].

In the process leading to the formation and development of CRC, CIN accounts for about 85%, while MSI accounts for only 15% [52]. 12% of MSI tumors are caused by hypermethylation of the MLH 1 gene promoter encoding the DNA MMR protein, while the remaining 3% of MSI tumors (Lynch syndrome) are caused by germline mutations of MLH 1, MSH 2, MSH 6 and PMS2 [53]. In MSI tumors, MSI-H and MSI-L also have defined characteristics. For example, patients with MSI-H CRCs are younger and have a better prognosis. The MSI-L phenotype accounted for 29%, 53%, and 83% of hyperplastic polyps, serrated adenomas, and mixed polyps, respectively. Hyperplastic polyps and other adenomas may be unique histological precursors that cause canceration [54–56]. Therefore, in the clinical diagnosis and treatment of CRC, we

should choose the appropriate treatment according to the causes and characteristics of CRC.

1.5 Tumor invasion and metastasis

Metastasis is a major feature of malignant tumors, distinguishing it from benign tumors [57]. It refers to the process whereby malignant tumor cells transfer from the primary site to other sites and continue to grow through lymph channels, blood vessels or body cavities [58]. There are four common types of metastasis: (a) spreading directly to adjacent sites; (b) lymphatic metastasis: cells of primary cancer follow the lymphatic drainage, from near to distant to lymph nodes at various levels [59]; (c) hematogenous metastasis: the cancer cells enter into the blood vessels and metastasize to distant sites; (d) implantation: after the tumor cells are shed, they are implanted in another site, such as splanchnic cancer being seeded into the peritoneum or pleura. Obviously, malignant tumor metastasis will increase the damage to the body and affect the prognosis. In many tumor entities, the metastatic transmission of a primary tumor is directly related to patient survival. In CRCs, metastasis accounts for about 90% of patients' deaths. Therefore, the malignant tumor metastasis is often the key to affecting tumor treatment [60–62].

Epithelial-Mesenchymal Transition (EMT) is a key link in the process of tumor metastasis, which is a process to that promotes tumors to obtain an aggressive phenotype (Fig. 2). Through this process, epithelial cells lose cell polarity and intercellular adhesion, and acquire migration and invasion properties to become mesenchymal stem cells, which can differentiate into a variety of pluripotent stromal cells. These cells lack this polarization and only interact with each other through the focal point [63]. The cells of the epithelial layer maintain the laminar structure intact through tight junctions, gap junctions and adhesive junctions, thereby forming a good barrier for the epithelial layer. The main component of the barrier is cadherin [64,65]. Therefore, during this process, the cells undergo profound morphological and phenotypic changes.

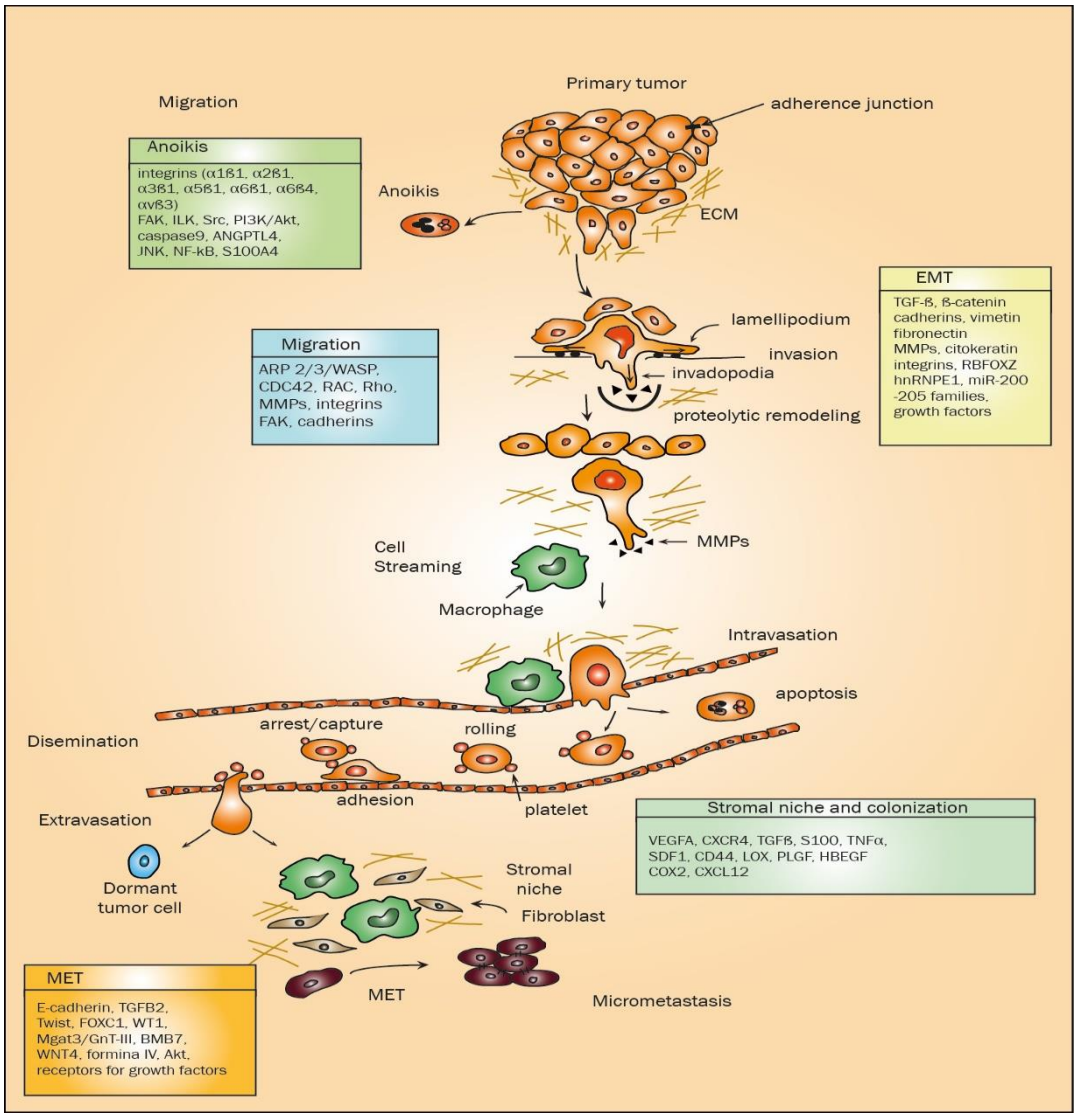

Fig. 2: Invasion and metastasis cascade. The process by which tumor cells leave the primary tumor, separate and migrate to reach the blood or lymphatic vessels and spread to the secondary site. This includes multiple gene expression and changes in cell morphology. In the figure, you can see the whole process [64].

At present, it is thought that there are three types of EMT: EMT type 1 is related to embryonic development, EMT type 2 is related to wound healing, and EMT type 3 is related to tumor cells [64,66]. There are many common pathways between embryonic and tumoral EMT, for example, stimulation of TGF-β can induce β-catenin phosphorylation, thereby causing the activation of transcription factors such as Snail [67], together with diverse growth factors and proteins. This is accompanied by the loss of a variety of epithelial proteins, such as E-Cadherin, α and β-catenins and cytokeratin, and the overexpression of mesenchymal proteins simultaneously [68]. E-cadherin is a protein that plays a key role in the process of cell migration. It prevents cell migration

and metastatic transmission by increasing the adhesion between epithelial cells and desmosomes [69]. At the beginning of metastasis, the absence of E-cadherin causes the adhesion between cancer cells in the primary tumor to weaken or disappear. Cancer cells can invade and penetrate the basement membrane and enter the bloodstream through intravasation. After entering the bloodstream, tumor cells recruit platelets to act as a physical barrier to help protect these cells from being cleared by immune cells. The metastatic cancer cells can adhere to the activated endothelial cells in the blood vessel wall due to the adhesion of platelets. They then leave the bloodstream at the second site and start to form a new tumor. Later, when these circulating tumor cells (CTCs) penetrate the blood vessel wall to form micrometastasis, they receive MET clone growth at these metastatic sites [70,71]. Therefore, EMT and Mesenchymal-Epithelial Transition (MET) form the initiation and completion of the invasion metastasis cascade [72].

Several oncogenic pathways (TGF-β, EGF, HGF, Wnt/β-catenin, etc.) and hypoxia can induce EMT [73]. In addition, p53 is also involved in the regulation of EMT induced by TGF-β by activating various microRNAs (miR-200 and miR-34) [74]. Besides this, there are other hypotheses about tumor metastasis, such as "seed and soil": cancer cells (“seed”) show matching compatibility and adaptive programs with the microenvironment of specific target sites (“soil”) [75]. For example, CRC tends to metastasize to the liver, while stomach cancer often metastasizes to the ovary in women, when it is called a Krukenberg tumor [76,77].

Because tumor metastasis has a major influence on tumor treatment, we study the mechanism of tumor invasion and metastasis, in order to discover more tumor markers to detect tumors before metastasis, improve the cure rate, and prolong the survival time of patients. For now, we still face great challenges.

1.6 Staging and treatment of CRC

According to different stages of CRC, the corresponding treatment plan can be made and the prognosis can be reasonably evaluated. Therefore, correct CRC staging is very important to guide the treatment of patients (Table 1). The primary tumor is usually staged according to its depth of penetration and the involvement of adjacent structures or distant sites [78].

Table 1. CRC TNM staging

AJCC stage	TNM stage	TNM stage criteria for CRC
Stage 0	Tis N0 M0	Tis: Tumor confined to muscosa; cancer-in-situ.
Stage I-A	T1 N0 M0	T1: Tumor invades submuscosa.
Stage I-B	T2 N0 M0	T2: Tumor invades muscularis propria.
Stage II-A	T3 N0 M0	T3: Tumor invades subserosa or beyond (without other organs involved).
Stage II-B	T4 N0 M0	T4: Tumor invades adjacent organs or perforates the visceral peritoneum.
Stage III-A	T1-2 N1 M0	N1: Metastasis to 1 to 3 regional lymph nodes. T1 or T2.
Stage III-B	T3-4 N1 M0	N1: Metastasis to 1 to 3 regional lymph nodes. T3 or T4.
Stage III-C	Any T, N2 M0	N2: Metastasis to 4 or more regional lymph nodes. Any T.
Stage IV	Any T, N2 M1	M1: Distant metastasis present. Any T, any N.

T: indicates the depth of tumor invasion, and its number range is 1 to 4. N: nodal status and 0, 1, or 2 indicates the number of affected lymph nodes around the region. M: metastasis. M0: no metastasis. M1: cancer has spread to distant organs [78].

There are many treatment methods for CRC, including surgery, chemotherapy, radiation therapy, hormone therapy, targeted therapy, and synthetic lethality. The specific treatment method needs to be selected based on comprehensive consideration of tumor location and stage as well as patient's general status [79]. However, surgical resection is still the main treatment for patients with CRC.

Stage I refers to tumor invasion of submucosa or muscularis propria, without local lymph node metastasis. At this stage, the main treatment is surgical resection, the prognosis is relatively ideal, and the 5-year survival rate is about 90% [80]. Stage II refers to the tumor invading subserosa, or invading adjacent organs, or perforating the visceral peritoneum. There is also no local lymph node metastasis, and the 5-year survival rate is about 70% -80%. At this stage, surgical resection is the first choice, and those with high-risk factors can consider postoperative chemotherapy [81]. Because CRC has no clinical symptoms at an early stage, it is difficult to detect and treat it early. As the tumor continues to grow, the 5-year survival rate also drops sharply from 40%-60%

at stage III to 10% at stage IV [82]. Stage III of cancer is that cancer cells have spread to lymph nodes, but not to other organs or body parts. At this stage, we need to choose a comprehensive treatment plan, initially surgical resection, which is then combined with chemotherapy to treat patients with CRC [83]. Patients with stage III and high-risk stage II (including perforation of the outermost layer of the colon or rectum, lymphatic infiltration (LVI), and perineural infiltration (PNI)) can also benefit from adjuvant chemotherapy 81,84. Stage IV requires a multidisciplinary discussion to make an accurate assessment. Based on these assessment results, you can select the appropriate treatment method to reduce patient suffering, improve quality of life, and prolong life [79,85].

With the development of science and technology, the level of treatment has improved. Although the 5-year survival rate of patients with early CRC has improved, there has been no significant change in patients with advanced cancer (stage IV) in the past few decades. Therefore, there is an urgent need for reliable and effective biomarkers for early prediction during tumor formation and subsequent treatment of tumors.

1.7 MACC1 - A newly identified prognostic and predictive biomarker

In 2009, our group conducted a genome-wide analysis of human CRC tissue, metastasis tissue and colorectal normal mucosa tissue by RT-qPCR, and found a promising prognostic marker named Metastasis associated in colon cancer 1 (MACC1), which has no similarity with the known gene [62].

Further analysis revealed that the expression of MACC1 mRNA in tumor tissues was significantly higher than in normal tissue, and compared with primary tumors, the MACC1 mRNA levels of metastatic tumors were significantly higher than non-metastatic tumors. The level of MACC1 mRNA expression is also closely related to the 5-year survival rate of patients. The 5-year survival rate of MACC1 high and low expression is 15% and 80%, respectively [62,86]. The level of MACC1 expression is negatively related to the survival rate (Fig. 3). This suggests that MACC1 plays a key role in tumor progression and metastasis, and can be used as an indicator of metastasis formation and non-metastasis survival. Since we discovered MACC1 in 2009, MACC1 has been established by many groups as being related to tumor progression and metastasis of more than 20 solid cancer types, such as CRC, bladder cancer, lung cancer, breast

cancer, esophageal cancer, cervical cancer, gallbladder cancer, gastric cancer, etc. [62,87–91]. This further confirms the value of MACC1 in tumor metastasis and progression. In addition, the MACC1 transcript or protein levels in liquid biopsies (such as the patient's blood) can be used to assess the tumor progression, metastasis formation and prognosis of patient survival in different solid tumors [92]. This is of great clinical significance and can provide timely clinical treatment for patients with high expression of MACC1.

Besides this, high expression of MACC1 has also been proven to predict the postoperative recurrence of the tumor and the response to conventional chemotherapy, such as the recurrence of gastric cancer after surgery, and the recurrence of cancer after resection liver metastases from CRC as well as 5-fluorouracil (5-FU) to treat gastric cancer [93–95]. It has also been confirmed in the adenoma-carcinoma sequence that we talked about in the previous section. As the tumor progresses, the expression of MACC1 increass, which help us to distinguish between high-grade and low-grade adenomas [96,97].

In summary, MACC1 can be used as a biomarker for a variety of solid tumors and plays a key role in tumor progression and metastasis.

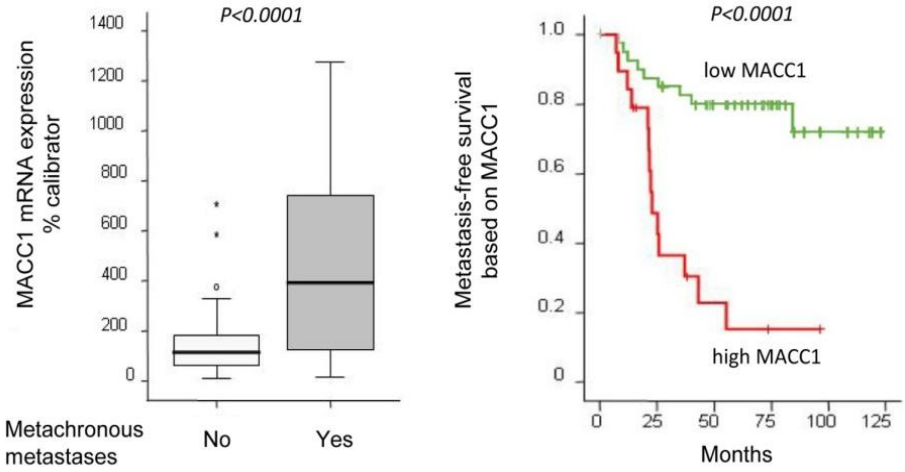

Fig. 3: MACC1 as a prognostic biomarker. MACC1 predicts metachronous metastasis and poor metastasis-free survival in tumors of patients without metastases at diagnosis [62].

1.7.1 MACC1 related signaling pathways

With the continuous development of science and technology, there is also in-depth research into molecular mechanisms in the process of tumorigenesis and development

is also in-depth. Since MACC1 can be used as a biomarker of many solid tumors, the signaling pathway associated with it has become very important (Fig. 4). For example, MACC1 induces angiogenesis through the TWIST1/2 signaling pathway, escapes growth inhibition through PI3K-AKT/ERK signaling pathway, and enables replication immortality through NANOG/OCT4 signaling pathway, and, in particular MACC1 maintains cell proliferation, migration, invasion and colony formation through HGF/c-MET [62,86,98,99]. These pathways play an important role in tumor formation, progression and metastasis, and MACC1 is at the core of these pathways.

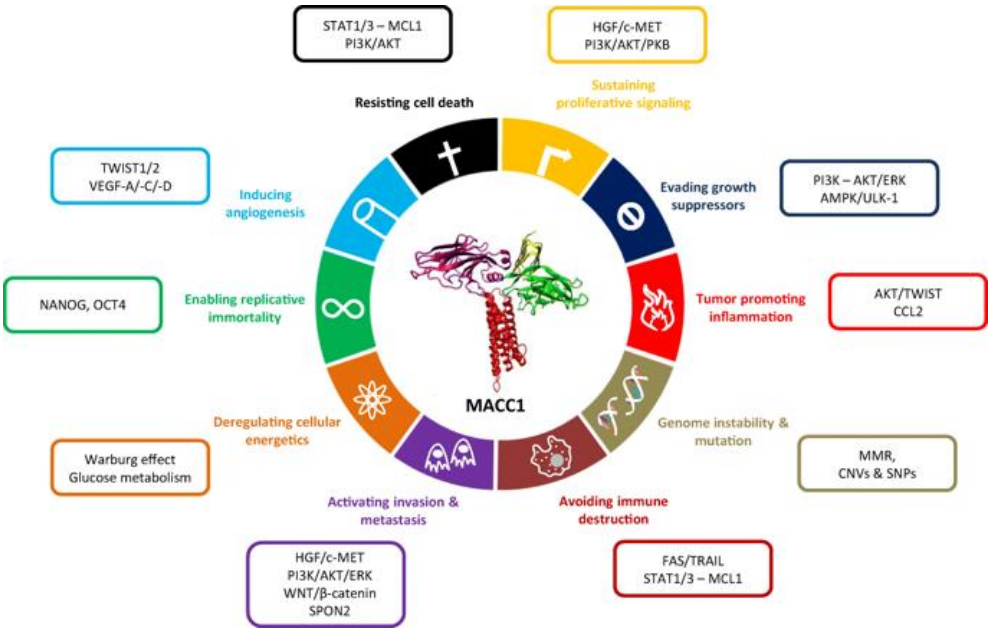

Fig. 4: Schematic of MACC1 related signaling pathways' impact on cancer hallmarks. MACC1 plays a key role in the progression and metastasis of tumors by regulating various pathways to promote the continuous proliferation, migration, invasion and metastasis of cells [86].

MACC1 is positively correlated with hepatocyte growth factor (HGF) receptor tyrosine kinase c-MET, which is its transcriptional activator. After overexpression of MACC1, the HGF/MET signaling pathway is activated and c-MET is upregulated, which results in cell proliferation, invasion and metastasis. If the expression of MACC1 is reduced, c-MET is downregulated, thereby reducing cell motility and proliferation. MACC1 activates its expression by binding to the promoter of the c-MET [62,100,101]. In addition, the activation of c-MET can trigger the downstream GAB1-SHP2-ERK/MAPK and PI3K/AKT axes, while the transcription factors of MACC1 itself are AP1 and Sp1, and the ERK

signal pathway can regulate its expression through the transcription factors of MACC1, and thus a positive feedback loop regulated by MACC1 is formed, which in turn leads to tumor progression and metastasis [86,102].

In short, MACC1 avoids the normal cell cycle by regulating different signaling pathways and inducing the continuous proliferation of cells, so that the tumor continues to progress to cancer. Similarly, because MACC1 involves many signaling pathways, this makes it possible to target MACC1 for intervention.

1.7.2 MACC1 protein structural features and inhibitory potential

MACC1 is a gene consisting of 2559 nucleotides located on human chromosome 7 (7p21.1). This gene was first discovered by our team in 2009. It contains seven exons and six introns. The encoded protein is composed of 852 amino acids and has a molecular weight of 97 kDa. The chromosome location of the MACC1 gene is a common mutation region that causes the occurrence or metastasis of gastrointestinal cancer, such as nearby Twist-related protein 1 (TWIST1), and Integrin beta 8 (ITGB8) [62,86,87,103]. The MET and HGF we introduced earlier are also located on chromosome 7. MACC1's transcription factors include SP1, AP1 and C/EBP. The promoter of MACC1 (-992 to -18bp upstream from the MACC1 transcriptional start site) drives transcription under the action of these transcription factors, and all three transcription factors are conducive to MACC1 expression [60,104].

Based on the translated MACC1 protein expression, five domains that mediate protein interaction are predicted（Fig. 5）: from the N-terminus, two domains resembling known structures of zonula occludens 1 and uncoordinated protein 5 (ZU5), p53-induced death domain, the domain of protein 1, and ankyrins domain (UPA). The C terminal of MACC1 contains an Src homology 3 (SH3) domain and a tandem of death domains (DD). MACC1 also contains a clathrin box, two Epsin 15 Homology interaction motifs (NPF), an interaction motif (DPF) for adaptor protein 2α (AP-2α), and proline-rich motifs (PxPxP, KxxPxxP) [62,87,105]. Among them, SH3 and proline-rich motifs (PxPxP, KxxPxxP) are involved in the process of MACC1 transport to the nucleus and affect the transcriptional activity of c-MET [106]. Since tyrosine phosphorylation is a very important part of the signal transduction process, interference with this process can affect the expression of MACC1, which further confirms that MACC1 can be used as a potential therapeutic target for cancer and metastasis.

MicroRNA (miRNA) is involved in the regulation of post-transcriptional gene expression. Abnormality of miRNA will affect the expression level of normal genes, which in turn will lead to the generation and development of tumors. In the past few years, a large number of studies have confirmed that many miRNAs cause abnormal cell activity by targeting MACC1. Overexpression of miRNAs associated with gastric cancer and CRC, such as miR-638, miR-3679-5p and miR-141, significantly reduced tumor growth and metastasis by downregulating MACCI in vivo [107–109]. This proves that MACC1 can be used as a target to limit the potential of tumor progression and metastasis.

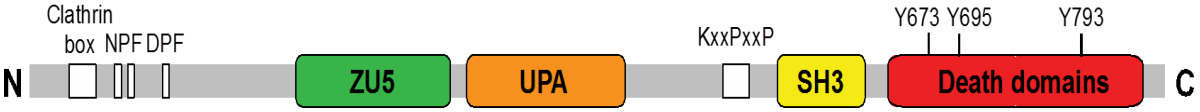

Fig. 5: Schematic of MACC1 protein domain structure. MACC1 protein expression domains that mediate protein interaction are predicted: from the N-terminus are ZU5 and UPA domains. The C terminal of MACC1 contains an SH3 domain and two death domains (DD). MACC1 also contains a clathrin box, two NPFs motifs, the DPF motif for adaptor protein 2α (AP-2α) and proline-rich motifs (PxPxP, KxxPxxP) [87].

Through the further analysis of the regulation of MACC1 transcription factors and the effect of post-transcriptional miRNA on its expression, it is known that MACC1 can be used as a clinical cancer treatment target, providing cancer patients with a new treatment method, which is of great clinical significance.

1.7.3 Discovery of MACC1 inhibitors

The screening of inhibitors is a very long and complicated process. There are many common screening techniques, such as tow-hybrid technology, genetic engineering technology, HTS, and so on [110–112]. With the development of advanced cell biology, as well as computer and automatic control technologies, the application of HTS technology in the screening of inhibitors is becoming more and more extensive. HTS uses the target of inhibitors for screening, which has the advantages of accuracy, rapidity and high efficiency. It can screen a large number of compounds in a short time, so it has become the main technical method of drug screening. Small molecule inhibitors have good spatial dispersion, and their chemical properties determine good drug-forming properties and pharmacokinetic properties, which makes small molecule compounds show great advantages in the screening process of inhibitors [113].

As mentioned above, MACC1 transcription factors play a vital role in the expression of MACC1. Therefore, if the inhibitors of these transcription factors can be found, the expression of MACC1 can be suppressed, which provides a new way for the treatment of cancer and its metastatic patients, or through the combined use of drugs to significantly improve the clinical treatment effect. Based on this idea, we found Lovastain and Rottlerin from small molecule compounds through HTS technology and verified the effects of these two inhibitors in vitro and in xenograft mice [60]. However, stains have been used clinically and have many contraindications. Therefore, we want to find novel MACC1 small molecule inhibitors through the above mentioned methods to provide more clinical treatment options.

1.8 Aims of the thesis

1. Identification of novel MACC1 transcriptional inhibitors from the largest academic library of Germany, the European Molecular Biology Laboratory, Heidelberg, Germany.

2. Evaluation of these inhibitors in vitro for the reduction of MACC1 expression and MACC1 associated functions.

3. In vivo validation for these inhibitors to restrict MACC1-induced tumor progression and metastasis formation in a xenografted mouse model.

2. Materials and Methods

2.1 Cell culture

In this study, all human CRC cell lines were obtained from the American Type Culture Collection (ATCC, USA). The medium used for cell growth was RPMI-1640 or Dulbecco's Modified Eagle medium (DMEM) containing 10% fetal bovine serum (FBS; Bio & Sell, Feucht, Germany). The cell was cultured at 37 °C in a humidified incubator with 5% CO2. Attention was paid to check the cell growth status, and cells were trypsinized and split in a 1:8 ratio every 3-4 days. Each culture flask was used no more than 3 times, so that the cells could better adhere to the bottom and to reduced the possibility of contamination. The plastic products used in the cell culture and experiments came from TPP (Trasadingen, Switzerland), BD Biosciences (Heidelberg, Germany) or Greiner BioOne (Kremsmünster, Austria). The MycoAlert® Mycoplasma detection kit (Lonza, Basel, Switzerland) was used to detect Mycoplasma regularly.

Table 2. All cell lines used in this study

Cell line	Medium	ATCC number
HCT116	RPMI 1640, 10% FBS	CCL-247
SW620	DMEM, 10% FBS	CCL-228

2.2 Cell cryopreservation and recovery

To prevent cells from being unsuitable for experiments after splitting too many times, it was necessary to know how to freeze cells. Preparation for cryopreservation: 10% Dimethylsulfoxide (DMSO, ⩾99.5%, bioscience-grade, Carl Roth, Germany)/FBS, cryopreservation tube and labelling it such as name, date, cell line, etc. Cell preparation: sufficient cells in the flask.

The medium was removed, washed one time with PBS, Trypsin/EDTA was added (Corning, USA), and it was placed in the incubator until the cells were completely detached, 10% FBS medium was added to stop the reaction, it was transferred to a 15ml high-clarity polypropylene conical tube (Falcon, Mexico), then centrifuged (Centrifuge 5810R, Eppendorf, Germany) at 1000 rpm for 4 min, and the medium was

removed and an appropriate amount of 10% DMSO/FBS medium was added after centrifugation. 1 ml of cell suspension was added to each cryopreservation tube after pipetting, then these were placed into the freezing box, and stored overnight in the refrigerator at - 80 ℃, and could then be transferred to a liquid nitrogen tank or stored at - 80 ℃ in the refrigerator.

Cell recovery: The cryopreservation tube was taken out, quickly and repeatedly pipetted with the medium containing 10% FBS medium until it was completely thawed, then transferred to the 15ml high-clarity polypropylene conical tube, centrifuged at 1000 rpm for 4 minutes, the medium was removed after centrifugation, fresh 10% FBS medium was added and all of the cell suspension was transferred to a flask, and it was checked whether the medium needed to be replaced or passaged after 1-2 days. Generally, it could be used for the experiment after splitting 2 times.

2.3 Cell counting

The purpose of cell counting was to determine the number of cells required for each experiment. The medium was removed, it was washed one time with PBS and Trypsin/EDTA was added, the flask was put into the incubator until the cells were detached, then medium was added to stop the reaction. Took 10 µl of cell suspension was taken and 10 µl of trypan blue was mixed it. Trypan blue is a vital stain used to selectively color dead tissues or color cells blue. 10 µl was taken to the cell counting slide (NanoEntek, Korea). The number of cells was automatically calculated by the cell counter (Live-cell movie analyzer, JuLI™ Br, Korea).

2.4 Derivative cell lines

To identify potential transcription inhibitors of MACC1, it was necessary to construct CRC derived cell lines for HTS. HCT116-MACC1p-Luc cells were generated by transfecting HCT116 cells with the plasmid pGL4.17 (Promega, Fitchburg, Wisconsin) containing the luciferase reporter gene. The luciferase expression was regulated by the human MACC1 promoter (-992 to -18 bp upstream of the MACC1 transcriptional start site).The HCT116-CMVp-Luc cells were HCT116 cells transfected with pcDNA3.1-puro-Luc. According to the manufacturer's instructions, the stable expression of the transgene was regularly controlled by the Steady Glow™ Luciferase Assay System (Promega) [60].

Table 3. All derivative cell lines used in this study

Cell line	Medium	Features
HCT116-MACC1p-Luc	RPMI 1640, 10% FBS	Firefly luciferase expression was regulated by MACC1 promoter
HCT116-CMVp-Luc	RPMI 1640, 10% FBS	Firefly luciferase expression was regulated by CMV promoter

2.5 Drug treatment

All of the small molecule compound inhibitors used for HTS came from the largest academic library of Germany, the European Molecular Biology Laboratory (EMBL), Heidelberg, Germany. Based on the results of HTS compound screening, small molecule compounds for further experiments in vitro were obtained from Enamine, Akos and Mcule (the compounds are the same as those used for HTS in EMBL). These compounds was dissolved in DMSO at a concentration of 10 mM, they were divided into multiple aliquots, and stored them at -80 °C to avoid repeated freezing and thawing. The experimental control group was also treated with the same concentration of solvent to exclude the adverse effects of DMSO.

2.6 Steady-Glo® Luciferase assay

The Steady-Glo® Luciferase Assay System can provide long-lived luminescence when added to cultured cells. HCT116-MACC1p-Luc cells were seeded into 96-well plates, $1.5x10^4$ cells/100 µl per well, this was down in triplicate for each concentration, then thy were put into the incubator. After 24 h of incubation, the cells were taken out and checked for growth status and density under a microscope. The prepared drug concentration of 10 mM was diluted according to the required experimental concentration and then the cells were treated for 24 h (since there was 100 µl medium in each well already, and the concentration should have been twice of that required). The plate was taken out after 24 h, 150 µl (or 100 µl) medium was removed from each well, and 50 µl (or 100 µl) of mixed reagent was added, so that the volume of the reagent was equal to the volume of culture medium in each well. The plate was rocked

slowly several times to ensure complete coverage of cells with Glo Lysis Buffer. Next, there was incubation for 5 min at room temperature to allow cell lysis in the dark. All the lysate was transfered to a white opaque 96-well plate, then the firefly luciferase was measure with a luminometer (Tecan, Infinite® 200 PRO, Austria).

2.7 Gene expression analysis

2.7.1 RNA isolation and reverse transcription

RNA was isolated using the GeneMATRIX Universal RNA Purification Kit (Roboklon, Berlin, Germany) according to the manufacturer´s instructions. Cells ($7.0x10^4$ cells/well) were seeded in a 24-well plate and incubated for 24 h. The appropriate concentration of drugs as required for another 24 h treatment was configured, and cells were washed with PBS and trypsinized. Pellet cells were lysed with 400 µl buffer RL, the lysate was transfered to the activated homogenization spin-column tube, then centrifuged at 11000 rpm for 2 min to remove DNA. This was pipetted with 250 µl of 96-100% ethanol and transferred to a RNA binding spin-column tube, and centrifuged at 11000 rpm for 1 min. Then it was rinsed with 400 µl wash DN1 buffer, washed with 600 µl RBW buffer and centrifuged. Finally, RNA samples were eluted with nuclease-free water (40 µl-100 µl) and quantified using a NanoDrop 1000 Spectrophotometer (Peqlab, Erlangen, Germany). The samples could be stored at -20℃ for further use.

The RNA samples without drug treatment were used as standard. 50 ng RNA was taken from each sample for reverse transcription (RT) with random hexamers in a reaction mix (25 µM hexamer primer, 200 U/µl reverse transcriptase, 40 U/µl RNase inhibitor, 5xSynthesis buffer, dNTP mix, PCR grade water; all from Biozym). The procedure (30 ℃ for 10min, 50 ℃ for 40min and 99 ℃ for 5 min with subcooling at 4 ℃ for 5 min) was set up in the RT machine (Mastercycler, Hamburg, Germany). The RT was carried out under these conditions. After the RT, all samples were diluted 1:1 with PCR Grade water, except the standard. The standard was used as the standard curve in the PCR process. Complementary DNA (cDNA) could be stored at - 20 ℃ or directly used for quantitative real-time PCR.

2.7.2 Quantitative real-time PCR

The primers for quantitative real-time amplification were obtained from Biotez, Berlin, and the blue S'Green qPCR was from Biozym, Hessisch Oldendorf. A total of 10 µl/well

of primers, dyes, and cDNA were added to a 96-well plate, 2-3 replicates were made for each concentration, and these were centrifuged briefly after attaching the membrane. G6PDH was selected as the housekeeping gene, LightCycler® 480 II (Roche Diagnostics, Risch, Switzerland) was used for quantitative polymerase chain reaction (qPCR) amplification of cDNA, and data was analyzed with the LightCycler® 480 Software release 1.5.0SP3 (Roche Diagnostics, Risch, Switzerland). The average values of repeated samples were taken and each mean value of expressed genes was normalized according to the results of housekeeping gene G6PDH. All expression analyses were performed three times independently.

Table 4. Primers used for quantitative real-time PCR

Primer	Sequence
MACC1-F	5'- TTCTTTTGATTCCTCCGGTGA -3'
MACC1-R	5'- ACTCTGATGGGCATGTGCTG -3'
G6PDH-F	5'- ATCGACCACTACCTGGGCAA -3'
G6PDH-R	5'- TTCTGCATCACGTCCCGGA -3'

2.8 Protein analysis

2.8.1 Protein extraction and quantification

3.0×10^5 cells per well were seeded in a 6-well plate, treated with drugs for 24 h (or 48 h), washed once with PBS and trypsinized. The cell suspension was transferred into a 1.5 ml tube, centrifuged at 1000 rpm for 5 min, and then the medium was removed. RIPA lysis buffer (50 mM Tris-HCl at pH 7.5, 150 mM NaCl, 1% NP-40; supplemented with protein and phosphate inhibitor cocktail tablets (Roche Diagnostics, Switzerland) was added, mixed and placed on ice for 30 min, and vortexed every 10 min. The tube was then centrifuged at 14800 rpm at 4 ℃ for 30 min to remove the cell debris. The supernatant was transferred to a new labeled tube and stored at – 20 ℃ or directly used for protein quantitative analysis.

The obtained supernatant was diluted with PBS at a ratio of 1:10 (or 1:5), such as 2.5 µl supernatant + 22.5 µl PBS (or 5 µl supernatant + 20 µl PBS). Replicates were done for each concentration. 2 mg/ml BSA solution was used to prepare a standard curve. According to the manufacturer's instructions, 200 µl Pierce ™ Bicinchoninic Acid (BCA)

Protein Assays Reagent (Thermo Scientific, USA) were added to each well. The plate was incubated in a 37°C incubator for 20 min and the absorbance at 560 nm was measured by Tecan infinite 200 PRO. A volume of 30 µl for each sample containing 20 µg protein was prepared based on the results of the measurement, which contained 10% DTT and 25% NuPAGE (Thermo Fisher Scientific, Invitrogen, USA). Finally, the samples were cooked (95°C, 700rpm, 10min). They were centrifuged after cooking and stored at 4 °C or directly used for Western blot analysis.

2.8.2 Western blot analysis

Sodium dodecyl sulfate-polyacrylamide gel electrophoresis (SDS-PAGE) was used to analyze protein expression levels. Protein samples were loaded onto a self-casted 10% Tris-glycine SDS-Polyacrylamide Gel (SDS-PAGE Calculator: http://www.changbioscience.com/calculator/sdspc4.htm). The Prestained Protein Ladder (PageRuler™ Plus, Thermo Scientific) was used to determine the band size. Electrophoresis was carried out in 1 x SDS running buffer. After the protein ran out of the stacking gel, the voltage was adjusted from 70 V to 130 V, and the electrophoresis was stopped after about 1.5 h. The gel was taken out the gel and the separating part was left for membrane transfer. In the TransBlot® Turbo™ system (2.5 A, 25 V, 7 min), used the TransBlot® Turbo™ Transfer Buffer was used to transfer the blot to the polyvinylidene difluoride (PVDF) membrane (all of them from Bio-Rad Laboratories Inc., Hercules, California). The PVDF membrane was activated with methanol for 1 min and rinsed with transfer buffer before use. The quality of the protein transfer was analyzed by protein staining with Ponceau S solution (Sigma, Taufkirchen). Then, it was washed with TBS-T (50 mM Tris-HCl, 150 mM NaCl, 0.05 % Tween 20, pH 7.5) and blocked with 5% milk (5% milk powder in TBS-T) for 1 h at room temperature. The membrane was washed with TBS-T after the blocking was completed. The location of the bands was determined according to the molecular weight. After the membrane was cut, put it into the corresponding primary antibody (Table 5) prepared with Albumin bovine fraction V (Serva, Heidelberg, Germany) at 4°C room for overnight. The membrane was washed with TBS-T for 30 min at room temperature and the TBS-T was replaced every 10 min. The membrane was put into horseradish peroxidase (HRP)-conjugated secondary antibodies (Table 5) prepared with TBS-T at room temperature for 1 h. The membrane washing process was repeated after incubation. Antibody-protein complexes were visualized with WesternBright (Advansta, Menlo Park, CA, USA) and subsequently

exposure to Fuji medical X-ray film SuperRX (Fujifilm, Tokyo, Japan). β-actin served as the protein loading control.

Table 5. Antibodies used for Western blot analysis, their dilutions and origins

Primary antibodies		
Anti-MACC1	1:3000	Rabbit polyclonal, Sigma
Anti-β-Actin	1:20000	Mouse monoclonal, Sigma
Secondary antibodies		
Anti-rabbit-HRP	1:10000	HRP conjugated antibody, Promega
Anti-mouse-HRP	1:40000	HRP conjugated antibody, Thermo Fisher

2.9 MTT cell viability assay

3-(4,5-dimethyl-2-thiazolyl)-2,5-diphenyl-2-H-tetrazolium bromide （MTT; Carl Roth, Germany）cell viability assay was used to determine the cell viability and proliferation of tumor cells after being treated by drugs. $7.5x10^3$ cells/well were seeded in a 96-well plate in triplicate for each concentration. After incubation for 24 h, the cells were treated with drugs for another 24 h. DMSO was used as the control group. MTT was prepared at a concentration of 5 mg/ml and added to each well (the concentration of MTT in each well was 0.1%).

The succinate dehydrogenase in the mitochondria of living cells can reduce the exogenous MTT to the water-insoluble blue-purple crystal formazan and deposit it in the cells, while dead cells have no such function. Thus, the medium was removed after 2 h incubation, 150 μl of DMSO was added to each well to dissolve the purple formazan crystals for 10 min, and an absorbance reader (Tecan infinite 200 PRO) was used to read the absorbance at 560 nm. This result can indirectly reflect the number of living cells. The results are expressed as percent viable cells compared to solvent-treated controls. Each experiment was performed in triplicate.

2.10 Transwell migration assay

The Boyden-chamber assay was performed for the evaluation of the migratory potential of cells. The cells were starved in serum-free medium for 6-8 h before seeding. A 96-well plate (REF 3384, Corning, USA) with an insert membrane pore size of 8 μm was used, each well was pre-soaked in 250 μl of medium without FBS for 30 min, and four replicates were made for each sample. 50 μl of starved cells (5 x 10^4 cells/well) were seeded in the upper chamber of the insert to avoid air bubbles during the operation. The target concentration of the drug was prepared two times, and 50μl per well was added to the upper chamber, so that there was a total of 100μl of cell and drug mixture in the upper chamber of each well. Medium containing 0.5% FBS was used in the upper chamber. In the lower chamber, 235 μl of drugs prepared with 10% FBS medium were added into each well to avoid bubbles during the operation. The drug concentrations in the upper and lower chambers were the same, with FBS concentrations of 0.5% and 10%, respectively. DMSO served as a control group. After 24 h of incubation, the medium in the upper chamber was removed and was transferred in the lower chamber to a new 96-well plate and marked accordingly. 75μl trypsin/EDTA was added to each well through the hole on the side of the insert, incubated for 15 min, and then transferred to the new 96-well plate, which contained the original medium and mixed. 100 μl of the mixture and 25 μl of CellTiter-Glo Reagents (Promega) were transferred to a white opaque 96-well plate, placed in the dark for 10 min, and then measured with the Infinite Pro multi-plate reader (Tecan, Infinite® 200 PRO, Austria).

2.11 Wound-healing assay

The wound-healing assay was used to analyze directed cell migration. On day 0, 1.1x10^5 cells per well were seeded into a 96-well plate (Imagelock 4379, Essen Bioscience, USA). Cells were not seeded in the outer ring of the plate, but replaced with 100 μl PBS to ensure that each well of the plate contained 100 μl of liquid (whether PBS or medium). After 6-8 h of incubation, the plate was taken out to prepare for the wound. Two trays were prepared, one for 45 ml of 75% ethanol and another for 45 ml of PBS. The scratch maker was first placed in a tray with ethanol for 5 min to sterilize it, and then washed with another one with PBS. The prepared 96-well plate was put into the cutting groove, the scratch maker was placed into the plate, and then the cutting key

was pressed. After that, the plate was put into the Incucyte Zoom (Essen Bioscience, USA). The system recorded cell migration every 2 h and analyzed the data after 72 h.

2.12 High-throughput drug screening (HTS)

In order to identify new transcription inhibitors of MACC1, we cooperated with the largest academic library in Germany, the EMBL and screened 118,500 compounds. HCT116-MACC1-Luciferase CRC cells stably expressing the human MACC1 promoter-driven luciferase reporter gene were seeded into 384-well plates. 4000 cells per well were seeded and the drug concentration was 50 µM-0.8 nM (serial 3x dilutions) in triplicates for each concentration. After 24 h of incubation, the 11 dose-response curves of different concentrations were measured with a Tecan (Infinite® 200 PRO, Austria) microplate reader. The most promising compounds were screened based on the inhibition of MACC1 mRNA expression and the relationship with cytotoxicity.

The drugs were stored according to the drug instructions and the stock solutions were prepared freshly. DMSO was used as the control group and the concentration of DMSO in each group of samples was ensured to be consistent.

2.13 The validation of novel MACC1 inhibitors on metastasis in vivo

To further investigate the effect of the novel MACC1 transcription inhibitors, these drugs were applied to in vivo experiments. All animal experiments were performed according to the United Kingdom Coordinating Committee of Cancer Research (UKCCCR) guidelines and in cooperation with Experimentelle Pharmakologie & Onkologie Berlin-Buch GmbH (EPO, Berlin, Germany). The State Office of Health and Social Affairs, Berlin, Germany granted the animal experiments under the permit Reg0010/19.

2.13.1 Maximum tolerated dose (MTD) experiment for Drug 22 in vivo

For MTD experiments, eight 6-week-old female severe combined immunodeficiency (SCID) mice were randomly divided into 4 groups. The dosages of Drug 22 were 25 mg/kg, 50 mg/kg, 100 mg/kg, and 200 mg/kg, respectively. The drug was applied by oral application. The toxicity effects of the drug were observed by analyzing the body weight of the mice daily. Due to the tumor load, the mice were sacrificed after they had been fed for 20 days.

2.13.2 Intrasplenal tumor transplantation

35 mg/kg Hypnomidate® (Janssen Pharmaceutica, Beerse, Belgium) was used to anesthetize the 6-week-old female SCID mice (EPO GmbH) for the spleen tumor cells transplantation. The spleen was externalized by incising the skin and peritoneum laterally. 3×10^6 of HCT116-CMVp-Luc cells were intrasplenically injected with a 27-gauge needle. The spleen was carefully placed back, the peritoneum was closed with Surgicryl ® absorbable suture and the skin was clamped twice.

2.13.3 In vivo drug application

Intrasplenically transplanted SCID-beige mice were randomly assigned to 4 groups of 10 animals each. Drug 22, Drug 22-10 and Drug 22-13 were orally administered at a daily dose of 50 mg/kg body weight 24 h after transplantation. Control animals received the corresponding amount of solvent. Due to the tumor load, the mice were sacrificed after they had been fed for 28 days.

2.13.4 In vivo bioluminescence imaging

The non-invasive bioluminescence imaging system NightOWL LB 981 (Berthold Technologies, Bad Wildbad, Germany) was used to monitor tumor growth and metastasis in mice. Isoflurane gas was used as the anesthetic for the mice in each test. D-luciferin (Biosynth, Staad, Switzerland) dissolved in PBS was injected intraperitoneally at a dose of 150 mg/kg. The tumor growth and metastasis formation were imaged and quantified by WinLight (Berthold Technologies) and ImageJ (version 1.53 J8, National Institutes of Health, USA). After the experiment, the isolated spleen (primary tumor) and liver (metastatic tumor) were frozen in liquid nitrogen for further analysis.

2.13.5 MACC1 expression in murine xenograft tissue

To isolate the mRNA, the mortar and pestle were pre-cooled with liquid nitrogen and then used to grind the tumor tissue into a fine powder. To ensure complete cell lysis, the tissue powder with RL buffer was sonicated 10 times at 40% output. RNA isolation and reverse transcription were performed as described in sections 2.7.1 and 2.7.2, respectively. The primers for quantification of MACC1 cDNA were designed to be specific for the human sequence of MACC1, excluding murine MACC1 cDNA to avoid interfere with the measurements.

2.14 Immunohistochemistry

For immunohistochemistry, previously frozen mouse liver tissues were sliced to a thickness of 5 μm. A Dako pen was used to draw a circle on the edge of the tissues to obtain more uniform immunohistochemical staining results, and this was left to dry for 30 min. After washing with PBS once, they were fixed with 4% paraformaldehyde PBS solution for 15 minutes at room temperature and washed with PBS three times. The sections were quenched with a solution containing 0.1 M glycine for 20 min and washed once with PBS. The endogenous peroxidase activity was inhibited by incubation for 10 min at room temperature in a 3% hydrogen peroxide buffer. After washing three times with PBS, the sections were immersed in PBS containing 0.2% TritonX-100 for 2 min. 5% albumin-free IgG was used for block for 1 h at room temperature. The slides were rinsed in PBS and subsequently incubated with anti-cytokeratin19 (CK19) rabbit monoclonal antibody (dilution 1:200; DB103-0.2, DB Biotech, Slovakia) overnight at 4˚C in a humidified chamber. Following this incubation, the slides were washed five times with PBS. The slides were then incubated with anti-rabbit HRP secondary antibody (dilution 1:500; HRP conjugated antibody, Promega) for 1 h in a humid condition at room temperature. After washing five times with PBS, 3,3'-diaminobenzidine (DAB) was added for a coloration for 2 min at room temperature, and then washed with distilled water. Then, the slices were stained with hematoxylin at room temperature for another 1 min. The slides were rinsed in running tap water, covered with a glass slide, and observed under an optical microscope. In the liver tissue, the CK19 positive reactant was brown in the cytoplasm [114].

2.15 Statistical analysis

GraphPad Prism 6.0 and Microsoft Excel 2010 were used for data statistics and analysis. The comparison between two groups was done by t-test, and the comparison of three or more groups was done by one-way analysis of variance (ANOVA) and Bonferroni post hoc multiple comparisons. The inhibiting concentration 50 (IC_{50}) and the effective concentration 50 (EC_{50}) were calculated by the sigmoidal dose-response inhibition curve fit of x=log(x) transformed data. All significance tests were two-sided with a confidence interval of 95% (* = $p < 0.05$, ** = $p < 0.01$, *** = $p < 0.001$, **** = $p < 0.0001$).

3. Results

Our lab cooperated with the EMBL, Heidelberg. They provided the largest academically available drug library in Germany to discover MACC1 transcription inhibitors through HTS. We discovered the S100A4 transcription inhibitor niclosamide and MACC1 transcription inhibitor statins through this method previously [60,115]. Now, we want to discover a new kind of compound through this method. This newly identified compound could be used as an efficient metastasis inhibitor targeting the metastasis inducer MACC1, and might even enhance this metastasis restriction when combined with further drugs known to act as metastasis inhibitors. However, since these compounds will be used to apply for a patent, the letter “R” replaces parts of the chemical structure of the compounds in the results section.

3.1 Screening of MACC1 transcription inhibitors by HTS

In this study, we aimed to elucidate a new strategy to prevent and interfere with tumor progression and metastasis formation by targeting the novel metastasis driver MACC1. Previously, our research team determined the promoter of MACC1, which we employed for reporter gene assays. Based on this, we used HCT116 cells that express the luciferase reporter gene under the control of the MACC1 promoter (HCT116-MACC1p-Luc), which is schematically represented in Fig. 6A. HTS was used to screen MACC1 transcription inhibitors from a library consisting of 118,500 compounds. The work flow chart is schematically depicted in Fig. 6B. Through luciferase and cytotoxicity tests, 66 compounds were selected from the library, then further verified by qRT-PCR. Finally, the MACC1 transcription inhibitor Drug 22 and derivatives thereof were identified (Fig. 6C).

The inhibitory effect of Drug 22 on MACC1 expression was further analyzed by qRT-PCR in two different cell lines and different concentrations, as well as by analysis of cell viability by the MTT assay. Taken together, Drug 22 inhibits the expression of MACC1, however, associated with some cytotoxicity (Fig. 6D). Therefore, we wanted to find suitable MACC1 inhibitors among the Drug 22 derivatives. We further compared the chemical structure of the inhibitors to define the main functional group (core structure) which is essential for efficient inhibition of MACC1expression.

A

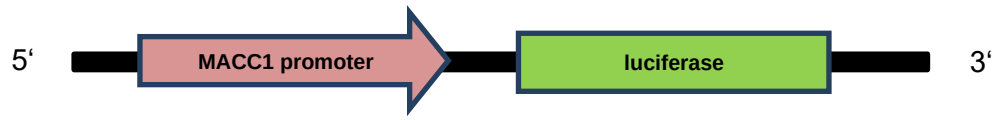
5‘
MACC1 promoter
luciferase
3‘

B

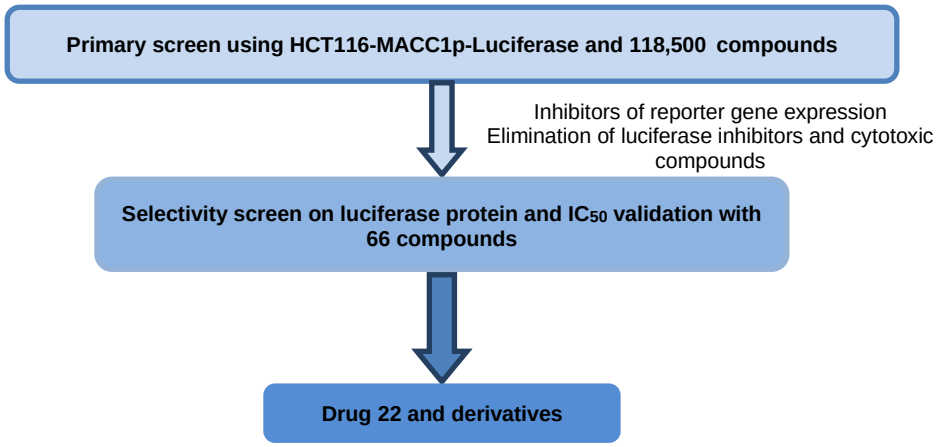
Primary screen using HCT116-MACC1p-Luciferase and 118,500 compounds
Inhibitors of reporter gene expression
Elimination of luciferase inhibitors and cytotoxic compounds
Selectivity screen on luciferase protein and IC50 validation with 66 compounds
Drug 22 and derivatives

C

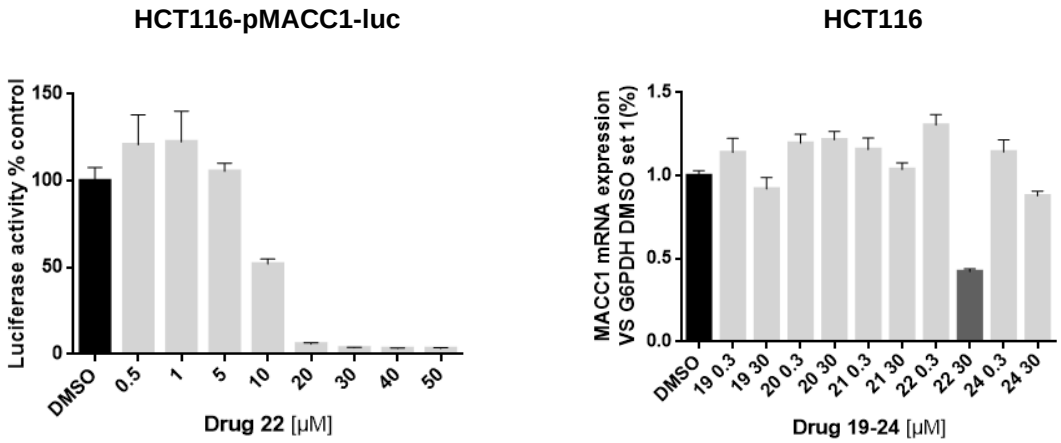
HCT116-pMACC1-luc
Luciferase activity % control
150
100
50
0
DMSO
0.5
1
5
10
20
30
40
50
Drug 22 [µM]
HCT116
MACC1 mRNA expression
VS G6PDH DMSO set 1(%)
1.5
1.0
0.5
0.0
DMSO
19 0.3
19 30
20 0.3
20 30
21 0.3
21 30
22 0.3
22 30
24 0.3
24 30
Drug 19-24 [µM]

D

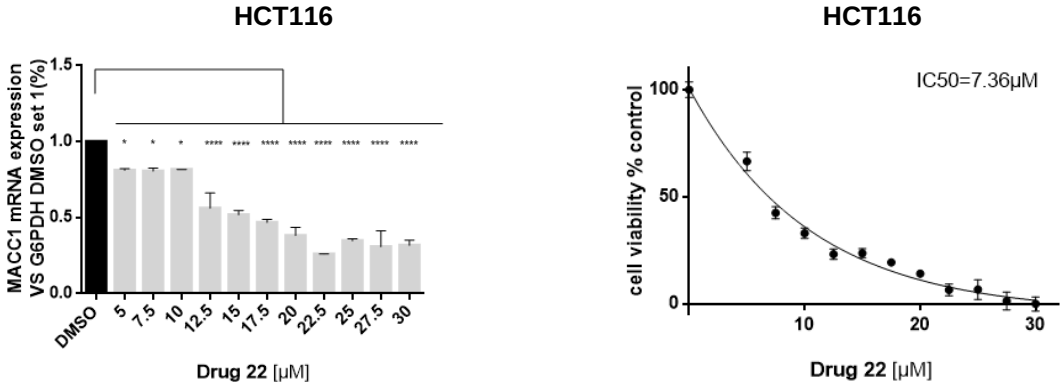
HCT116
MACC1 mRNA expression
VS G6PDH DMSO set 1(%)
1.5
1.0
0.5
0.0
DMSO
5
7.5
10
12.5
15
17.5
20
22.5
25
27.5
30
Drug 22 [µM]
HCT116
IC50=7.36µM
cell viability % control
100
50
0
10
20
30
Drug 22 [µM]

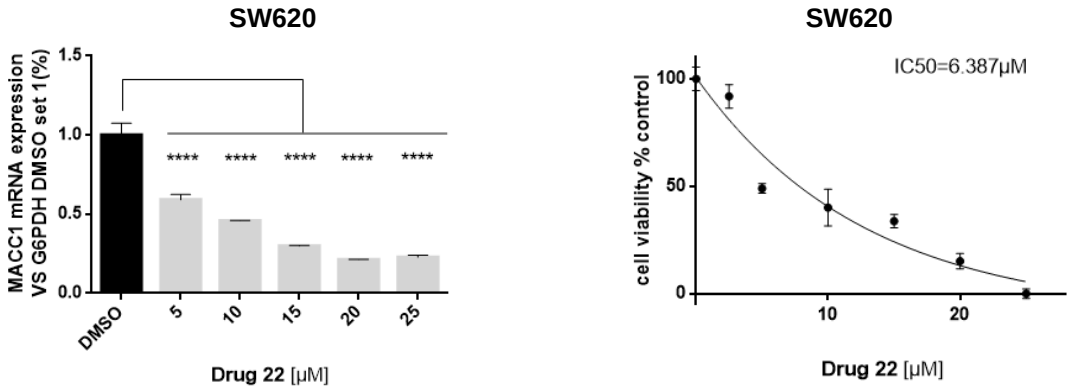

Fig. 6: MACC1 inhibitor screening flowchart and verification of Drug 22 mediated inhibition of MACC1 expression. (A) Scheme of construct expressed in HCT116-MACC1p-Luc cells used for HTS. The luciferase reporter gene expression is controlled by the human MACC1 promoter (MACC1p). (B) The transcription inhibitors of MACC1 were gradually identified from the library through HTS and in vitro verification. (C) HCT116-MACC1p-Luc cells and HCT116 cells were treated with increasing concentrations of Drug 22 for 24 h. Compared with the control group, Drug 22 significantly reduced the expression of luciferase at 10 μM. Similarly, when qRT-PCR was performed to verify the 66 small molecule compounds, only Drug 22 significantly reduced the expression of MACC1 mRNA. (D) Drug 22 can inhibit the expression of MACC1 in different cell lines, but the cytotoxicity is relatively high (IC_{50}=7.36 μM in HCT116 cell line and IC_{50}=6.387 μM in SW620 cell line). MACC1 mRNA levels were normalized to G6PDH mRNA expression and respective DMSO control (black bar). Results for mRNA represent means ± standard error of the mean (SEM) of three independent experiments. Significant results were determined by one-way ANOVA and multiple comparison was done by Dunnett's method (* = $p < 0.05$, **** = $p < 0.0001$).

3.2 Derivatives of Drug 22

In order to better analyze the chemical structure of the Drug 22 derivatives, we divided commercially available derivatives into five parts according to their different structure variations. In vitro, qRT-PCR, Western blot, cell viability, migration assay and wound-healing assay were used to verify MACC1 expression and its functional consequences in two different cell lines, HCT116 and SW620. Compared with the initial structural features of Drug 22, and according to the change of the chemical structure of the derivatives, the screening scope gradually narrowed. As a result of this, the substructure that is essential for inhibition of MACC1 expression is clearly defined.

3.2.1 Part 1: Drug 22-2 to Drug 22-9

In this part, through experimental verification, it was found that four of eight Drug 22 derivatives can inhibit the expression of MACC1, namely: Drug 22-5, Drug 22-7, Drug

22-8 and Drug 22-9 (Fig. 7). The other four didn't work. Combined with qRT-PCR and MTT analysis (EC_{50} and IC_{50}), it was found that out of these four drugs, Drug 22-7 and Drug 22-8 out of these four drugs were more efficient than the other two.

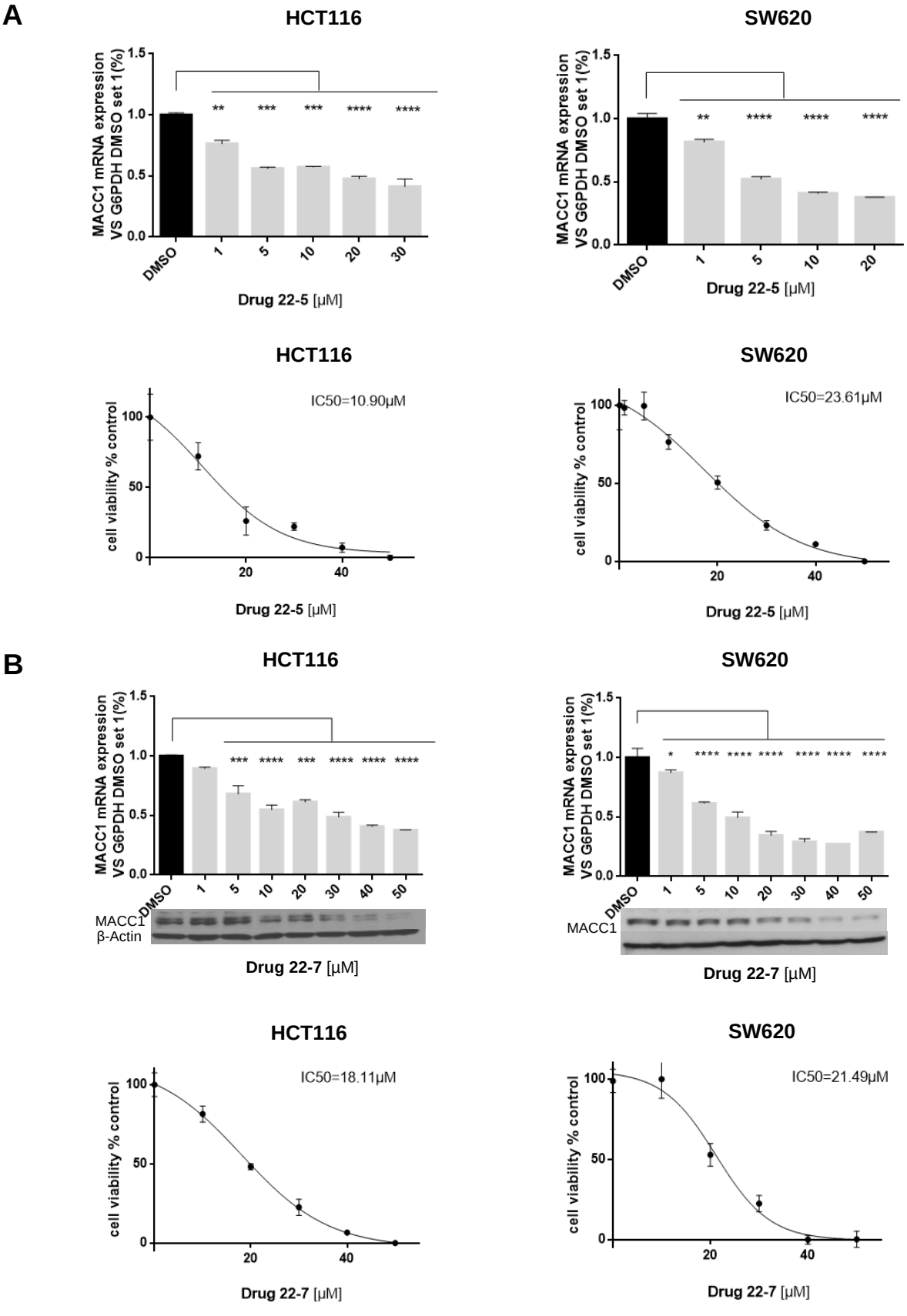

C

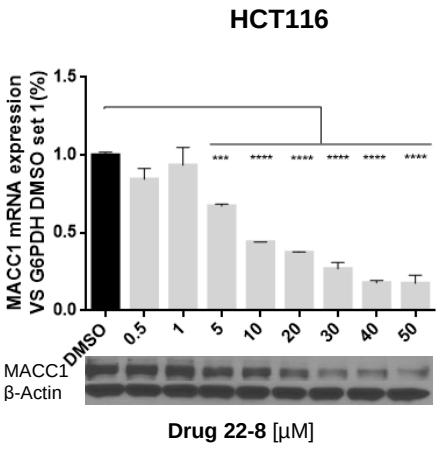
HCT116
MACC1 mRNA expression
VS G6PDH DMSO set 1(%)
1.5
1.0
0.5
0.0
DMSO
0.5
1
5
10
20
30
40
50
MACC1
β-Actin
Drug 22-8 [μM]

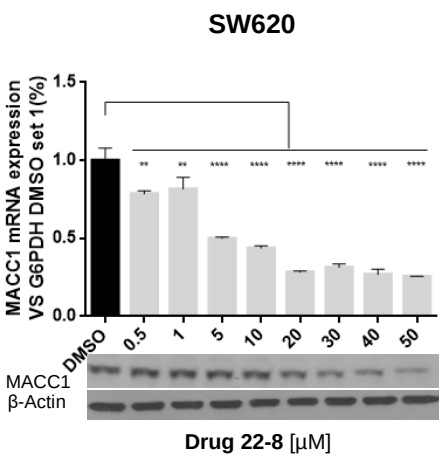
SW620
MACC1 mRNA expression
VS G6PDH DMSO set 1(%)
1.5
1.0
0.5
0.0
DMSO
0.5
1
5
10
20
30
40
50
MACC1
β-Actin
Drug 22-8 [μM]

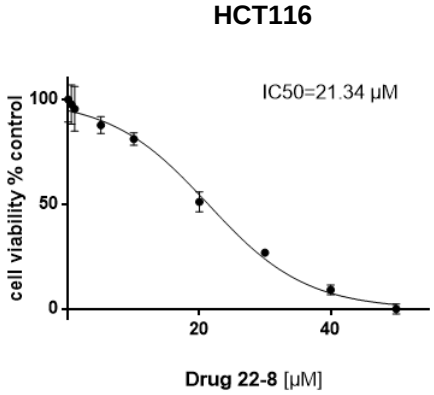
HCT116
IC50=21.34 μM
cell viability % control
100
50
0
20
40
Drug 22-8 [μM]

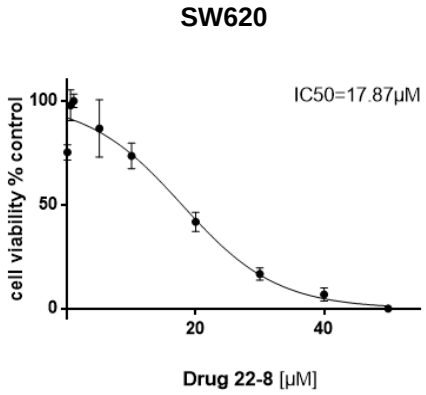
SW620
IC50=17.87μM
cell viability % control
100
50
0
20
40
Drug 22-8 [μM]

D

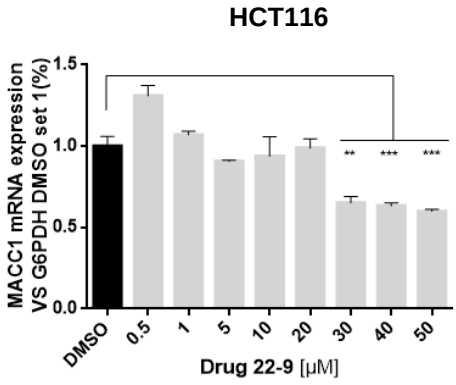
HCT116
MACC1 mRNA expression
VS G6PDH DMSO set 1(%)
1.5
1.0
0.5
0.0
DMSO
0.5
1
5
10
20
30
40
50
Drug 22-9 [μM]

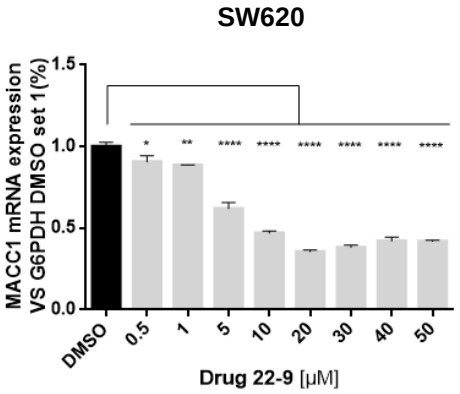
SW620
MACC1 mRNA expression
VS G6PDH DMSO set 1(%)
1.5
1.0
0.5
0.0
DMSO
0.5
1
5
10
20
30
40
50
Drug 22-9 [μM]

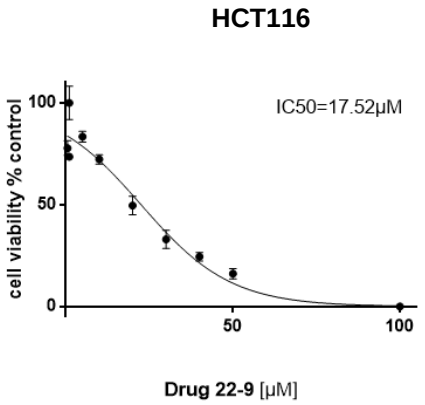
HCT116
IC50=17.52μM
cell viability % control
100
50
0
50
100
Drug 22-9 [μM]

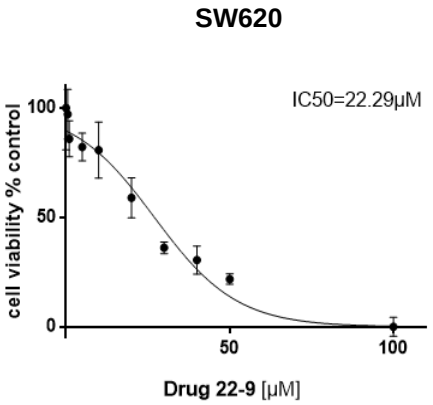
SW620
IC50=22.29μM
cell viability % control
100
50
0
50
100
Drug 22-9 [μM]

Fig. 7：The effect of Drug 22 derivatives on MACC1 expression and cell viability. (A, B, C, D) represent Drug 22-5, Drug 22-7, Drug 22-8 and Drug 22-9, respectively. HCT116 cells were treated for 24 h, and SW620 cells for 48 h with the Drug 22 derivatives. Cells for qRT-PCR and MTT assays were treated for 24 h. MACC1 mRNA levels were normalized to G6PDH mRNA expression and respective DMSO control (black bar). Results for mRNA represent means ± SEM of three independent experiments and for the WB one representative example of three independent experiments is shown. In the WB, β-actin served as a loading control. Cell viability was measured independently by MTT assay. Results are shown as mean ± SEM of three independent experiments performed in triplicate. Significant results were determined by one-way ANOVA and multiple comparison was done by Dunnett's method (* = $p < 0.05$, ** = $p < 0.01$, *** = $p < 0.001$, **** = $p < 0.0001$).

Based on whether these derivatives inhibited the expression of MACC1, a structure analysis was performed (Fig. 8). Drug 22 and all derivatives have a similar chemical substructure: "R1+R2". This shows that this part contributes strongly to the inhibitory effect. Four Drugs that have no inhibitory effect on MACC1, it may be considered that the changing part (marked in red) may affect the function of the main group, such as increased cytotoxicity and insolubility, etc. Based on the results of this analysis, in the following sections, we have further analyzed this main functional group.

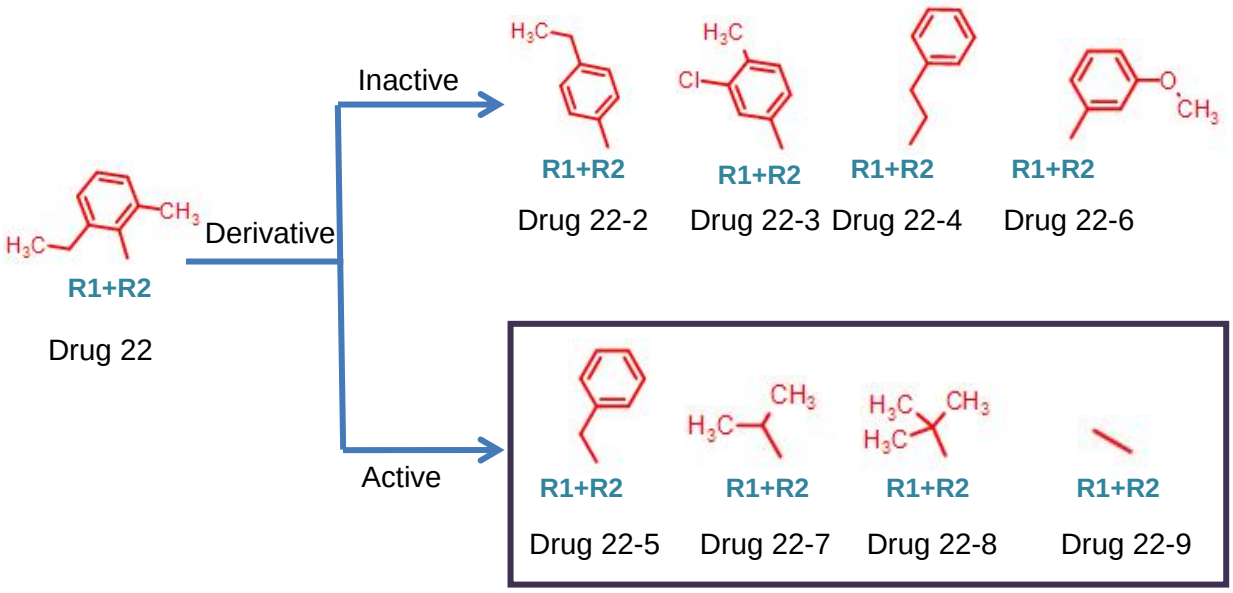

Fig. 8 The chemical structures of Drug 22 and derivatives thereof. The common substructure of all derivatives are the same as Drug 22, and the chemical substructure marked in red are the changing parts. The derivatives inside the box inhibit the expression of MACC1.

3.2.2 Part 2: Drug 22-19 to Drug 22-22

In this part, all the derivatives have the same substructure, i.e., R2 (except Drug 22-21 in part 4). Through experimental verification, it was found that all of the derivatives in part 2 have no effect on the expression of MACC1 (Fig. 9).

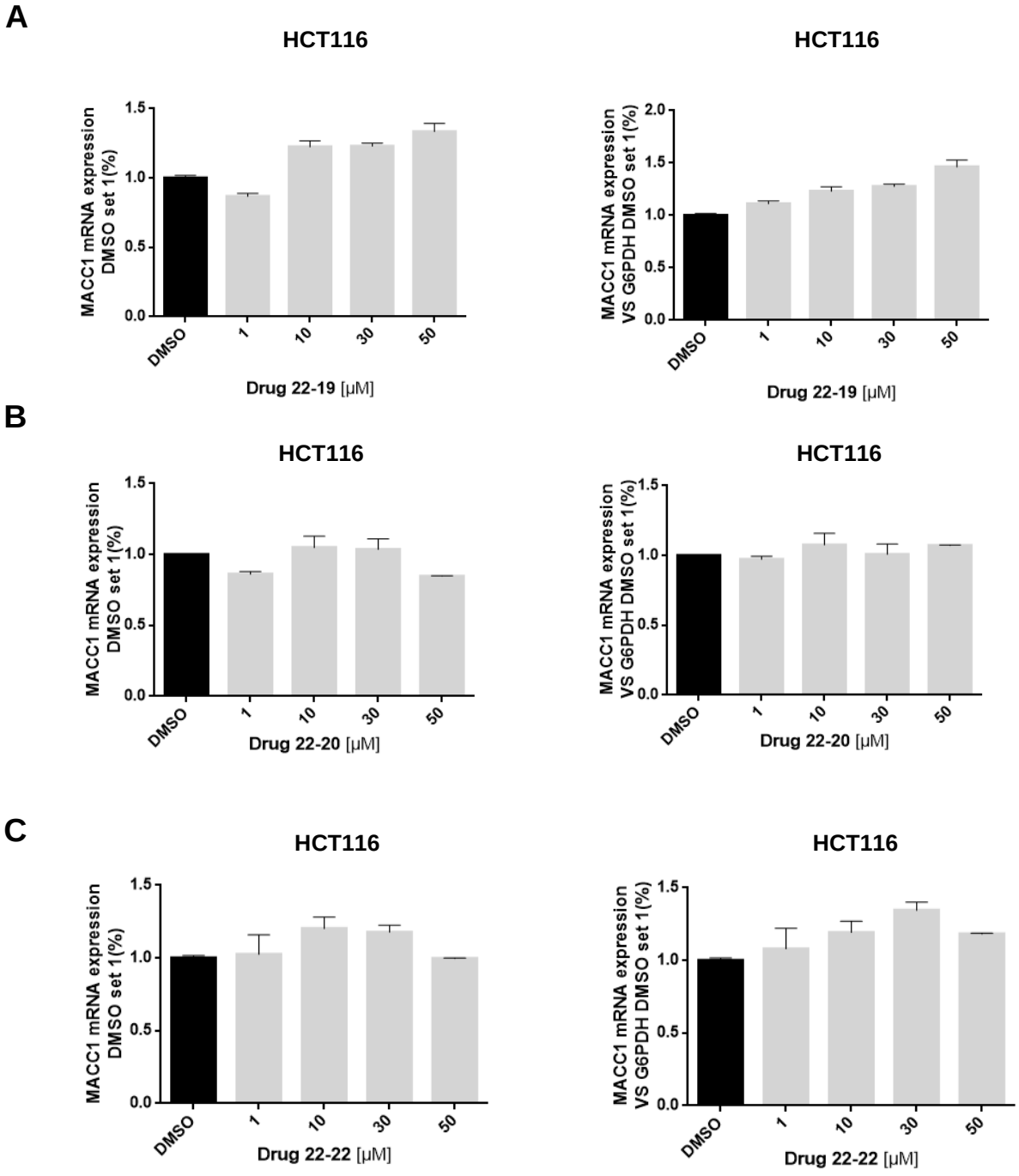

Fig. 9: The effect of Drug 22 derivatives on MACC1 expression. (A, B, C) represent Drug 22-19, Drug 22-20, and Drug 22-22, respectively. Treatment with these derivatives for 24 h in the HCT116 cell line had no effect on MACC1 mRNA expression. Results for mRNA represent means ± SEM of two independent experiments.

We continue to analyze the structures of these derivatives. Their common substructure has been marked in red, but alterations had no inhibitory effect on the expression of MACC1 (Fig. 10). Based on our previous analysis of effective structures, we did further screening to analyze and confirm the part that inhibits the expression of MACC1.

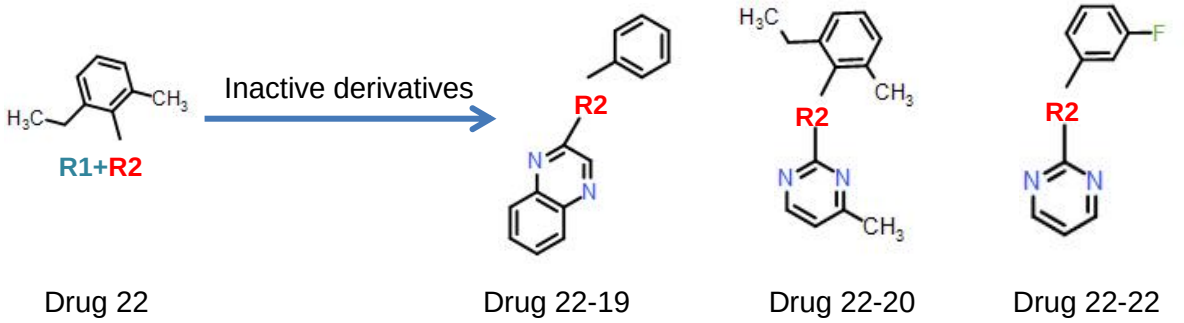

Fig. 10: The chemical structure of Drug 22 and derivatives thereof. The red part marked in all derivatives is the same as Drug 22, and the other part of the chemical structures are the changing parts. All of these derivatives have no inhibitory effect on the expression of MACC1.

3.2.3 Part 3: Drug 22-10 to Drug 22-18

We checked 9 different derivatives in part 3. Through qRT-PCR, Western blot and MTT assay we found that Drug 22-10 and Drug 22-13 inhibit the expression of MACC1 (Fig. 11). Drug 22-15 and Drug 22-17 also inhibited the expression of MACC1, but they were excluded from further evaluations because of their cytotoxicity. Other derivatives have no effect.

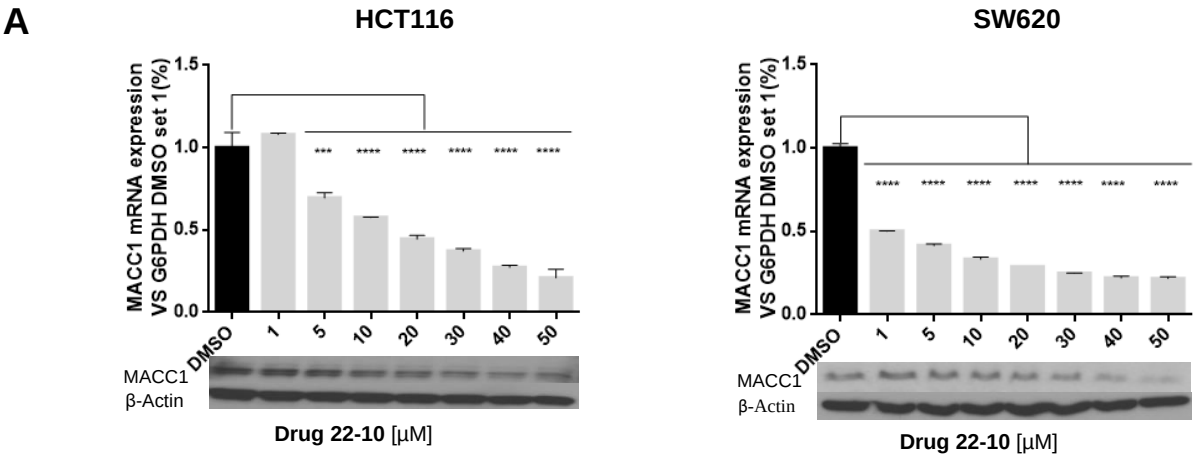

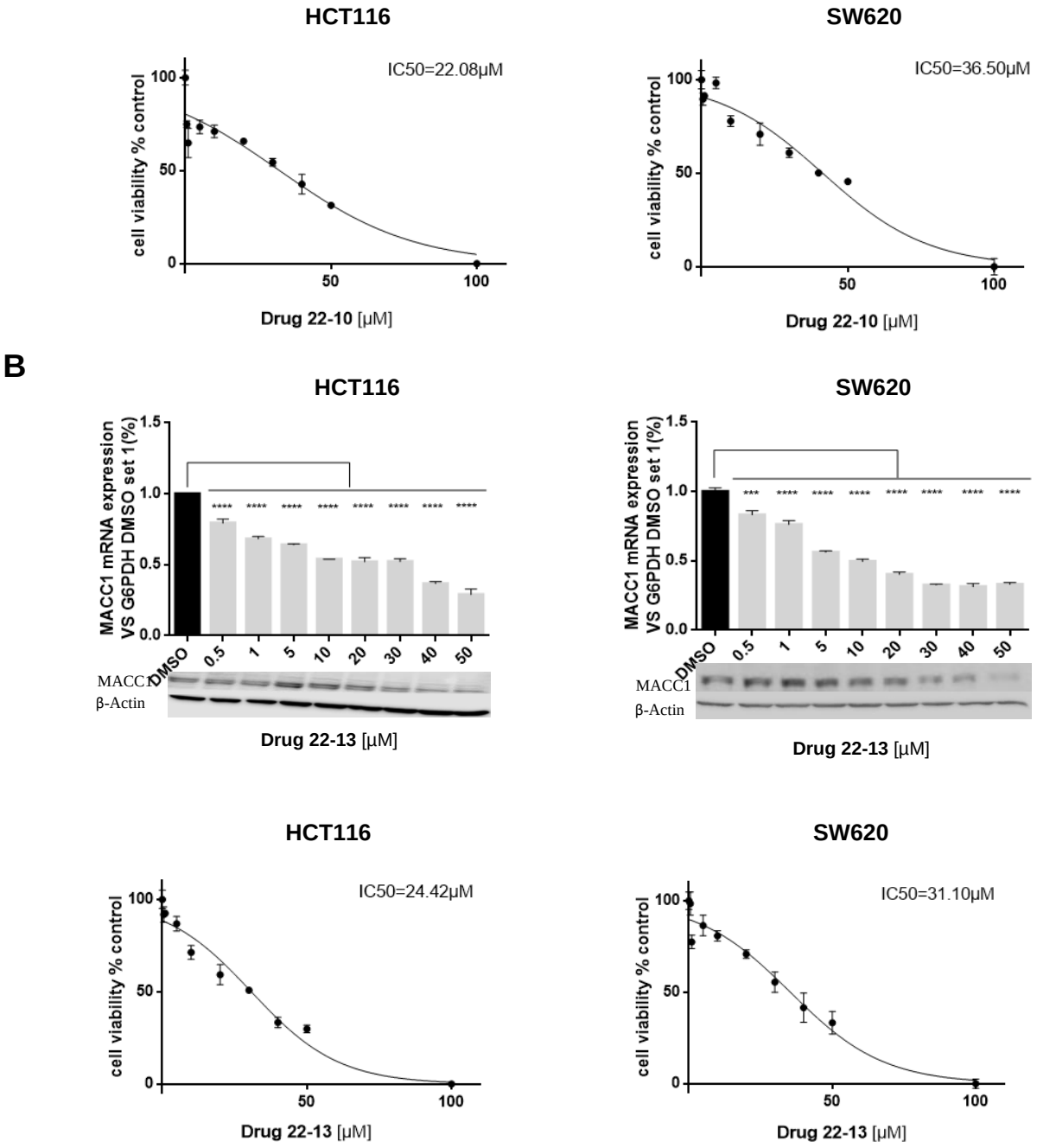

Fig. 11：The effect of Drug 22 derivatives on MACC1 expression. (A, B) represent Drug 22-10 and Drug 22-13, respectively. HCT116 cells and SW620 cells were treated with the inhibitors for 24 h and 48 h, respectively, and Western blots (WB) were performed. The qRT-PCR and MTT assays were treated for 24 h. MACC1 mRNA levels were normalized to G6PDH mRNA expression and the respective DMSO control (black bar). Results for mRNA represent means ± SEM of three independent experiments and for WB one representative example of three independent experiments is shown. In the WB, β-actin served as a loading control. Cell viability was measured independently by MTT assay. Results are shown as mean ± SEM of three independent experiments performed in triplicate. Significant results were determined by one-way ANOVA and multiple comparison was done by Dunnett's method (*** = $p < 0.001$, **** = $p < 0.0001$).

Similarly, the chemical structure of these derivatives was compared with Drug 22, and it was found that all derivatives that can inhibit the expression of MACC1 have the same substructure as Drug 22 — R1 (marked red), Even just replacing a sulfoether linkage from R1 whit an amine linker R3 (marked in red) affects the inhibition of MACC1 (Fig. 12). Therefore, we speculate that the R1 may be the working substructure that can inhibit the expression of MACC1. In response to this inference, we made further a verification in part 4.

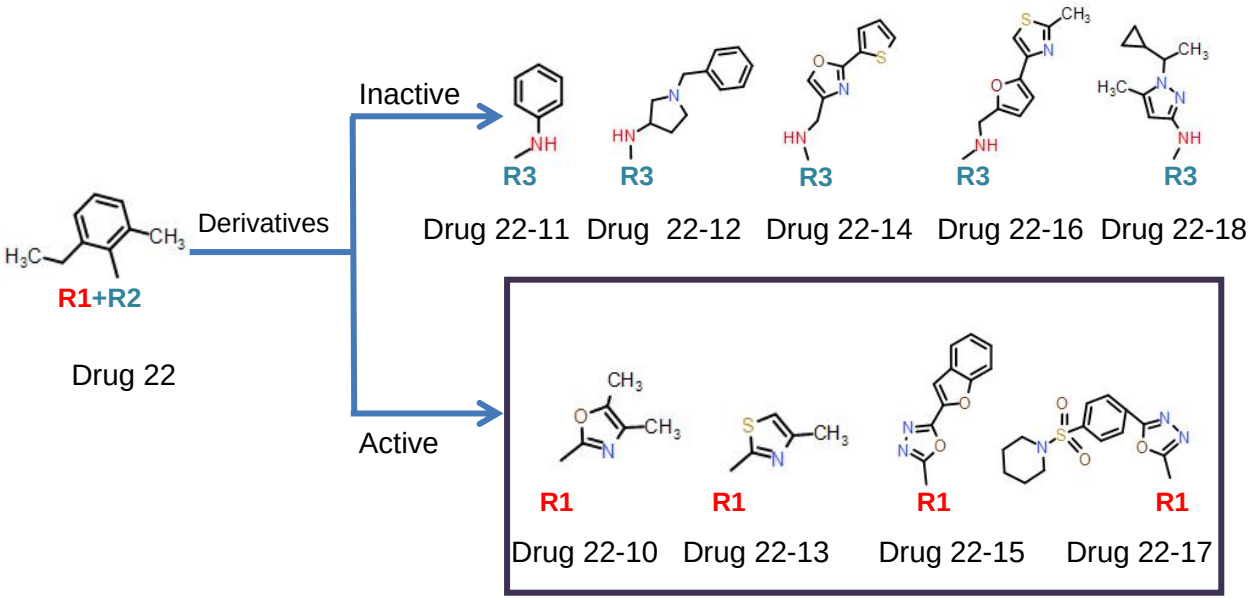

Fig. 12： The chemical structure of Drug 22 and derivatives thereof. The red part marked in all derivatives is the same as Drug 22, and the other part of the chemical structures are the changing parts. The derivatives in the box can inhibit MACC1 expression. Since a sulfoether linker is replaced by an amine linker, other derivatives have no inhibitory effect on MACC1 (R1 is R3 and sulfoether linkage).

3.2.4 Part 4: Drug 22-21 to Drug 22-28

Through the previous analysis, the screening scope was narrowed, and the effective substructure was gradually clarified. We therefore screened another 8 derivatives for verification (Fig. 13). MTT and qRT-PCR assay were used to analyze the drug toxicity and the inhibitory effect on MACC1 mRNA expression, respectively.

A

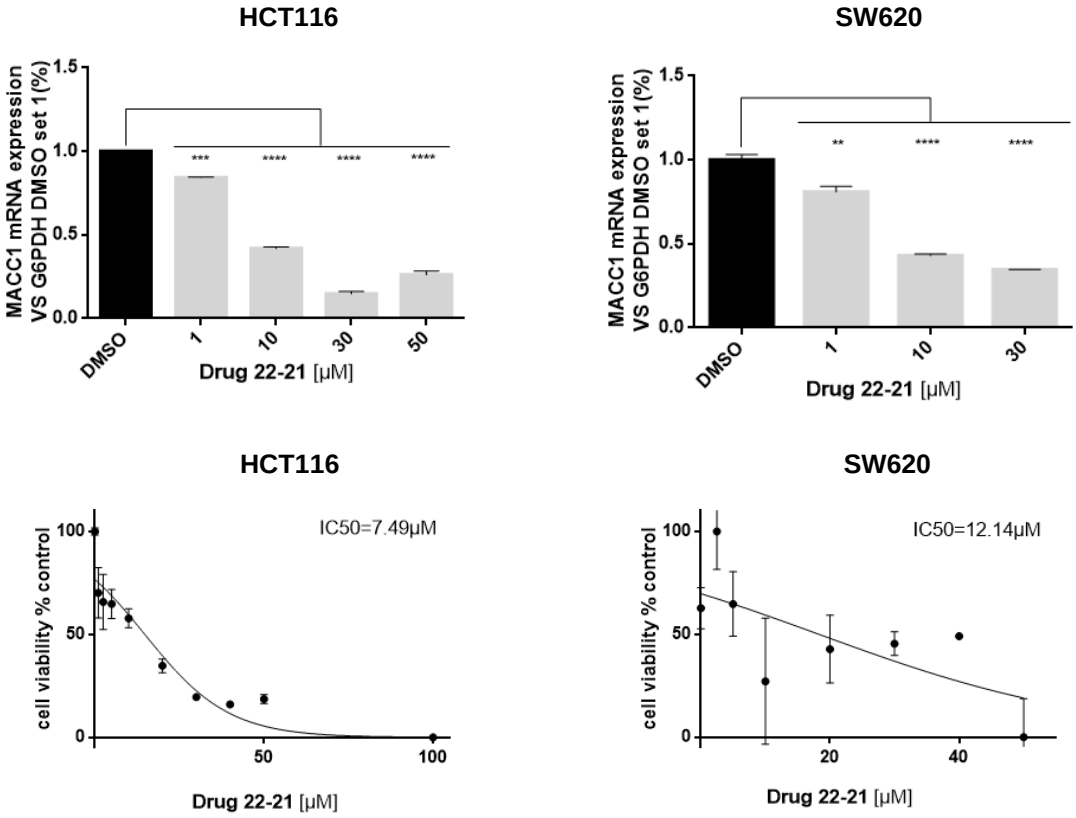
HCT116
SW620
MACC1 mRNA expression VS G6PDH DMSO set 1(%)
1.5
1.0
0.5
0.0
***
****
****
****
**
****
****
DMSO
1
10
30
50
Drug 22-21 [μM]
HCT116
SW620
cell viability % control
100
50
0
IC50=7.49μM
IC50=12.14μM
50
100
20
40
Drug 22-21 [μM]

B

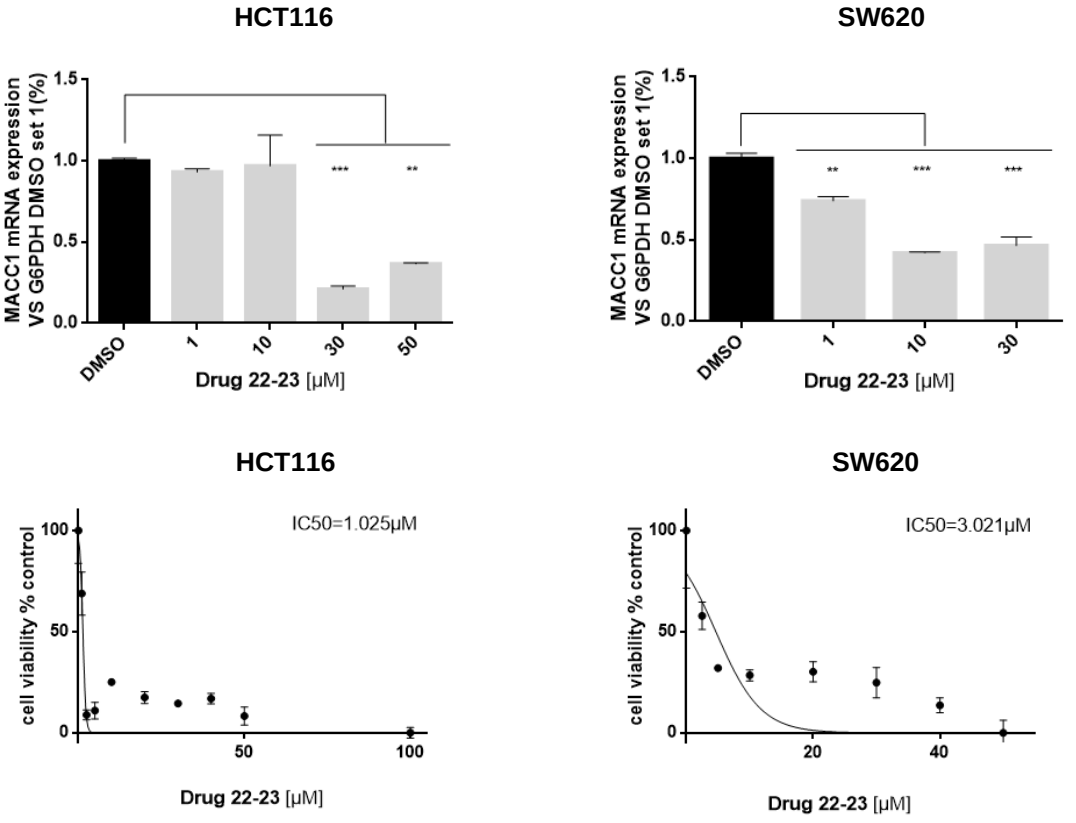
HCT116
SW620
MACC1 mRNA expression VS G6PDH DMSO set 1(%)
1.5
1.0
0.5
0.0
***
**
**
***
***
DMSO
1
10
30
50
Drug 22-23 [μM]
HCT116
SW620
cell viability % control
100
50
0
IC50=1.025μM
IC50=3.021μM
50
100
20
40
Drug 22-23 [μM]

C

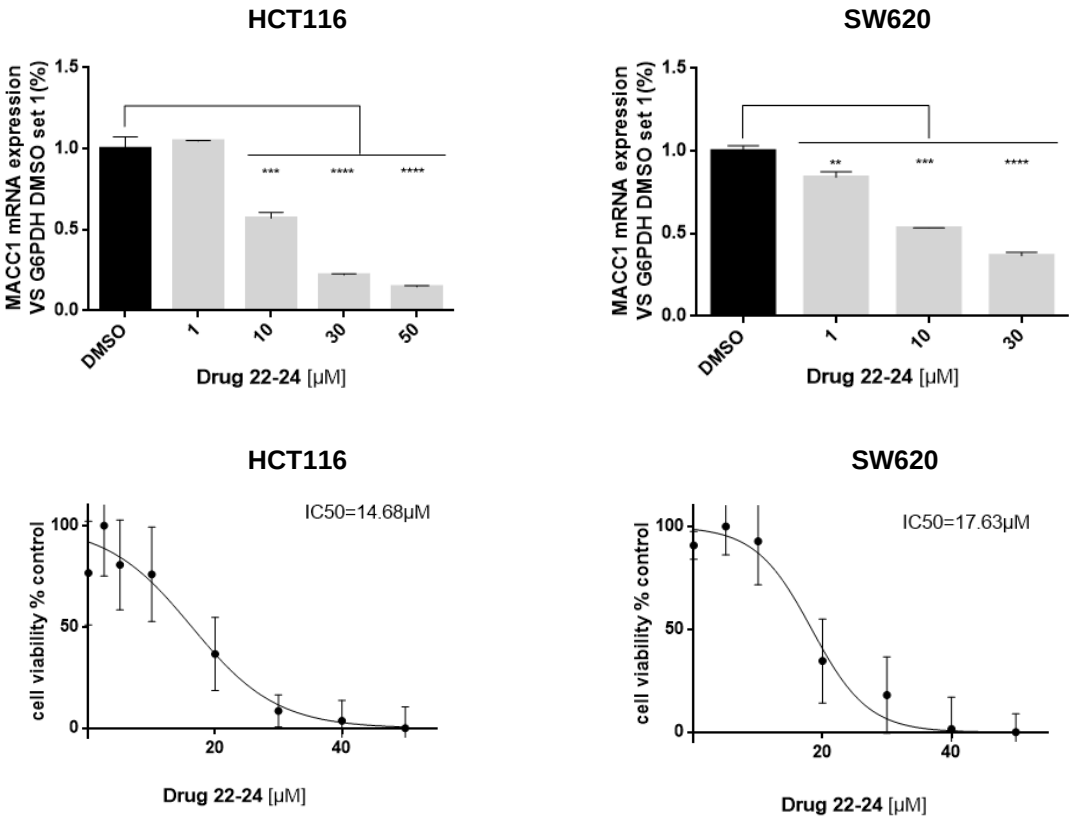
HCT116
SW620
MACC1 mRNA expression VS G6PDH DMSO set 1(%)
1.5
1.0
0.5
0.0
DMSO
1
10
30
50
Drug 22-24 [μM]
HCT116
SW620
IC50=14.68μM
IC50=17.63μM
cell viability % control
100
50
0
20
40
Drug 22-24 [μM]

D

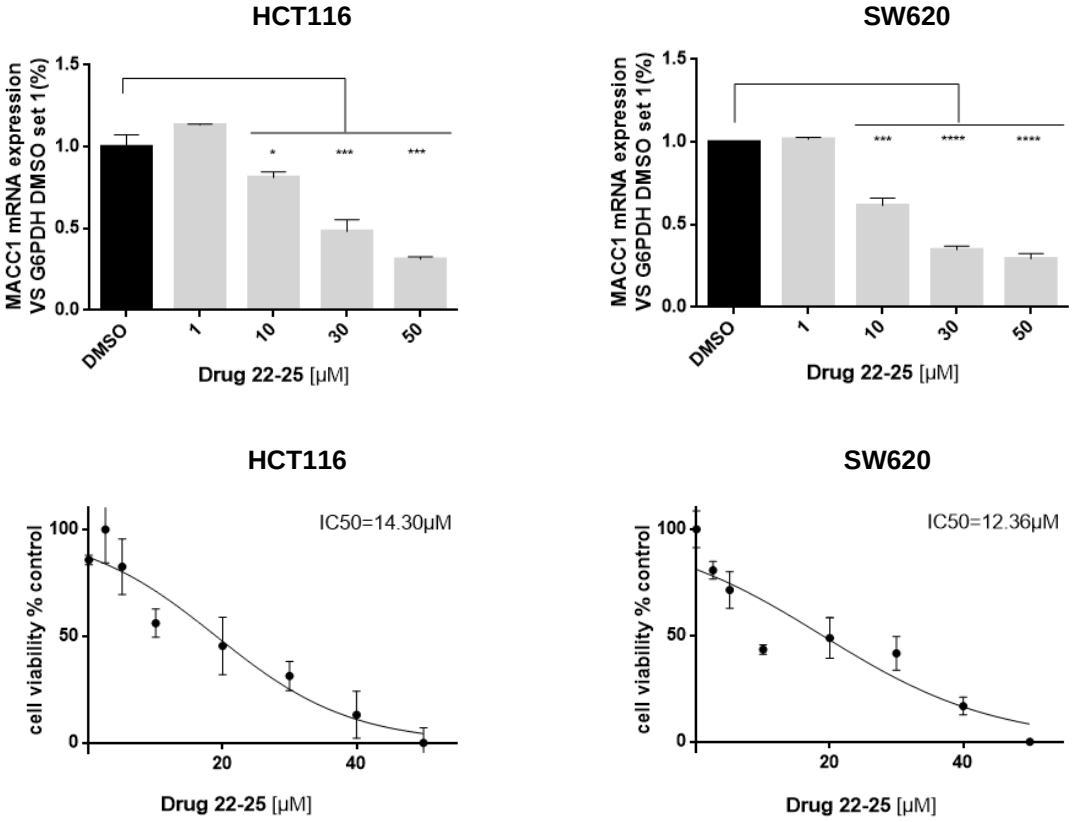
HCT116
SW620
MACC1 mRNA expression VS G6PDH DMSO set 1(%)
1.5
1.0
0.5
0.0
DMSO
1
10
30
50
Drug 22-25 [μM]
HCT116
SW620
IC50=14.30μM
IC50=12.36μM
cell viability % control
100
50
0
20
40
Drug 22-25 [μM]

E

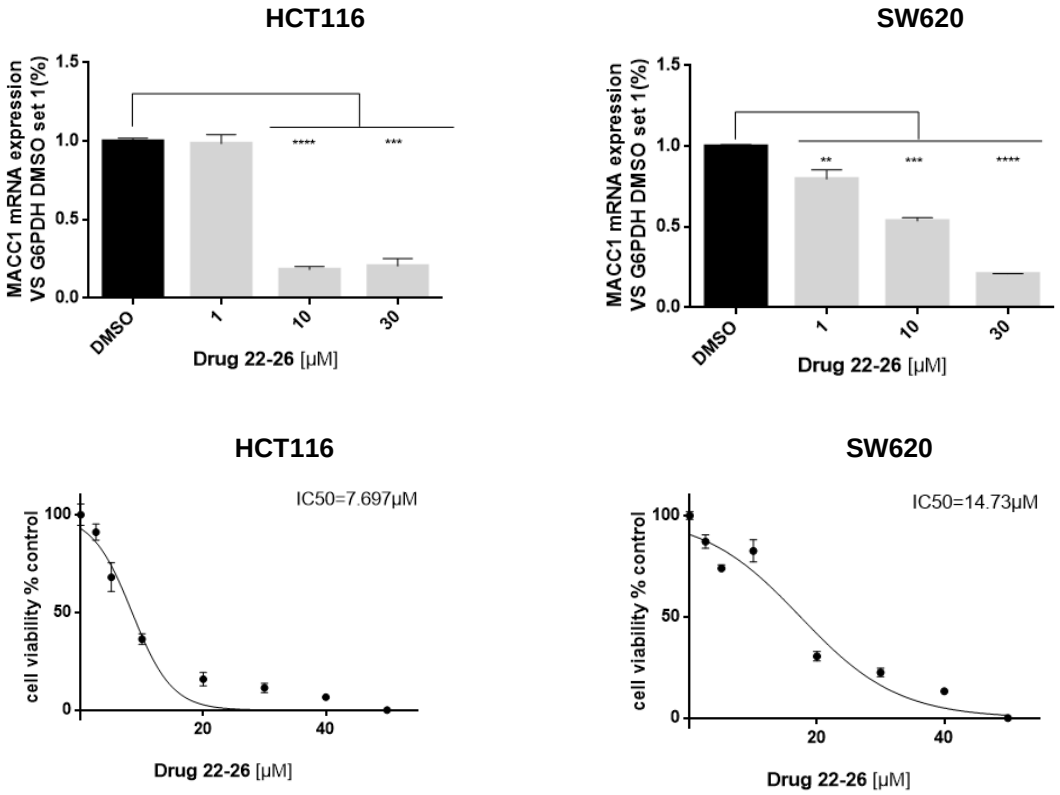

Fig. 13: The effect of Drug 22 derivatives on MACC1 expression. (A, B, C, D, E) represent Drug 22-21, Drug 22-23, Drug 22-24, Drug 22-25, and Drug 22-26, respectively. The qRT-PCR and MTT assays were treated for 24 h. MACC1 mRNA levels were normalized to G6PDH mRNA expression and the respective DMSO control (black bar). MACC1 showed a dose-dependent decrease of mRNA. Results for mRNA represent means ± SEM of two independent experiments. Cell viability was measured independently by MTT assay. Results are shown as mean ± SEM of three independent experiments performed in triplicate. Significant results were determined by one-way ANOVA and multiple comparison was done by Dunnett's method (* = $p < 0.05$, ** = $p < 0.01$, *** = $p < 0.001$, **** = $p < 0.0001$).

Through this screening, we compared the structure of the derivatives with Drug 22 (the red marked part) and found that the derivatives that have an inhibitory effect on MACC1 expression all contain the substructure of R1 (marked in red), which proves our previous inference (Fig. 14). However, the effective group of some derivatives is not the same as the party marked in red, such as Drug 22-25 and Drug 22-26. What we named R4 lacks one nitrogen of R1. In addition, it carries a bulky trifluoromethyl group. But they are also structural modifications based on this, which also reminded us that we could find improved drugs by modifying the most effective group so far.

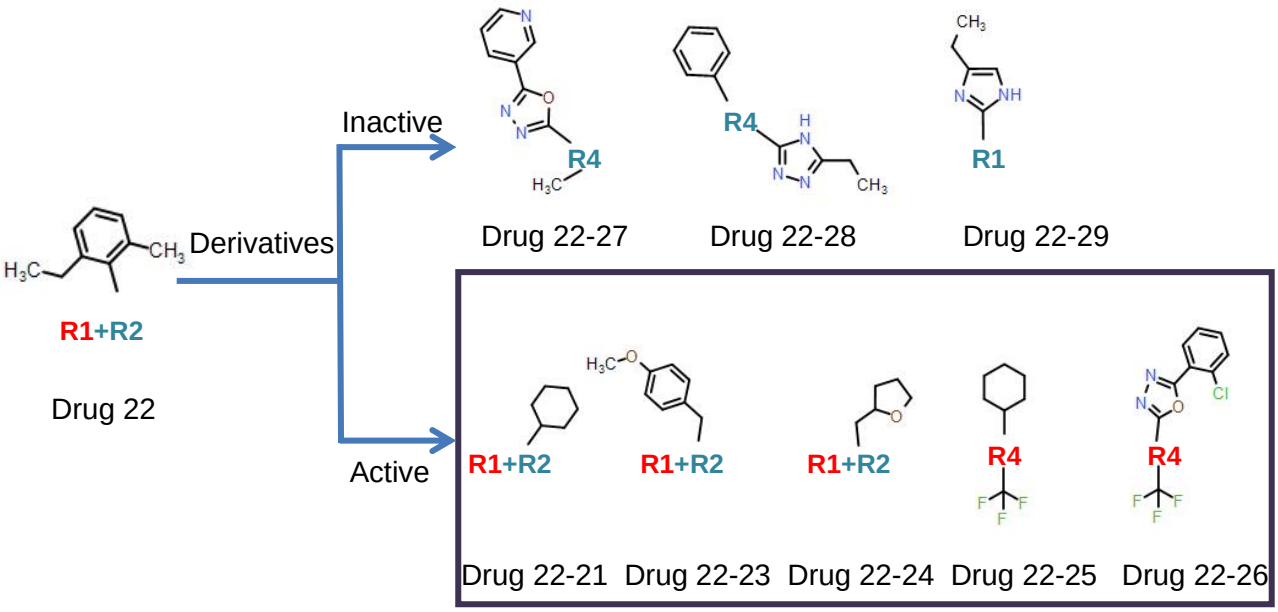

Fig. 14： The chemical structure of Drug 22 and derivatives thereof. The red part marked in all derivatives is the same as Drug 22 (R4 lacks one nitrogen of R1), and the other part of the chemical structures are the changing parts. The names marked in the box are derivatives that can inhibit MACC1 expression.

3.2.5 Part 5: Drugs from Medchem

Through Part 4, we found that R4 (lacking one nitrogen of R1) adds a bulky trifluoromethyl group that can also inhibit the expression of MACC1. To further prove the effectiveness of this structure, we obtained 48 new compounds from Medchem. Here, we listed some compounds with the same structure as R4 and made drug screenings on this structure. The effect of these drugs was further verified by qRT-PCR in the HCT116 cell line (Fig. 15).

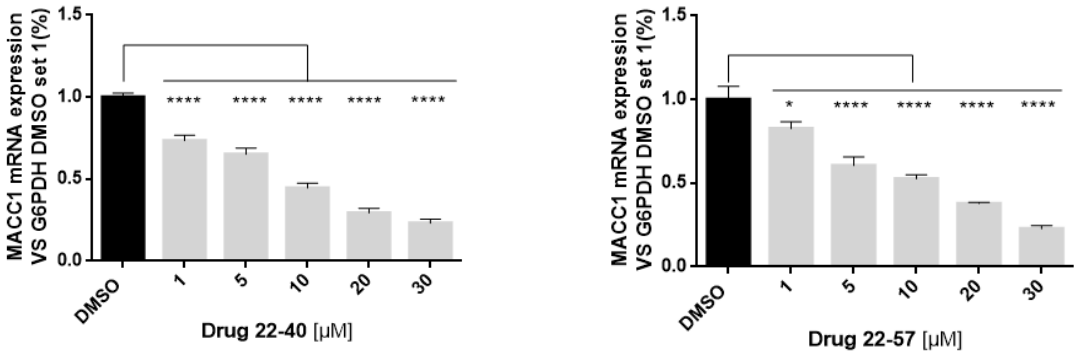

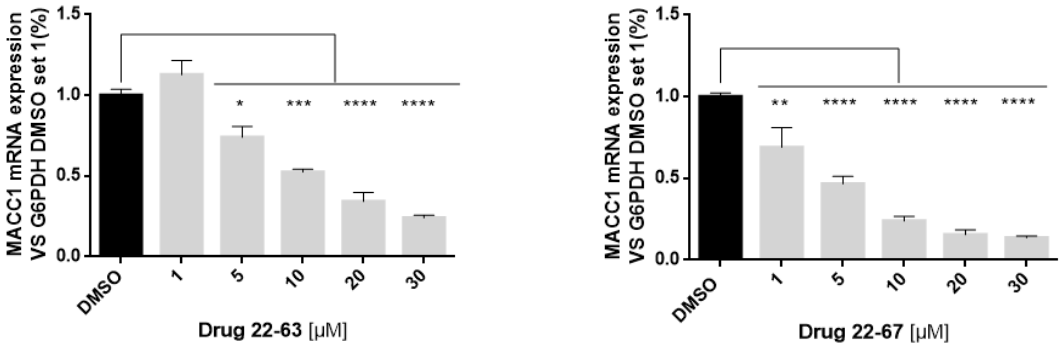

Fig. 15: The effect of Drug 22 derivatives on MACC1 expression. The qRT-PCR assay was treated for 24 h. MACC1 mRNA levels were normalized to G6PDH mRNA expression and the respective DMSO control (black bar). MACC1 showed a dose-dependent decrease of mRNA. Results for mRNA represent means ± SEM of two independent experiments. Significant results were determined by one-way ANOVA and multiple comparison was done by Dunnett's method (* = $p < 0.05$, ** = $p < 0.01$, *** = $p < 0.001$, **** = $p < 0.0001$).

Combined with the results of qRT-PCR, through the analysis of the chemical structures of these drugs, it was found that, for example, when the trifluoromethyl group behind R4 was changed, the drug would no longer inhibit the expression of MACC1 (Fig. 16), or even modify the groups other than R4, which could also change the inhibitory effect of this drug on MACC1, like Drug 22-32. This situation provided us with the good idea to change the effect of these drugs by modifying the main chemical structure. At the same time, these verified drug modifying groups would provide a great reference for our subsequent drug structure modification.

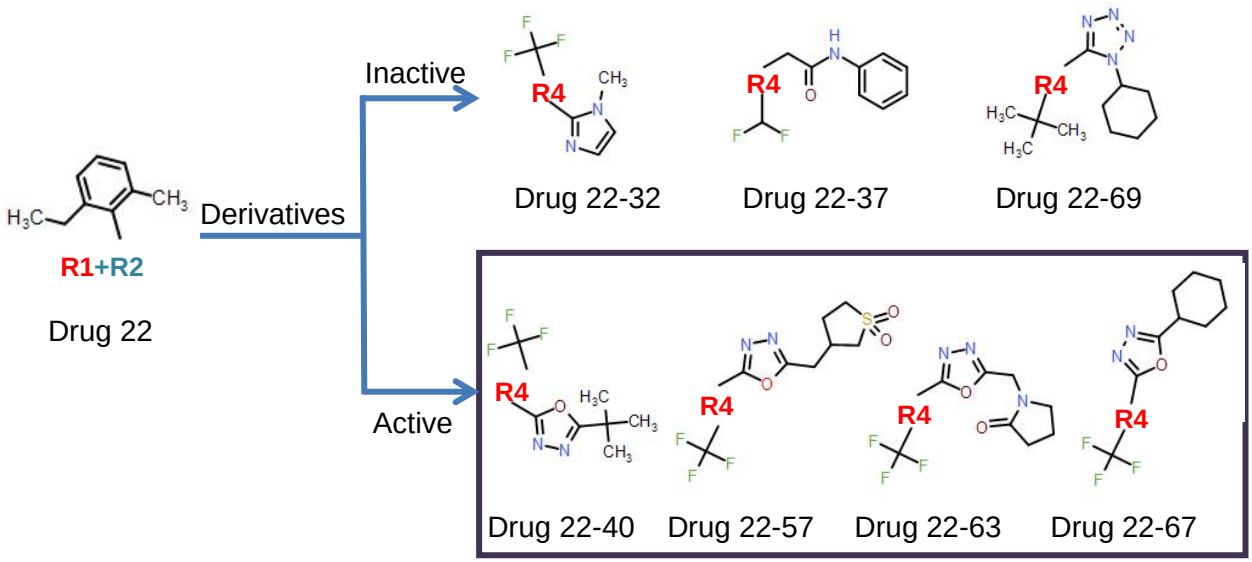

Fig. 16： The chemical structure of Drug 22 and derivatives thereof. The red part marked in all derivatives is R4 (lacking one nitrogen of R1), and the other part of the chemical structures are the changing parts. The names marked in the box are derivatives that can inhibit MACC1 expression.

3.3 Inhibition on MACC1-associated migration in CRC cells

Through the experiments using MTT, qRT-PCR and WB, we screened the drugs that inhibit the expression of MACC1. Based on cell viability and mRNA expression after drug treatment, we further analyzed IC_{50} and EC_{50}. Based on these two results, all effective compounds are classified into two groups: highly active drugs (Table 6) and active drugs (Table 7; Appendix table: inactive drugs). Since the major phenotype imparted by MACC1 is the increased migration of CRC cells, after classification, migration and wound-healing assays were performed on these four highly active drugs.

Table 6. Four highly active drugs

Compound	Structure	Cell line	Maximal inhibition %	At concentration [μM]	Active concentration [μM]	EC50 (activity) [μM]	IC50 (Tox/MTT) [μM]
						normalized	normalized
Drug 22-7	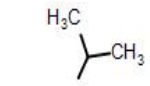 R1+R2	HCT116	77	50	10-50	12.3	18.11
		SW620	69	50	5-50	10.99	21.49
Drug 22-8	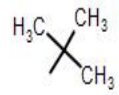 R1+R2	HCT116	90	50	0.5-50	6.79	21.34
		SW620	82	50	0.5-50	6.6	17.87
Drug 22-10	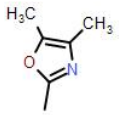 R1	HCT116	56	50	1-50	4.42	22.08
		SW620	78	40	1-50	2.6	36.5
Drug 22-13	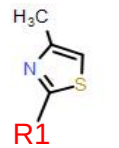 R1	HCT116	70	50	0.5-50	9.44	24.42
		SW620	63	50	1-50	8.73	31.1

Table 7. Twenty four active drugs

Compound	Structure	Cell line	Maximal inhibiton %	At concentration [μM]	Active concentration [μM]	EC50 (activity) [μM]	IC50 (Tox/MTT) [μM]
						normalized	normalized
Drug 22	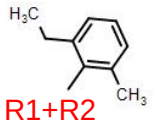 R1+R2	HCT116	85.4	30	5-30	11.31	7.36
		SW620	78	25	5-25	7.359	6.38
Drug 22-5	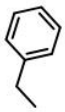 R1+R2	HCT116	80	30	5-30	12.96	10.9
		SW620	53.5	20	1-20	2.302	23.61
Drug 22-9	 R1+R2	HCT116	64	50	30-50	29.64	17.52
		SW620	66	40	10-50	12.16	22.29
Drug 22-21	 R1+R2	HCT116	91	30	1-50	6.78	7.49
		SW620	72	30	1-30	9.96	12.14
Drug 22-23	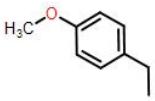 R1+R2	HCT116	88	30	10-50	10.82	1.025
		SW620	75	30	1-30	0.88	3.021
Drug 22-24	 R1+R2	HCT116	90	50	10-50	11.49	14.68
		SW620	69	30	10-30	10.53	17.63
Drug 22-25	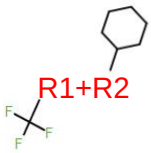 R1+R2	HCT116	68	50	30-50	17.64	14.3
		SW620	65	50	1-50	8.4	12.36
Drug 22-26	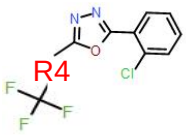 R4	HCT116	87	30	10-30	7.089	7.697
		SW620	79	30	1-30	5.987	14.73

Compound	Structure	Cell line	Maximal inhibition %	At concentration [μM]	Active concentration [μM]	EC50 (activity) [μM] normalized	IC50 (Tox/MTT) [μM] normalized
Drug 22-29	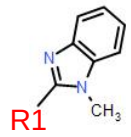 R1	HCT116	47.34	30	5-30	★	74.51
Drug 22-30	R1 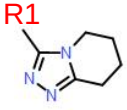	HCT116	35.24	30	5-30	★	133.70
Drug 22-38	 R1+R2	HCT116	70.02	30	5-30	7.993	23.37
Drug 22-40	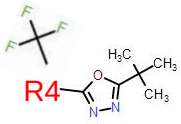 R4	HCT116	76.89	30	1-30	3.278	19.88
Drug 22-42	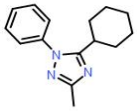 R1	HCT116	54.17	30	20-30	12.45	21.16
Drug 22-47	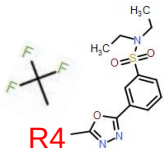 R4	HCT116	62.16	30	10	7.217	5.95
Drug 22-48	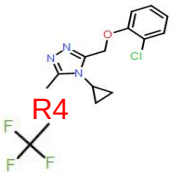 R4	HCT116	53.28	30	20-30	8.483	16.93
Drug 22-52	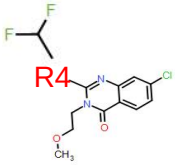 R4	HCT116	87.41	20	5-30	4.973	10.66

Compound	Structure	Cell line	Maximal inhibition %	At concentration [μM]	Active concentration [μM]	EC50 (activity) [μM]	IC50 (Tox/MTT) [μM]
						normalized	normalized
Drug 22-57		HCT116	77.33	30	1-30	4.558	23.94
Drug 22-63	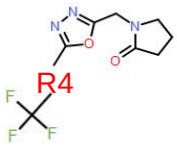	HCT116	75.89	30	5-30	6.1	22.33
Drug 22-66	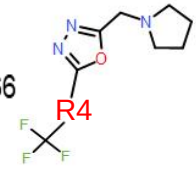	HCT116	83.08	30	10-30	8.369	15.42
Drug 22-67	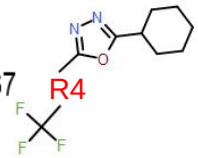	HCT116	86.46	30	1-30	2.042	18.91
Drug 22-72	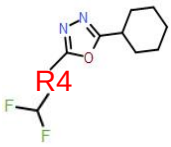	HCT116	78.03	30	1-30	3.203	20.70
Drug 22-74	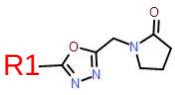	HCT116	83.32	20	1-30	1.207	4.83
Drug 22-75	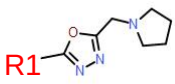	HCT116	87.79	30	1-30	1.149	10.18
Drug 22-76	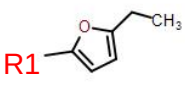	HCT116	86.72	30	1-30	1.013	12.57

Through the qRT-PCR and MTT assay, we knew the EC_{50} and IC_{50} of these four highly active drugs, so we choose the drug concentration lower than IC_{50} for the migration assay. We investigated the effect of these four highly active drugs on MACC1-mediated cell migration of HCT116 cells using the Boyden chamber assay. HCT116 cells treated with different drug concentrations for 24 h showed more inhibition of cell migration than solvent-treated control cells (Fig. 17). And from the results, it can be seen that the effects of these three drugs (Drug 22-7, Drug 22-8 and Drug 22-10) in inhibiting the expression of MACC1 are concentration-dependent, which is consistent with the results obtained by qRT-PCR and WB. However, Drug 22-13 has no inhibitory effect on cell migration at low concentrations of 0.5 µM and 1 µM.

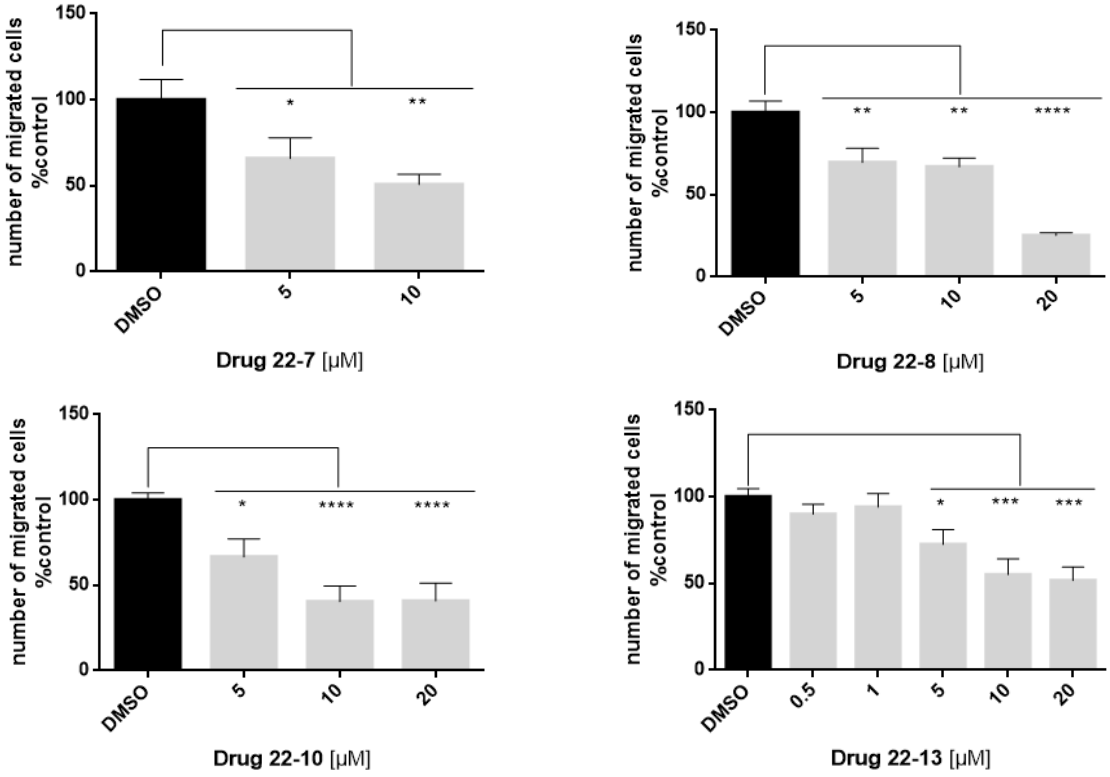

Fig. 17: The effect of four highly active drugs on cell migration. HCT116 cells were treated with different drug concentrations lower than IC_{50} for 24 h. Migration was measured with the Boyden chamber assay. These four highly active drugs inhibited the migration of HCT116 cells by inhibiting the expression of MACC1. Results are shown as mean ± SEM of three independent experiments performed in quadruplicate. Control cells were treated with an equivalent amount of DMSO in all assays. Significant results were determined by one-way ANOVA and multiple comparison was done by Dunnett's method (* = $p < 0.05$, ** = $p < 0.01$, *** = $p < 0.001$, **** = $p < 0.0001$).

We further analyzed the effect of these four drugs on directed migration in a wound-healing assay (Fig. 18A). As with the migration assay, the effective concentrations lower than IC_{50} were selected for the experiments. From the figures, we could see that in the control group without these drugs, HCT116 cells completely closed the inserted wound in 48 h, which corresponds to a value of 100%. However, wound confluence was impaired in drug-treated HCT116 cells. For example, Drug 22-7 started to show a different wound confluence curve from the control group after 12 h of drug treatment. The high concentration of 10 μM was the first to started to be different from the control group, and then the low concentration of 5 μM followed, which indicated that the migration of HCT116 cells was inhibited after drug treatment, and the wound confluence was slower than that of the control group. The inhibitory effect reached its maximum when the drug was treated for 24 h to 36 h, and then started to weaken until the curve overlapped with the control group at 48 h, which corresponds to a value of 100%. This means that the wound was completely closed at this time, and the drug no longer had any effect. The wound confluence curves of the other three drugs were the same as this analysis, but the wound confluence curves started to change and the time for the wound closure curves to overlap with the control group was different.

During the experiment, we also took photos of wound confluence so that we could understand the process of wound confluence more intuitively (Fig. 18B). After 24 h of drug treatment, we could see that the growth of the wound cells treated by the drug was significantly slower than that of the control group. After 48 h, the wound in the control group had been completely closed, while for the other groups the wounds had not. Among them, the remaining wound of Drug 22-8 was the largest.

Through migration assay and wound-healing assay, it was confirmed that these four highly active drugs can inhibit cell migration by inhibiting the expression of MACC1 in HCT116 cells.

A

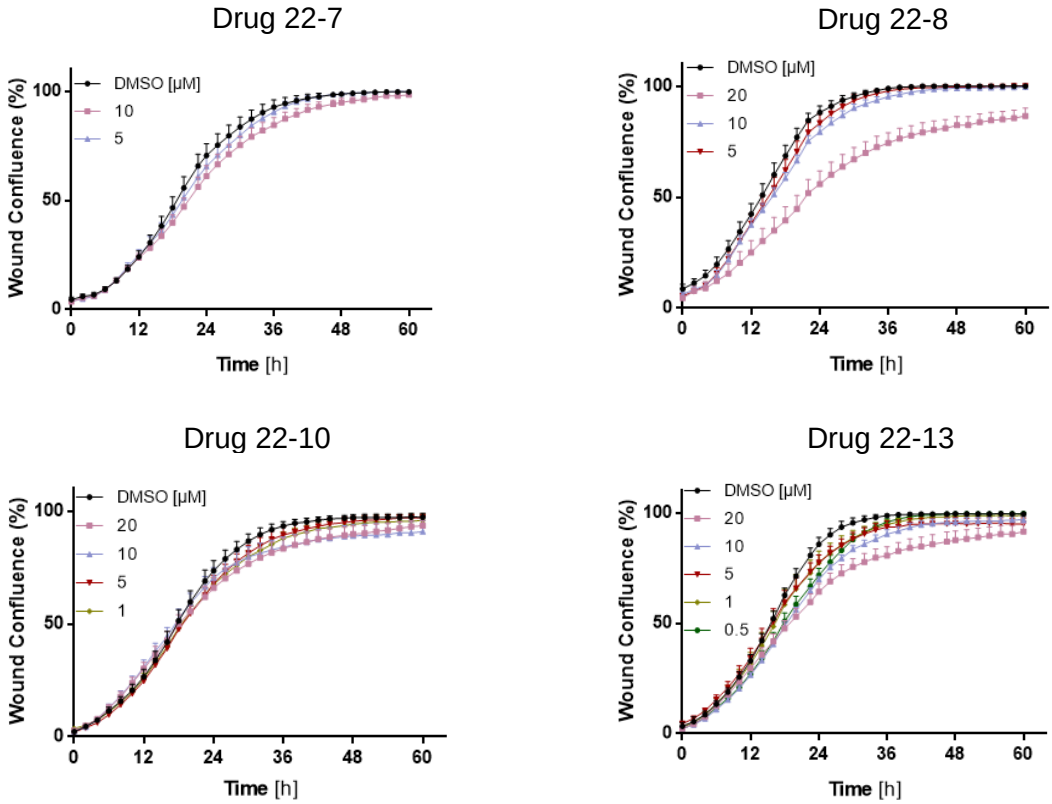
Drug 22-7
DMSO [µM]
10
5
Wound Confluence (%)
Time [h]
Drug 22-8
DMSO [µM]
20
10
5
Wound Confluence (%)
Time [h]
Drug 22-10
DMSO [µM]
20
10
5
1
Wound Confluence (%)
Time [h]
Drug 22-13
DMSO [µM]
20
10
5
1
0.5
Wound Confluence (%)
Time [h]

B

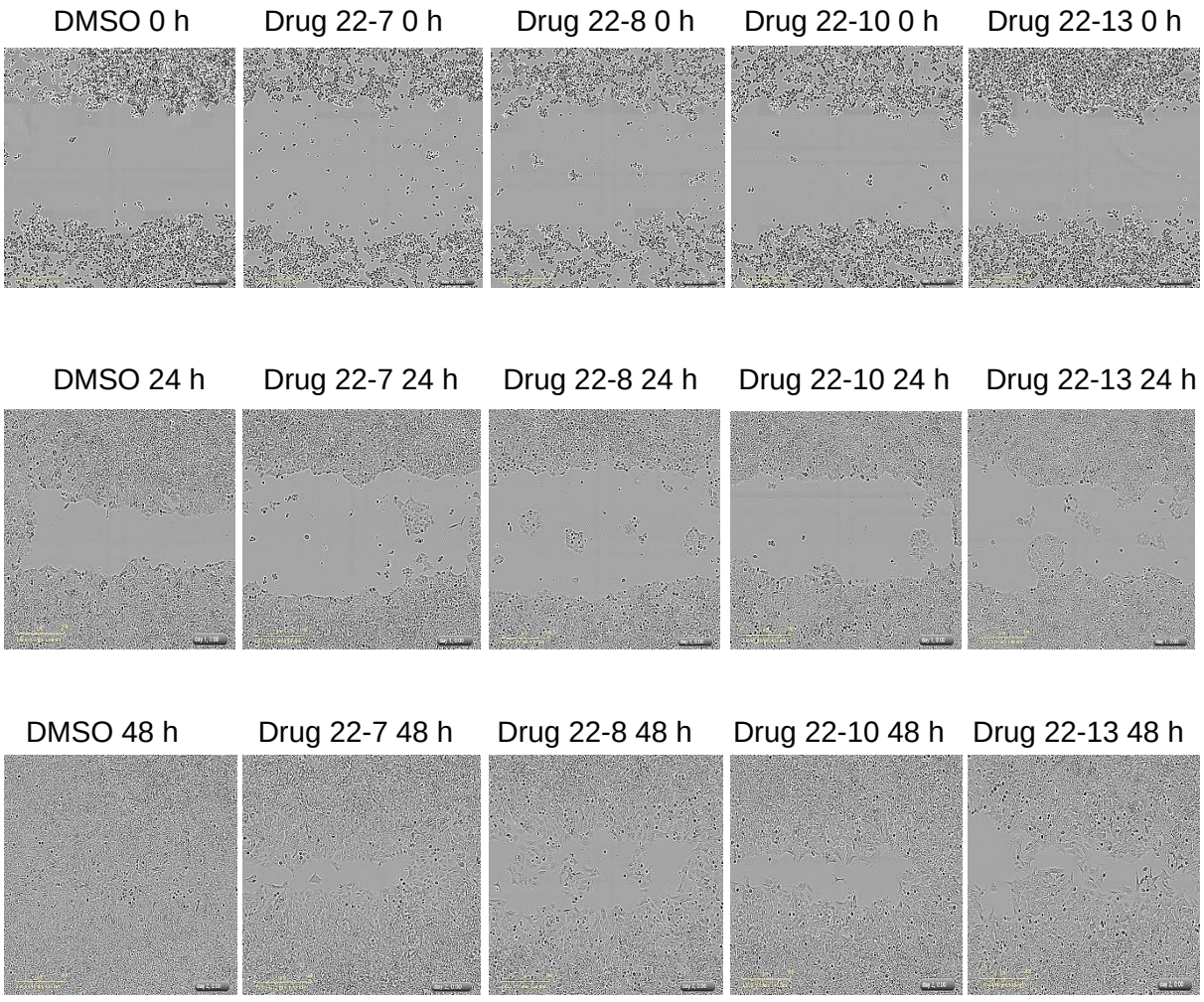
DMSO 0 h
Drug 22-7 0 h
Drug 22-8 0 h
Drug 22-10 0 h
Drug 22-13 0 h
DMSO 24 h
Drug 22-7 24 h
Drug 22-8 24 h
Drug 22-10 24 h
Drug 22-13 24 h
DMSO 48 h
Drug 22-7 48 h
Drug 22-8 48 h
Drug 22-10 48 h
Drug 22-13 48 h

Fig. 18: The effect of four highly active drugs on wound healing. HCT116 cells were treated with different drug concentrations lower than IC_{50} for 24 h. The wound was measured using Incucyte. (A) Under the action of these four highly active drugs, the percentage of wound confluence of HCT116 cells moved over time. (B) The photos of the wound confluence of HCT116 cells were taken every two hours in Incucyte. From top to bottom, the different wound states at 0 h, 24 h and 48 h under different drug concentrations are shown, respectively. Results are shown as mean ± SEM of three independent experiments performed in triplicate. Control cells were treated with an equivalent amount of DMSO in all assays.

3.4 Novel compounds inhibit metastasis formation in mice

As shown previously, MACC1 promotes tumor growth and induces metastasis formation. To analyze whether these novel drugs have an inhibitory effect on tumor metastasis in mice, we conducted animal experiments. Drug 22 is the first novel MACC1 expression inhibitor we discovered and has strong toxicity in in *vitro* experiments. Therefore, we first conducted an MTD experiment with Drug 22 to verify the effects in vivo. We had four groups, with two animals in each group, and the dosages were 25 mg/kg, 50 mg/kg, 100 mg/kg and 200 mg/kg, respectively. With the oral application route for 20 consecutive days, we did not observe any toxicity (as a measure of body weight and general health condition) (Fig. 19A) [116]. Finally, we selected a concentration of 50 mg/kg for further studies in vivo.

We used Drug 22 and randomly selected Drug 22-10 and Drug 22-13 from the four highly active derivatives for animal bioluminescence experiments (each group with 10 mice). Since the toxicity of these two derivatives was significantly lower than that of Drug 22, the concentration of 50 mg/kg was therefore selected. In cooperation with EPO Berlin-Buch GmbH, SCID-beige mouse spleens were transplanted with HCT116-CMVp-Luc cells. Tumor growth and metastasis formation were continuously monitored by non-invasive bioluminescence imaging over 21 days until the ethical endpoint (cancer burden of control group animals) was reached. We monitored the weight and health condition of the mice, which also showed no toxicities (Fig. 19B). The lateral view captures the bioluminescent signals emitted by the tumor cells growing in the spleen that form the primary tumor, while the ventral view represents the signal from the liver where the tumor had metastasized. The signal was quantified by ImageJ software. Compared with the control group, Drug 22 significantly inhibited the formation of liver metastasis and had some effect on the primary tumor of the spleen (Fig. 19C, D). From the overlay figures, comparing the luminous intensity of the control group and the drug-treated groups on the 21st day, it was found that the ventral area of the control group

was larger and the signal intensity was stronger, while the signal of the drug-treated group was weakened, which indicated that liver metastasis was inhibited. These drugs also had an inhibitory effect on the primary tumor in the spleen (Fig. 19E, H). Representative images of the liver isolated signals on day 21 are also shown in these figures.

We next analyzed the presence of human satellite DNA in the liver of the control versus the drug-treated mice as a molecular marker for the appearance of metastases (Fig. 19F). The analysis showed that compared with the three different drug-treated groups (Drug 22, Drug 22-10 and Drug 22-13), the human satellite DNA carried by the liver was reduced by 55%, 75% and 70%, respectively, which supported our bioluminescence experiments. In addition, MACC1 mRNA levels were quantified by qRT-PCR to verify drug-mediated transcriptional inhibition of MACC1 in vivo (Fig. 19G, I). Drug-treated animals showed significantly reduced MACC1 mRNA expression in the liver and spleen, confirming that the drugs act as transcriptional inhibitors of MACC1 and thus inhibit MACC1-induced metastasis formation in vivo.

We used the tissue adjacent to the part where the human microsatellite DNA and MACC1 mRNA were detected conduct immunohistochemistry to ensure the accuracy of the results and detect the expression of CK19 (Fig. 19J). It can be seen from the figures that compared with the control group, the number of micrometastases and the expression of CK19 in the drug-treated groups were decreased. The liver tissue treated with Drug 22-13 showed that the metastases were reduced and the middle part was necrotic. The liver tissues treated with Drug 22-10 showed that there were only a small amount of micrometastases and no large metastases. In comparison, the effect of Drug 22-10 on metastasis inhibition was better than that of Drug 22-13, and the therapeutic effects of these two derivatives were significantly better than that of Drug 22, which was also consistent with our previous data. In vitro and in vivo experiments were carried out to verify the newly discovered inhibitors of MACC1 expression, and these finally proved the effectiveness of these inhibitors.

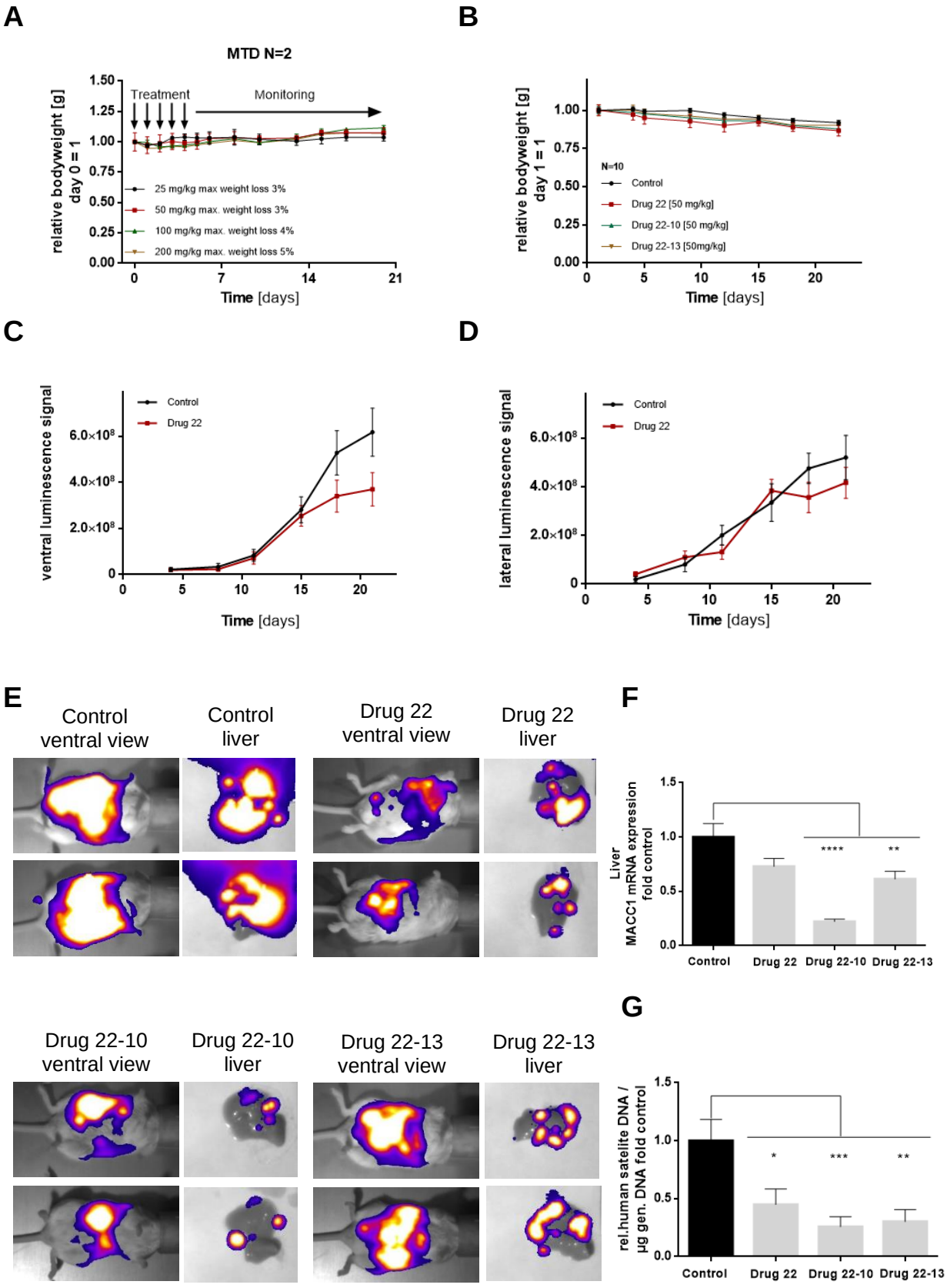
A
MTD N=2
Treatment
Monitoring
relative bodyweight [g]
day 0 = 1
25 mg/kg max weight loss 3%
50 mg/kg max. weight loss 3%
100 mg/kg max. weight loss 4%
200 mg/kg max. weight loss 5%
Time [days]
B
relative bodyweight [g]
day 1 = 1
N=10
Control
Drug 22 [50 mg/kg]
Drug 22-10 [50 mg/kg]
Drug 22-13 [50mg/kg]
Time [days]
C
ventral luminescence signal
Control
Drug 22
Time [days]
D
lateral luminescence signal
Control
Drug 22
Time [days]
E
Control ventral view
Control liver
Drug 22 ventral view
Drug 22 liver
Drug 22-10 ventral view
Drug 22-10 liver
Drug 22-13 ventral view
Drug 22-13 liver
F
Liver MACC1 mRNA expression fold control
Control
Drug 22
Drug 22-10
Drug 22-13
G
rel.human satelite DNA / µg gen. DNA fold control
Control
Drug 22
Drug 22-10
Drug 22-13

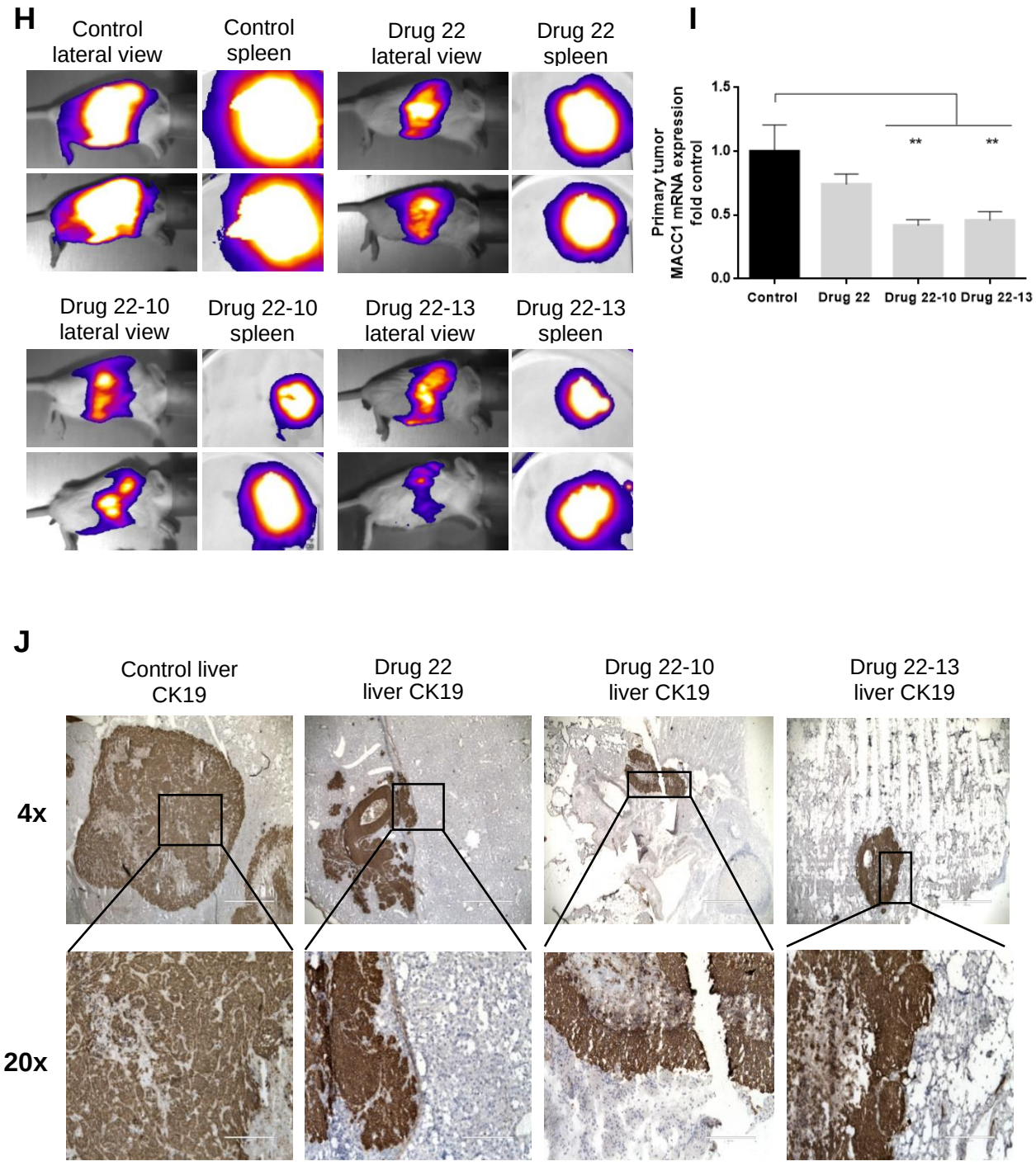

Fig. 19: The effect of novel MACC1 inhibitors on metastasis in mice. SCID-beige mice were intrasplenically transplanted with HCT116-CMVp-Luc cells and treated orally with novel MACC1 inhibitors daily. Bioluminescence was measured by an intraperitoneal application of 150 mg/kg D-Luciferin and a sequence exposure of 20 s. (A) MTD assay was used to evaluate the toxicity of Drug 22 in mice. Body weight was measured daily for 20 days and is shown relative to day 0. (B) Acute toxicity was assessed in healthy animals treated with 50 mg/kg of novel MACC1 inhibitors. Body weight was measured daily for 21 days and is shown relative to day 1. (C, D) The ventral signals (C) and lateral signals (D) from metastases and tumors were monitored via bioluminescence imaging and quantified over time in solvent-treated and Drug 22-treated mice. Bioluminescence intensity was quantified via ImageJ and averaged per group and day. (E, H) Representative bioluminescence pictures showing in vivo and ex vivo imaging of isolated

organs from each group on day 21 of SCID-beige mice. All images are overlaid with the corresponding bright-field pictures. (F) Human satellite DNA was quantified using a quantitative polymerase chain reaction (qPCR) with equivalent amounts of genomic DNA obtained from the liver of each mouse. (G, I) MACC1 mRNA levels were determined from the livers (G) and the spleens (I) using qRT-PCR. (J) The expression of CK19 in liver metastases was detected by immunohistochemistry. Data represent mean ± SEM. Significant results were determined by one-way ANOVA and multiple comparison was done by Dunnett's method (n = 10 animals/group, * = $p < 0.05$, ** = $p < 0.01$, *** = $p < 0.001$, **** = $p < 0.0001$).

MACC1 is a biomarker highly related to tumor formation and progression as well as tumor metastasis. Therefore, it is of great clinical significance to find inhibitors that can inhibit the expression of MACC1. Through HTS, we found a small molecule inhibitor of MACC1 expression. On this basis, we continuously narrowed the scope of screening, and finally found several derivatives of Drug 22 that inhibit the expression of MACC1. During this screening process, we identified effective substructures, which are essential for the transcriptional inhibition of MACC1. Some of these Drug 22 derivatives showed high activity, therefore, they indicate the direction of further structural modifications for improved efficacy. In conclusion, Drug 22 and derivatives thereof provide new options for the selective anti-metastatic treatment of tumor patients in the future.

4. Discussion

The occurrence and development of cancer is a very complicated process. Although people have been continuously deepening their research on cancer in the past few decades, trying to find new effective treatments, the current treatment effects for cancer are still unsatisfactory. Among them, the mortality caused by CRC is the second highest among all cancers, and has become one of the main causes of cancer-related death in the world [2]. Conventional treatment methods such as surgery, chemotherapy, and radiotherapy have a better effect on early CRC, but the treatment effect is poor for advanced patients with metastasis. For example, the five-year survival rate of early local tumor patients is 90%, but when the regional lymph nodes or even distant metastases are formed, the five-year survival rate drops to 10%. Therefore, the metastatic transmission of primary colon cancer accounts for 90% of all colon cancer deaths, which makes the formation of metastasis a key process in the treatment of CRC [7].

In 2009, our lab discovered MACC1. The gene can be used as a biomarker for a variety of solid tumors and plays a key role in tumor progression and metastasis [62]. In a large number of follow-up studies, it has been confirmed that tumor progression and metastasis of more than 20 solid tumors is related to this gene [86]. Therefore, the finding of a transcription inhibitor that inhibits the expression of this gene has become a new treatment for CRC. Previously, we found the MACC1 transcription inhibitors statins and rottlerin in our lab, and conducted in vivo experiments with good results [60]. This highlights the key role of MACC1 in the metastasis of CRC and the necessity to find inhibitors to inhibit the expression of this gene.

Therefore, through HTS screening, we discovered new compounds that inhibit the expression of MACC1, and verified the effect of the inhibitors through experiments in vitro and in vivo. These compounds that inhibit the expression of MACC1 will provide a new treatment for patients with advanced CRC.

4.1 HTS identifies novel compounds as MACC1 inhibitors

The screening of inhibitors is a very complicated and long process. However, with the development of cell biology, as well as computer and automatic control technology, HTS, with the advantages of accuracy, rapidity and high efficiency, has become the main method in the process of inhibitor screening [110–112]. HTS is designed according to the target and hypothesis, which can identify the desired ideal compounds from the large compound library in a short time, so HTS can be applied to a wide range of biological problems. However, it must be noted that screening is only the beginning of the drug discovery and development process. Generally, HTS cannot evaluate all the properties of compounds required for final drug discovery, so further validation and modification of the selected compounds are required [117].

We previously described the key role that MACC1 plays in the process of tumor metastasis. Therefore, the discovery of novel compounds that can inhibit the expression of MACC1 has become a promising new treatment method to inhibit tumor metastasis. In order to identify compounds targeting the MACC1 gene, more than 118,500 compounds from the academic library of EMBL were screened using HCT116 cells stably transfected with MACC1 promoter-luciferase constructs [60]. Then, the most promising compounds were identified by evaluating cytotoxicity. Among these 118,500 compounds, 66 compounds were selected as potential candidates, and further verified by qRT-PCR. Finally, Drug 22 was found. Through the analysis of the chemical structure of different parts of Drug 22, the effective functional groups were finally determined. Combined with the comprehensive analysis of IC_{50} and EC_{50} results, four highly active compounds were found from 76 derivatives of drug 22, including drug 22-7, drug 22-8, drug 22-10 and drug 22-13. The effectiveness of these four highly active drugs in inhibiting MACC1 expression was further verified by in vitro and in vivo experiments.

4.2 Identifying effective substructure groups and the highly active derivative compounds

Through HTS, we found that Drug 22 has an inhibitory effect on the expression of MACC1, but combined with EC_{50} and IC_{50} analysis, we found that Drug 22 is too toxic for in vitro experiments. Therefore, we wanted to find suitable small molecule compounds from its derivatives and analyze them for effective chemical substructures.

This required the constant comparison of the structure and effectiveness of different derivatives of Drug 22 to determine the trend of the relationship between structure and activity, and to screen out effective drug substructures through experimental verification [117].

First of all, we selected 8 derivatives with similar main substructures from Drug 22: Drug 22-2 to Drug 22-9. These eight derivatives all have the substructure of R1+R2. Further verification by qRT-PCR showed that the four derivatives of Drug 22-5, Drug 22-7, Drug 22-8 and Drug 22-9 inhibited the expression of MACC1 in HCT116 and SW620 - two different CRC cell lines - while the other four did not. Through MTT assay, it was found that the IC_{50} of these eight derivatives was different because of the different structures apart from the R1+R2 substructure. Among them, the IC_{50} of Drug 22-7 and Drug 22-8 was the largest, indicating that the toxicity was the lowest, which was 18.11 μM and 21.34 μM in the HCT116 cell line and 21.49 μM and 17.87 μM in the SW620 cell line, respectively. Combined with EC_{50} and IC_{50} analysis, it was concluded that among the four derivatives which had an inhibitory effect on MACC1 expression, Drug 22-7 and Drug 22-8 had relatively better effects. Therefore, we verified the effect of two derivatives of Drug 22-7 and Drug 22-8 at the protein level by WB. It was found that MACC1 at the protein level in these two cell lines could also be inhibited. This indicates that the part outside the main substructure of R1 + R2 can affect the effectiveness and toxicity of the whole compound.

Based on the idea of screening the chemical substructure of derivatives from Drug 22, we wanted to verify which part of these two substructures R1 and R2 is really effective. We also selected three derivatives containing the same part of R2 as Drug 22, namely Drug 22-19, Drug 22-20 and Drug 22-22. It was found through qRT-PCR that these three derivatives had no inhibitory effect on the expression of MACC1 in HCT116 and SW620 CRC cell lines, that is, the substructure R2 part had no inhibitory effect on the expression of MACC1. Therefore, R1 may be an effective substructure that works.

In order to verify the substructure inhibitory effect of R1 on MACC1 expression, we selected nine Drug 22 derivatives: Drug 22-10 to Drug 22-18. Four of these nine derivatives contain R1 substructure, namely Drug 22-10, Drug 22-13, Drug 22-15 and Drug 22-17. The other five derivatives replace the sulfoether on R1 with an amine linker (even just replacing a sulfoether linkage from R1 to an amine linker R3 will affect the

inhibition of MACC1 expression), which we named R3. The results of qRT-PCR showed that all of the nine derivatives with R1 substructure could inhibit MACC1 expression in HCT116 and SW620 CRC cell lines, while the other five derivatives with R3 substructure could not. This fully demonstrates the effectiveness of the R1 substructure. By MTT assay, among these four effective derivatives, Drug 22-10 and Drug 22-13 had the lowest toxicity, which was 22.08 μM and 24.42 μM in the HCT116 cell line and 36.50 μM and 31.10 μM in the SW620 cell line, respectively. Combined with EC_{50} and IC_{50} analysis, it was concluded that among these four derivatives with the inhibitory effect on MACC1 expression, the effects of Drug 22-10 and Drug 22-13 were relatively better. Therefore, we verified the effect of two derivatives of Drug 22-10 and Drug 22-13 at the protein level by WB. It was found that MACC1 protein expression in HCT116 and SW620 cell lines was also inhibited.

In order to clarify the inhibitory effect of the integrity of R1 substructure on MACC1 expression, we screened another eight derivatives, referred to as Drug 22-21, and Drug 22-23 to Drug 22-29, respectively. Among these eight derivatives, four of them changed the substructure of R1, which were Drug 22-25, Drug 22-26, Drug 22-27 and Drug 22-28. They have one nitrogen less than R1, which we named R4. The results of qRT-PCR showed that Drug 22-21, Drug 22-23 and Drug 22-24 with R1 substructure had an inhibitory effect on the expression of MACC1, while Drug 22-27 and Drug 22-28 did not inhibit the expression of MACC1. Drug 22-29 contains an R1 substructure, but it had no inhibitory effect on the expression of MACC1. This may be due to the structure groups other than the R1 substructure affecting its function, which is also consistent with our analysis above. The two derivatives of Drug 22-25 and Drug 22-26 also inhibited the expression of MACC1 by replacing one nitrogen on R1 with a bulky trifluoromethyl group in the chemical structure.

To verify the effectiveness of this replacement, we cooperated with Medchem to select another 48 derivatives of Drug 22 (see table 7 and the Appendix table for details), 39 of which have R4 substructures. Only 9 of these 39 derivatives were able to inhibit the expression of MACC1. Here, we listed 7 representative derivatives for analysis, namely Drug 22-32, Drug 22-37, Drug 22-40, Drug 22-57, Drug 22-63, Drug 22-67 and Drug 22-69. Among the seven derivatives, four derivatives containing R4 and a bulk trifluoromethyl group substructure, which were drug 22-40, drug 22-57, drug 22-63 and

drug 22-67, had inhibitory effects on the expression of MACC1. Drug 22-37 and Drug 22-69, containing the R4 structure but replacing the bulky trifluoromethyl group with other groups, had no effect. Drug 22-32, containing R4 and the bulky trifluoromethyl group, also had no inhibitory effect. Only 9 of the 39 derivatives had an inhibitory effect on the expression of MACC1, which accounted for a very small proportion. This indicated that after R4 destroyed the substructural integrity of R1, it reduced the inhibitory effect of derivatives on MACC1 expression. At the same time, when replacing the nitrogen on R1 with other groups, although a small amount of the combination of R4 and the bulky trifluoromethyl group was effective, most of this and other combinations were ineffective. This means that only a few substitution groups can be effective after destroying the R1 substructure, which makes it clear that the integrity of the R1 substructure is very important for inhibiting the expression of MACC1.

Through the above analysis of the substructure of Drug 22 derivatives, we found that the R1 structure is the main functional substructure to inhibit MACC1 expression, and that destroying the integrity of the R1 substructure will weaken or cause the inhibitory effect of the compound on MACC1 expression to be lost. At the same time, it also reminds us that modifying R1 with other groups can reduce toxicity or increase effectiveness.

By analyzing the EC_{50} and IC_{50} of all the derivatives, we found four highly active drugs: Drug 22-7, Drug 22-8, Drug 22-10 and Drug 22-13. These four highly active drugs not only inhibit the expression of MACC1 mRNA but also inhibit the expression of MACC1 protein. On this basis, we further verified these four highly active drugs in vitro and in vivo. However, these four highly active drugs are merely the best drugs found to date, and there is still much room for improvement in efficacy and toxicity. At present, we are cooperating with the Leibniz-Forschungsinstitut für Molekulare Pharmakologie (FMP) to screen out the most effective inhibitor for MACC1 expression by modifying the drug structure.

4.3 Novel compounds inhibit MACC1-associated migration in vitro

Many papers have confirmed that MACC1 plays a key role in the metastasis of various tumors. MACC1 can promote the invasion and migration of tumor cells through the HGF/c-MET, WINT/β-catenin, PI3K/AKT/ERK and SPON2 pathways. By reducing the

expression of MACC1, it can significantly reduce tumor cell metastasis [62,100,101,116,117]. MACC1 promotes tumor cell proliferation and migration to distant organs to form new tumor cell colonies, which is also inseparable from the process of EMT-MET [86]. Therefore, it is very important to interfere with tumor metastasis by targeting MACC1. We have screened out four highly active MACC1 expression inhibitors by comparing the chemical structure of the drugs, using qRT-PCR, WB and MTT assays. Then through the transwell migration assay, it was found that in the effective concentration range lower than IC_{50}, Drug 22-7, Drug 22-8, Drug 22-10 and Drug 22-13 can significantly inhibit the migration of HCT116 cells. In the wound-healing assay, it was observable that treating the cells with these four different highly active derivatives can inhibit the migration properties of HCT116 cells in the confluent monolayer of cells at two different time points, 24 h and 48 h, and the effect of 24 h is better than 48 h. This shows that CRC cells treated with these four highly active drugs can reduce cell migration and colony formation by reducing the expression of MACC1.

Previously, our lab discovered for the first time that statins and rottlerin can be used as MACC1 inhibitors, and statins have achieved good results as drugs that have been used in clinical practice [60,118]. In contrast, the newly discovered inhibitors are less effective in inhibiting cell migration. This proves the necessity of further optimizing the drug structure to improve the efficacy and safety of the drug. Although the specific mechanism of these new drugs acting on MACC1 is still unclear, as novel MACC1 inhibitors, they also provide new expectations for our anti-cancer therapy. Therefore, we decided to choose two of these four drugs: Drug 22-10 and Drug 22-13 for the first in vivo study to evaluate their effectiveness as MACC1 inhibitors, thereby evaluating their role as inhibitors of CRC progression. It has provided pre-clinical data to provide a basis for clinical studies as a treatment method for human CRC.

4.4 Novel compounds inhibit MACC1-driven metastasis in vivo

As previously shown, we wanted to use three MACC1 expression inhibitors, Drug 22, Drug 22-10 and Drug 22-13 for in vivo experiments. However, Drug 22 was the most toxic compound in vitro experiments. Therefore, we used Drug 22 for MTD experiments. MTD studies are used to determine the highest dose at which a compound can be administered without side effects or overt toxicity [119]. The MTD results showed that the body weight of mice was reduced by 3%, 3%, 4% and 5% after 20 days of treatment

with four different doses of 25 mg/kg, 50 mg/kg, 100 mg/kg and 200 mg/kg, respectively. The drug toxicity was within the tolerance range of mice. Finally, a dose of 50 mg/kg was selected for the bioluminescence experiment in the SCID mouse model.

Mouse models have been essential in advancing our understanding of the biological processes that drive tumor progression. Since xenografts involve the implantation of human tumor cells into mice, in order to prevent host rejection, human tissues must be introduced into immunocompromised mice or immune-deficient mice. One advantage of these tumor models is that the donor cells originated from humans. The disadvantage is the lack of the host adaptive immune system and the microenvironment for human tumor growth. However, they can reflect the potential clinical activity of the drug according to the different effects of the drug treatment between the primary lesion and the metastatic lesion, thereby reflecting the clinical situation [120,121]. Therefore, tumor xenografts in immune-deficient mice are recognized animal models for human cancer research.

The metastasis cascade of the original tumor is very complex, as we mentioned in the previous introduction. The disadvantages of simulating the whole metastasis cascade in orthotopic xenograft mice are obvious. First of all, metastasis formation takes a long time and can not guarantee the success of the surgery. Secondly, in successful transplanted mice, most of the tumors metastasize to the lymph nodes and peritoneum, and rarely to the liver. Furthermore, in most cases, the tumor burden can lead to death before liver metastasis is visible [122,123]. The unfavoured organ tropism can be solved by transplanting tumor cells directly into the spleen. The spleen has an abundant blood supply and fast blood circulation, which can make tumor cells enter the blood circulation quickly and avoid the metastasis process in tissues and lymph nodes. Therefore, the intrasplenic metastasis model partially represents the process of metastasis formation, which can produce liver metastases derived from the spleen [124].

In this study, we used the SCID mouse model to transplant HCT116-CMVp-Luc cells into the spleen to evaluate the potential of novel MACC1 inhibitors to prevent tumor progression and metastasis caused by MACC1. These cells can stably express luciferase. Tumor progression was monitored by using non-invasive bioluminescence imaging to track the progression of human CRC induced by MACC1 in vivo. Compared with magnetic resonance imaging, computed tomography and other methods, this non-

invasive bioluminescence imaging system has the advantages of easy application and high sensitivity [125].

By detecting the fluorescence signal, it was found that in the primary tumor of the spleen, the fluorescence signal intensity of the drug-treated groups was significantly lower than that of the control group, especially for the mice treated with Drug 22-10, and the treatment effect was better than that of the drug 22 and Drug 22-13 groups. Then, through the detection of MACC1 mRNA expression in the primary tumor, it was found that Drug 22-10 and Drug 22-13 treated groups decreased it by 58.2% and 54.2%, respectively. The MACC1 mRNA expression of the mice treated with Drug 22 was decreased, albeit it had no biological significance. This was also consistent with the fluorescence signal intensity and the primary tumor growth curve drawn by continuous detection of the fluorescence signal expression. Through fluorescence detection of the liver, it was found that the fluorescence signals of the three groups treated with novel drugs were significantly lower than those of the control group, especially the group treated with Drug 22-10, and only weak fluorescence signals appeared in the isolated liver. By detecting the human satellite DNA and MACC1 mRNA expression in isolated liver, we found that Drug 22-10 and Drug 22-13 have biological significance in inhibiting tumor metastasis. In the detection of human satellite DNA, it was reduced by 75% and 70%, respectively, and the expression of MACC1 mRNA was reduced by 78% and 39%. Although Drug 22 inhibited the mRNA expression of MACC1 to some extent, it had no biological significance. This conclusion is also consistent with the results we got from in vitro experiments.

CK19 is a tumor biomarker which exists in a variety of normal epithelial tissues. When epithelial cells transform into tumors, their expression increases. Many studies have shown that the expression of CK19 is positively correlated with the development and prognosis of liver cancer [126–128]. CK19 does not stain normal mouse liver cells but has specific staining for bile duct epithelium and liver cancer cells. Therefore, we performed immunohistochemical staining to investigate the expression of CK19 at the protein level on liver tissue sections. Compared with the control group, the area of metastases in the Drug 22 treatment group was reduced. The metastases in the Drug 22-10 and Drug 22-13 treatment groups were significantly smaller than the control group, and necrosis occurred in the metastases. In particular, in the group treated with Drug 22-10, not only was the necrotic area inside the metastasis larger, but the edge of

the metastasis was not as dense as in other groups. This indicates that these inhibitors can also inhibit the formation of tumor metastasis at the protein level.

The experiments with these drugs in vitro and in vivo have proved that these novelly discovered MACC1 expression inhibitors can not only inhibit MACC1 expression in vitro, but also can better inhibit the metastasis caused by MACC1 in vivo.

4.5 Small molecule inhibitors of MACC1 can be used as potential drugs for the treatment of CRC

Small molecules refer to organic compounds that can regulate biological processes, and their molecular weight is usually less than 800 Daltons. This characteristic determines that the small molecule compound has good spatial dispersion, can easily pass through the cell membrane, and can enter the cytoplasm to bind to the corresponding target, block its upstream or downstream signal pathway conduction, and achieve the purpose of the treatment. Such good drug-forming properties make small molecule compounds show great advantages in the screening process of inhibitors [129,130].

Traditional “cytotoxic drugs” such as cisplatin, 5-FU and other drugs mainly act on the cell division and proliferation stage. These drugs widely act on various types of cells in the body and are prone to severe side effects due to their lack of specificity. In contrast, small molecule targeted therapy can overcome this problem well. Targeted therapy is based on the molecular biology of the tumor, which can prevent the growth of cancer cells by interfering with the specific targeted molecules required by cancer transformation and tumor growth [131]. These kinds of drugs have strong specificity and cause little damage to normal cells, so the side effects of treatment are also small and have good application prospects.

MACC1 is a tumor biomarker discovered by our lab in 2009. It plays a key role in tumor progression and metastasis and has been confirmed in more than 20 solid tumors. As mentioned in our previous introduction, tumor metastasis is the main cause of death. Our newly discovered small molecule targeted drugs have been proved to be effective in *in vitro* and *in vivo* experiments. Therefore, these small molecule drugs targeting MACC1 can effectively inhibit tumor metastasis. This may provide a new treatment option for CRC patients in the future.

5. Conclusion & Outlook

MACC1 has been confirmed to be closely related to the development and metastasis of a variety of solid tumors. In this study, through HTS, we discovered Drug 22, a novel transcription inhibitor of MACC1. Because of its toxicity in *in vitro* experiments, we searched for effective inhibitors from a large number of its derivatives, and finally found four highly effective derivatives. During the screening process, the core chemical structure that played an effective role was gradually discovered, and it was realized that the parts separate to the core chemical structure can affect the effectiveness, solubility and toxicity of the whole drug. This idea has laid a foundation for our future drug structure modification. Finally, we further verified the inhibitory effect of these drugs on MACC1 expression in vivo through animal experiments. These results indicate that these drugs have the potential to act as inhibitors of CRC progression by inhibiting the transcription of MACC1.

The process of drug development is long and complicated, and it is still in the initial screening stage for this study. It is necessary to collect data through continuous screening, designing and experimenting of drug structure. Then, the toxicity, solubility and efficacy of the drug should be evaluated comprehensively to determine whether it can become the most ideal drug. After the determination of the most ideal drug, it is necessary to conduct more in-depth research on its molecular mechanism and pharmacokinetics, such as which pathway of signal transduction it acts on and organs of drug metabolism, etc. We need to get more preclinical data to lay the foundation for future clinical trials based on the high expression of MACC1 in CRC patients.

Although this research still has a long way to go, we have anyway taken a crucial first step anyway. This step fully demonstrates the value of these drugs in inhibiting tumor metastasis. This targeted therapy based on MACC1 can provide more options for the future anti-cancer treatment of CRC patients.

Appendix table:

Forty eight inactive drugs

Compound	Structure	Compound	Structure
Drug 22-2	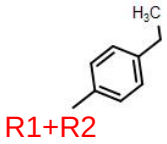	Drug 22-16	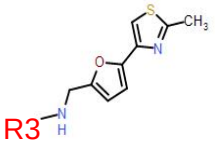
Drug 22-3	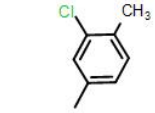	Drug 22-17	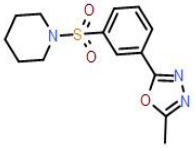
Drug 22-4	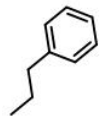	Drug 22-18	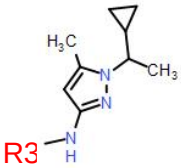
Drug 22-6	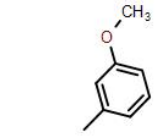	Drug 22-19	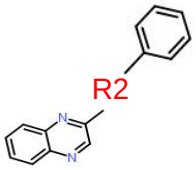
Drug 22-11	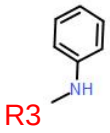	Drug 22-20	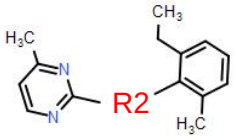
Drug 22-12	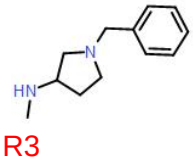	Drug 22-22	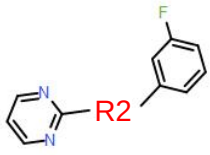
Drug 22-14	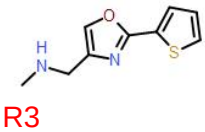	Drug 22-27	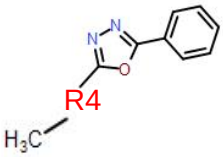
Drug 22-15	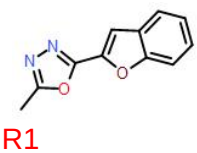	Drug 22-28	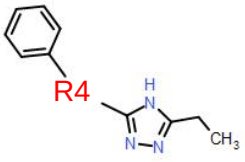

Compound	Structure	Compound	Structure
Drug 22-31	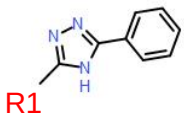	Drug 22-41	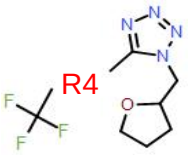
Drug 22-32	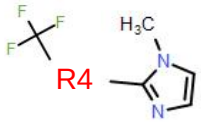	Drug 22-43	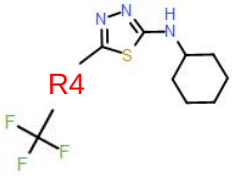
Drug 22-33	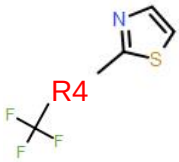	Drug 22-44	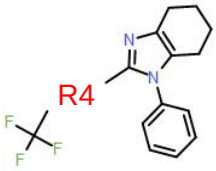
Drug 22-34	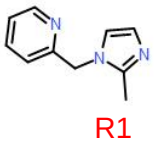	Drug 22-45	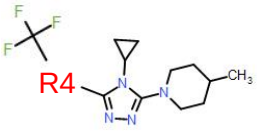
Drug 22-35	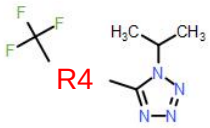	Drug 22-46	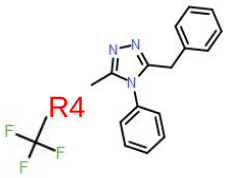
Drug 22-36	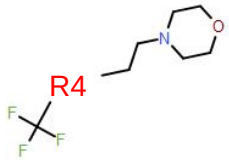	Drug 22-49	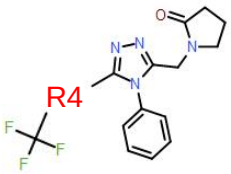
Drug 22-37	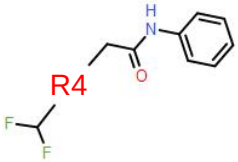	Drug 22-50	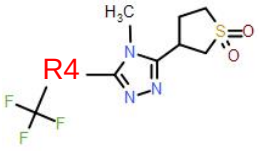
Drug 22-39	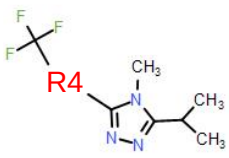	Drug 22-51	

Compound	Structure	Compound	Structure
Drug 22-53		Drug 22-62	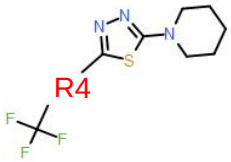
Drug 22-54	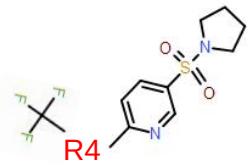	Drug 22-64	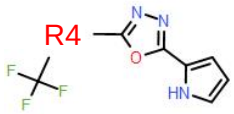
Drug 22-55	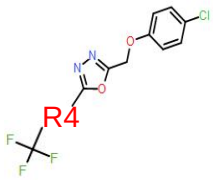	Drug 22-65	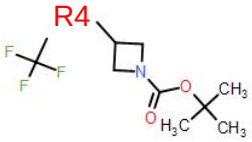
Drug 22-56	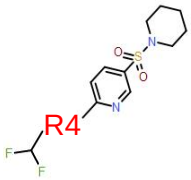	Drug 22-68	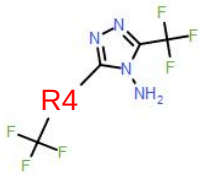
Drug 22-58	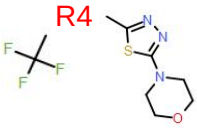	Drug 22-69	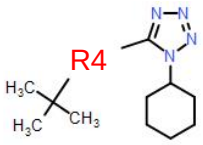
Drug 22-59	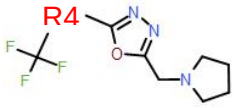	Drug 22-70	
Drug 22-60	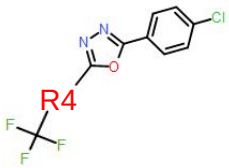	Drug 22-71	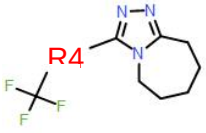
Drug 22-61	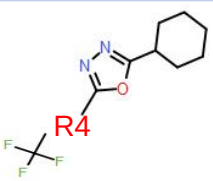	Drug 22-73	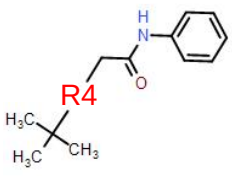

References

(1) Brenner, H.; Kloor, M.; Pox, C. P. Colorectal Cancer. *The Lancet* **2014**, *383* (9927), 1490–1502. https://doi.org/10.1016/S0140-6736(13)61649-9.

(2) Sankaranarayanan, R. Cancer Survival in Africa, Asia, the Caribbean and Central America. Introduction. *IARC Sci. Publ.* **2011**, No. 162, 1–5.

(3) Cancer survival in five continents: a worldwide population-based study (CONCORD) - ScienceDirect https://www.sciencedirect.com/science/article/pii/S1470204508701797?via%3Dihub (accessed Jan 14, 2020).

(4) BW, S.; CP, W. *World Cancer Report 2014*.

(5) Torre, L. A.; Siegel, R. L.; Ward, E. M.; Jemal, A. Global Cancer Incidence and Mortality Rates and Trends—An Update. *Cancer Epidemiol. Prev. Biomark.* **2016**, *25* (1), 16–27. https://doi.org/10.1158/1055-9965.EPI-15-0578.

(6) Survival from colorectal cancer in Germany in the early 21st century | British Journal of Cancer https://www.nature.com/articles/bjc2012189 (accessed Jan 14, 2020).

(7) Stein U; Schlag PM. Clinical, biological, and molecular aspects of metastasis in colorectal cancer Recent Results Cancer Res (accessed Jan 14, 2020).

(8) Worthley, D. L.; Whitehall, V. L.; Spring, K. J.; Leggett, B. A. Colorectal Carcinogenesis: Road Maps to Cancer. *World J. Gastroenterol.* **2007**, *13* (28), 3784–3791. https://doi.org/10.3748/wjg.v13.i28.3784.

(9) Murphy, K. M.; Zhang, S.; Geiger, T.; Hafez, M. J.; Bacher, J.; Berg, K. D.; Eshleman, J. R. Comparison of the Microsatellite Instability Analysis System and the Bethesda Panel for the Determination of Microsatellite Instability in Colorectal Cancers. *J. Mol. Diagn.* **2006**, *8* (3), 305–311. https://doi.org/10.2353/jmoldx.2006.050092.

(10) Wolff, R. K.; Hoffman, M. D.; Wolff, E. C.; Herrick, J. S.; Sakoda, L. C.; Samowitz, W. S.; Slattery, M. L. Mutation Analysis of Adenomas and Carcinomas of the Colon: Early and Late Drivers. *Genes. Chromosomes Cancer* **2018**, *57* (7), 366–376. https://doi.org/10.1002/gcc.22539.

(11) Cunningham, J. M.; Christensen, E. R.; Tester, D. J.; Kim, C.-Y.; Roche, P. C.; Burgart, L. J.; Thibodeau, S. N. Hypermethylation of the HMLH1 Promoter in Colon Cancer with Microsatellite Instability. *Cancer Res.* **1998**, *58* (15), 3455–3460.

(12) De Palma, F. D. E.; D'Argenio, V.; Pol, J.; Kroemer, G.; Maiuri, M. C.; Salvatore, F. The Molecular Hallmarks of the Serrated Pathway in Colorectal Cancer. *Cancers* **2019**, *11* (7), 1017. https://doi.org/10.3390/cancers11071017.

(13) Leslie, A.; Carey, F. A.; Pratt, N. R.; Steele, R. J. C. The Colorectal Adenoma–Carcinoma Sequence. *BJS Br. J. Surg.* **2002**, *89* (7), 845–860. https://doi.org/10.1046/j.1365-2168.2002.02120.x.

(14) Wu, Z.; Liu, Z.; Ge, W.; Shou, J.; You, L.; Pan, H.; Han, W. Analysis of Potential Genes and Pathways Associated with the Colorectal Normal Mucosa–Adenoma–Carcinoma Sequence. *Cancer Med.* **2018**, *7* (6), 2555–2566. https://doi.org/10.1002/cam4.1484.

(15) Thiruvengadam, S.; O'Malley, M.; LaGuardia, L.; Lopez, R.; Wang, Z.; Shadrach, B.; Chen, Y.; Li, C.; Veigl, M.; Barnholtz-Sloan, J.; Pai, R.; Church, J.; Kalady, M.; Walsh, R.; Burke, C. Gene Expression Changes Accompanying the Duodenal Adenoma-Carcinoma Sequence in Familial Adenomatous Polyposis. *Clin. Transl. Gastroenterol.* **2019**, *10* (6). https://doi.org/10.14309/ctg.0000000000000053.

(16) Norollahi, S. E.; Hamidian, S. M. T.; Kohpar, Z. K.; Azadi, R.; Rostami, P.; Vahidi, S.; Ghazanfari, S.; Shabe, F. A.; Khaksar, R.; Samadani, A. A. The Fluctuation of APC Gene in WNT Signaling with Adenine Deletion of Adenomatous Polyposis Coli, Is Associated in Colorectal Cancer. *J. Coloproctology* **2019**. https://doi.org/10.1016/j.jcol.2019.11.487.

(17) Lesko, A. C.; Goss, K. H.; Yang, F. F.; Schwertner, A.; Hulur, I.; Onel, K.; Prosperi, J. R. The APC Tumor Suppressor Is Required for Epithelial Cell Polarization and Three-Dimensional Morphogenesis. *Biochim. Biophys. Acta* **2015**, *1854* (3), 711–723. https://doi.org/10.1016/j.bbamcr.2014.12.036.

(18) Tanaka, N.; Mashima, T.; Mizutani, A.; Sato, A.; Aoyama, A.; Gong, B.; Yoshida, H.; Muramatsu, Y.; Nakata, K.; Matsuura, M.; Katayama, R.; Nagayama, S.; Fujita, N.; Sugimoto, Y.; Seimiya, H. APC Mutations as a Potential Biomarker for Sensitivity to Tankyrase Inhibitors in Colorectal Cancer. *Mol. Cancer Ther.* **2017**, *16* (4), 752–762. https://doi.org/10.1158/1535-7163.MCT-16-0578.
(19) Sawa, M.; Masuda, M.; Yamada, T. Targeting the Wnt Signaling Pathway in Colorectal Cancer. *Expert Opin. Ther. Targets* **2016**, *20* (4), 419–429. https://doi.org/10.1517/14728222.2016.1098619.
(20) Aghabozorgi, A. S.; Bahreyni, A.; Soleimani, A.; Bahrami, A.; Khazaei, M.; Ferns, G. A.; Avan, A.; Hassanian, S. M. Role of Adenomatous Polyposis Coli (APC) Gene Mutations in the Pathogenesis of Colorectal Cancer; Current Status and Perspectives. *Biochimie* **2019**, *157*, 64–71. https://doi.org/10.1016/j.biochi.2018.11.003.
(21) Jass, J. R.; Whitehall, V. L. J.; Young, J.; Leggett, B. A. Emerging Concepts in Colorectal Neoplasia. *Gastroenterology* **2002**, *123* (3), 862–876. https://doi.org/10.1053/gast.2002.35392.
(22) Green, R. A.; Wollman, R.; Kaplan, K. B. APC and EB1 Function Together in Mitosis to Regulate Spindle Dynamics and Chromosome Alignment. *Mol. Biol. Cell* **2005**, *16* (10), 4609–4622. https://doi.org/10.1091/mbc.e05-03-0259.
(23) Wen, Y.; Eng, C. H.; Schmoranzer, J.; Cabrera-Poch, N.; Morris, E. J. S.; Chen, M.; Wallar, B. J.; Alberts, A. S.; Gundersen, G. G. EB1 and APC Bind to MDia to Stabilize Microtubules Downstream of Rho and Promote Cell Migration. *Nat. Cell Biol.* **2004**, *6* (9), 820–830. https://doi.org/10.1038/ncb1160.
(24) Barth, A. I. M.; Siemers, K. A.; Nelson, W. J. Dissecting Interactions between EB1, Microtubules and APC in Cortical Clusters at the Plasma Membrane. *J. Cell Sci.* **2002**, *115* (8), 1583–1590.
(25) Tsuchida, N.; Ohtsubo, E.; Ryder, T. Nucleotide Sequence of the Oncogene Encoding the P21 Transforming Protein of Kirsten Murine Sarcoma Virus. *Science* **1982**, *217* (4563), 937–939. https://doi.org/10.1126/science.6287573.
(26) Haigis, K. M.; Kendall, K. R.; Wang, Y.; Cheung, A.; Haigis, M. C.; Glickman, J. N.; Niwa-Kawakita, M.; Sweet-Cordero, A.; Sebolt-Leopold, J.; Shannon, K. M.; Settleman, J.; Giovannini, M.; Jacks, T. Differential Effects of Oncogenic K-Ras and N-Ras on Proliferation, Differentiation and Tumor Progression in the Colon. *Nat. Genet.* **2008**, *40* (5), 600–608. https://doi.org/10.1038/ng.115.
(27) Corcoran, R. B.; André, T.; Atreya, C. E.; Schellens, J. H. M.; Yoshino, T.; Bendell, J. C.; Hollebecque, A.; McRee, A. J.; Siena, S.; Middleton, G.; Muro, K.; Gordon, M. S.; Tabernero, J.; Yaeger, R.; O'Dwyer, P. J.; Humblet, Y.; Vos, F. D.; Jung, A. S.; Brase, J. C.; Jaeger, S.; Bettinger, S.; Mookerjee, B.; Rangwala, F.; Cutsem, E. V. Combined BRAF, EGFR, and MEK Inhibition in Patients with BRAFV600E-Mutant Colorectal Cancer. *Cancer Discov.* **2018**, *8* (4), 428–443. https://doi.org/10.1158/2159-8290.CD-17-1226.
(28) Porru, M.; Pompili, L.; Caruso, C.; Biroccio, A.; Leonetti, C. Targeting KRAS in Metastatic Colorectal Cancer: Current Strategies and Emerging Opportunities. *J. Exp. Clin. Cancer Res.* **2018**, *37* (1), 1–10. https://doi.org/10.1186/s13046-018-0719-1.
(29) Lundberg, I. V.; Wikberg, M. L.; Ljuslinder, I.; Li, X.; Myte, R.; Zingmark, C.; Löfgren-Burström, A.; Edin, S.; Palmqvist, R. MicroRNA Expression in KRAS- and BRAF-Mutated Colorectal Cancers. *Anticancer Res.* **2018**, *38* (2), 677–683.
(30) Bos, J. L.; Fearon, E. R.; Hamilton, S. R.; Vries, M. V.; van Boom, J. H.; van der Eb, A. J.; Vogelstein, B. Prevalence of Ras Gene Mutations in Human Colorectal Cancers. *Nature* **1987**, *327* (6120), 293–297. https://doi.org/10.1038/327293a0.
(31) Kim, B. J.; Jang, H. J.; Kim, J. H.; Kim, H. S.; Lee, J. KRAS Mutation as a Prognostic Factor in Ampullary Adenocarcinoma: A Meta-Analysis and Review. *Oncotarget* **2016**, *7* (36), 58001–58006. https://doi.org/10.18632/oncotarget.11156.
(32) Cox, A. D.; Fesik, S. W.; Kimmelman, A. C.; Luo, J.; Der, C. J. Drugging the Undruggable RAS: Mission Possible? *Nat. Rev. Drug Discov.* **2014**, *13* (11), 828–851. https://doi.org/10.1038/nrd4389.
(33) Caputo, F.; Santini, C.; Bardasi, C.; Cerma, K.; Casadei-Gardini, A.; Spallanzani, A.; Andrikou, K.; Cascinu, S.; Gelsomino, F. BRAF-Mutated Colorectal Cancer: Clinical and Molecular Insights. *Int. J. Mol. Sci.* **2019**, *20* (21), 5369. https://doi.org/10.3390/ijms20215369.

(34) Maraka, S.; Janku, F. BRAF Alterations in Primary Brain Tumors. *Discov. Med.* **2018**, *26* (141), 51–60.
(35) Cohen, R.; Cervera, P.; Svrcek, M.; Pellat, A.; Dreyer, C.; de Gramont, A.; André, T. BRAF-Mutated Colorectal Cancer: What Is the Optimal Strategy for Treatment? *Curr. Treat. Options Oncol.* **2017**, *18* (2), 9. https://doi.org/10.1007/s11864-017-0453-5.
(36) Rajagopalan, H.; Jallepalli, P. V.; Rago, C.; Velculescu, V. E.; Kinzler, K. W.; Vogelstein, B.; Lengauer, C. Inactivation of HCDC4 Can Cause Chromosomal Instability. *Nature* **2004**, *428* (6978), 77–81. https://doi.org/10.1038/nature02313.
(37) Reed, S. E.; Spruck, C. H.; Sangfelt, O.; Drogen, F. van; Mueller-Holzner, E.; Widschwendter, M.; Zetterberg, A.; Reed, S. I. Mutation of HCDC4 Leads to Cell Cycle Deregulation of Cyclin E in Cancer. *Cancer Res.* **2004**, *64* (3), 795–800. https://doi.org/10.1158/0008-5472.CAN-03-3417.
(38) Kemp, Z.; Rowan, A.; Chambers, W.; Wortham, N.; Halford, S.; Sieber, O.; Mortensen, N.; Herbay, A. von; Gunther, T.; Ilyas, M.; Tomlinson, I. CDC4 Mutations Occur in a Subset of Colorectal Cancers but Are Not Predicted to Cause Loss of Function and Are Not Associated with Chromosomal Instability. *Cancer Res.* **2005**, *65* (24), 11361–11366. https://doi.org/10.1158/0008-5472.CAN-05-2565.
(39) SMAD4 SMAD family member 4 [Homo sapiens (human)] - Gene - NCBI https://www.ncbi.nlm.nih.gov/gene/4089 (accessed Feb 3, 2020).
(40) Itatani, Y.; Kawada, K.; Sakai, Y. Transforming Growth Factor-β Signaling Pathway in Colorectal Cancer and Its Tumor Microenvironment. *Int. J. Mol. Sci.* **2019**, *20* (23). https://doi.org/10.3390/ijms20235822.
(41) Zhao, M.; Mishra, L.; Deng, C.-X. The Role of TGF-β/SMAD4 Signaling in Cancer. *Int. J. Biol. Sci.* **2018**, *14* (2), 111–123. https://doi.org/10.7150/ijbs.23230.
(42) Siraj, A. K.; Pratheeshkumar, P.; Divya, S. P.; Parvathareddy, S. K.; Bu, R.; Masoodi, T.; Kong, Y.; Thangavel, S.; Al-Sanea, N.; Ashari, L. H.; Abduljabbar, A.; Al-Homoud, S.; Al-Dayel, F.; Al-Kuraya, K. S. TGFβ-Induced SMAD4-Dependent Apoptosis Proceeded by EMT in CRC. *Mol. Cancer Ther.* **2019**, *18* (7), 1312–1322. https://doi.org/10.1158/1535-7163.MCT-18-1378.
(43) Reference, G. H. SMAD4 gene https://ghr.nlm.nih.gov/gene/SMAD4 (accessed Feb 3, 2020).
(44) Mills, A. A. P53: Link to the Past, Bridge to the Future. *Genes Dev.* **2005**, *19* (18), 2091–2099. https://doi.org/10.1101/gad.1362905.
(45) Baugh, E. H.; Ke, H.; Levine, A. J.; Bonneau, R. A.; Chan, C. S. Why Are There Hotspot Mutations in the TP53 Gene in Human Cancers? *Cell Death Differ.* **2018**, *25* (1), 154–160. https://doi.org/10.1038/cdd.2017.180.
(46) Teodoro, J. G.; Evans, S. K.; Green, M. R. Inhibition of Tumor Angiogenesis by P53: A New Role for the Guardian of the Genome. *J. Mol. Med.* **2007**, *85* (11), 1175–1186. https://doi.org/10.1007/s00109-007-0221-2.
(47) Assadian, S.; El-Assaad, W.; Wang, X. Q. D.; Gannon, P. O.; Barrès, V.; Latour, M.; Mes-Masson, A.-M.; Saad, F.; Sado, Y.; Dostie, J.; Teodoro, J. G. P53 Inhibits Angiogenesis by Inducing the Production of Arresten. *Cancer Res.* **2012**, *72* (5), 1270–1279. https://doi.org/10.1158/0008-5472.CAN-11-2348.
(48) Ellegren, H. Microsatellites: Simple Sequences with Complex Evolution. *Nat. Rev. Genet.* **2004**, *5* (6), 435–445. https://doi.org/10.1038/nrg1348.
(49) Schlötterer, C.; Harr, B. Microsatellite Instability. In *eLS*; American Cancer Society, 2004. https://doi.org/10.1038/npg.els.0000840.
(50) Hoeijmakers, J. H. J. Genome Maintenance Mechanisms for Preventing Cancer. *Nature* **2001**, *411* (6835), 366–374. https://doi.org/10.1038/35077232.
(51) Larrea, A. A.; Lujan, S. A.; Kunkel, T. A. SnapShot: DNA Mismatch Repair. *Cell* **2010**, *141* (4), 730.e1. https://doi.org/10.1016/j.cell.2010.05.002.
(52) Gupta, R.; Sinha, S.; Paul, R. N. The Impact of Microsatellite Stability Status in Colorectal Cancer. *Curr. Probl. Cancer* **2018**, *42* (6), 548–559. https://doi.org/10.1016/j.currproblcancer.2018.06.010.
(53) Boland, C. R.; Goel, A. Microsatellite Instability in Colorectal Cancer. *Gastroenterology* **2010**, *138* (6), 2073-2087.e3. https://doi.org/10.1053/j.gastro.2009.12.064.

(54) Koopman, M.; Kortman, G. a. M.; Mekenkamp, L.; Ligtenberg, M. J. L.; Hoogerbrugge, N.; Antonini, N. F.; Punt, C. J. A.; van Krieken, J. H. J. M. Deficient Mismatch Repair System in Patients with Sporadic Advanced Colorectal Cancer. *Br. J. Cancer* **2009**, *100* (2), 266–273. https://doi.org/10.1038/sj.bjc.6604867.
(55) Iino, H.; Jass, J. R.; Simms, L. A.; Young, J.; Leggett, B.; Ajioka, Y.; Watanabe, H. DNA Microsatellite Instability in Hyperplastic Polyps, Serrated Adenomas, and Mixed Polyps: A Mild Mutator Pathway for Colorectal Cancer? *J. Clin. Pathol.* **1999**, *52* (1), 5–9. https://doi.org/10.1136/jcp.52.1.5.
(56) Popat, S.; Hubner, R.; Houlston, R. s. Systematic Review of Microsatellite Instability and Colorectal Cancer Prognosis. *J. Clin. Oncol.* **2005**, *23* (3), 609–618. https://doi.org/10.1200/JCO.2005.01.086.
(57) Girotti, M. R.; Salatino, M.; Dalotto-Moreno, T.; Rabinovich, G. A. Sweetening the Hallmarks of Cancer: Galectins as Multifunctional Mediators of Tumor Progression. *J. Exp. Med.* **2020**, *217* (2). https://doi.org/10.1084/jem.20182041.
(58) What is Metastasis? https://www.cancer.net/navigating-cancer-care/cancer-basics/what-metastasis (accessed Feb 6, 2020).
(59) Lin, Y.; Sun, L.; Zeng, F.; Wu, S. An Unsymmetrical Squaraine-Based Activatable Probe for Imaging Lymphatic Metastasis by Responding to Tumor Hypoxia with MSOT and Aggregation-Enhanced Fluorescent Imaging. *Chem. – Eur. J.* **2019**, *25* (72), 16740–16747. https://doi.org/10.1002/chem.201904675.
(60) Juneja, M.; Kobelt, D.; Walther, W.; Voss, C.; Smith, J.; Specker, E.; Neuenschwander, M.; Gohlke, B.-O.; Dahlmann, M.; Radetzki, S.; Preissner, R.; Kries, J. P. von; Schlag, P. M.; Stein, U. Statin and Rottlerin Small-Molecule Inhibitors Restrict Colon Cancer Progression and Metastasis via MACC1. *PLOS Biol.* **2017**, *15* (6), e2000784. https://doi.org/10.1371/journal.pbio.2000784.
(61) Stein, U. MACC1 – a Novel Target for Solid Cancers. *Expert Opin. Ther. Targets* **2013**, *17* (9), 1039–1052. https://doi.org/10.1517/14728222.2013.815727.
(62) Stein, U.; Walther, W.; Arlt, F.; Schwabe, H.; Smith, J.; Fichtner, I.; Birchmeier, W.; Schlag, P. M. MACC1, a Newly Identified Key Regulator of HGF-MET Signaling, Predicts Colon Cancer Metastasis. *Nat. Med.* **2009**, *15* (1), 59–67. https://doi.org/10.1038/nm.1889.
(63) Thiery, J. P.; Sleeman, J. P. Complex Networks Orchestrate Epithelial–Mesenchymal Transitions. *Nat. Rev. Mol. Cell Biol.* **2006**, *7* (2), 131–142. https://doi.org/10.1038/nrm1835.
(64) Hernández-Caballero, M. E. Molecular Mechanisms of Metastasis: Epithelial-Mesenchymal Transition, Anoikis and Loss of Adhesion. *Carcinogenesis* **2013**. https://doi.org/10.5772/55399.
(65) Turner, J. R. Intestinal Mucosal Barrier Function in Health and Disease. *Nat. Rev. Immunol.* **2009**, *9* (11), 799–809. https://doi.org/10.1038/nri2653.
(66) Kalluri, R.; Weinberg, R. A. The Basics of Epithelial-Mesenchymal Transition. *J. Clin. Invest.* **2009**, *119* (6), 1420–1428. https://doi.org/10.1172/JCI39104.
(67) Li, W.; Kidiyoor, A.; Hu, Y.; Guo, C.; Liu, M.; Yao, X.; Zhang, Y.; Peng, B.; Zheng, J. Evaluation of Transforming Growth Factor-B1 Suppress Pokemon/Epithelial–Mesenchymal Transition Expression in Human Bladder Cancer Cells. *Tumor Biol.* **2015**, *36* (2), 1155–1162. https://doi.org/10.1007/s13277-014-2625-2.
(68) Campbell, K. Contribution of Epithelial-Mesenchymal Transitions to Organogenesis and Cancer Metastasis. *Curr. Opin. Cell Biol.* **2018**, *55*, 30–35. https://doi.org/10.1016/j.ceb.2018.06.008.
(69) Coopman, P.; Djiane, A. Adherens Junction and E-Cadherin Complex Regulation by Epithelial Polarity. *Cell. Mol. Life Sci.* **2016**, *73* (18), 3535–3553. https://doi.org/10.1007/s00018-016-2260-8.
(70) Schlesinger, M. Role of Platelets and Platelet Receptors in Cancer Metastasis. *J. Hematol. Oncol.J Hematol Oncol* **2018**, *11* (1), 125. https://doi.org/10.1186/s13045-018-0669-2.
(71) Menter, D. G.; Kopetz, S.; Hawk, E.; Sood, A. K.; Loree, J. M.; Gresele, P.; Honn, K. V. Platelet "First Responders" in Wound Response, Cancer, and Metastasis. *Cancer Metastasis Rev.* **2017**, *36* (2), 199–213. https://doi.org/10.1007/s10555-017-9682-0.
(72) Chaffer, C. L.; Weinberg, R. A. A Perspective on Cancer Cell Metastasis. *Science* **2011**, *331* (6024), 1559–1564. https://doi.org/10.1126/science.1203543.
(73) Lindsey, S.; Langhans, S. A. Crosstalk of Oncogenic Signaling Pathways during Epithelial–Mesenchymal Transition. *Front. Oncol.* **2014**, *4*. https://doi.org/10.3389/fonc.2014.00358.

(74) Kaller, M.; Hermeking, H. Interplay Between Transcription Factors and MicroRNAs Regulating Epithelial-Mesenchymal Transitions in Colorectal Cancer. In *Non-coding RNAs in Colorectal Cancer*; Slaby, O., Calin, G. A., Eds.; Advances in Experimental Medicine and Biology; Springer International Publishing: Cham, 2016; pp 71–92. https://doi.org/10.1007/978-3-319-42059-2_4.
(75) Fidler, I. J. The Pathogenesis of Cancer Metastasis: The "seed and Soil" Hypothesis Revisited. *Nat. Rev. Cancer* **2003**, *3* (6), 453–458. https://doi.org/10.1038/nrc1098.
(76) Paschos, K. A.; Majeed, A. W.; Bird, N. C. Natural History of Hepatic Metastases from Colorectal Cancer - Pathobiological Pathways with Clinical Significance. *World J. Gastroenterol.* **2014**, *20* (14), 3719–3737. https://doi.org/10.3748/wjg.v20.i14.3719.
(77) Jin, X.; Zhu, Z.; Shi, Y. Metastasis Mechanism and Gene/Protein Expression in Gastric Cancer with Distant Organs Metastasis. *Bull. Cancer (Paris)* **2014**, *101* (1), E1-12.
(78) *AJCC Cancer Staging Manual*, 7. ed.; Edge, S. B., American Joint Committee on Cancer, Eds.; Springer: New York, 2010.
(79) Benson, A. B.; Venook, A. P.; Al-Hawary, M. M.; Cederquist, L.; Chen, Y.-J.; Ciombor, K. K.; Cohen, S.; Cooper, H. S.; Deming, D.; Engstrom, P. F.; Garrido-Laguna, I.; Grem, J. L.; Grothey, A.; Hochster, H. S.; Hoffe, S.; Hunt, S.; Kamel, A.; Kirilcuk, N.; Krishnamurthi, S.; Messersmith, W. A.; Meyerhardt, J.; Miller, E. D.; Mulcahy, M. F.; Murphy, J. D.; Nurkin, S.; Saltz, L.; Sharma, S.; Shibata, D.; Skibber, J. M.; Sofocleous, C. T.; Stoffel, E. M.; Stotsky-Himelfarb, E.; Willett, C. G.; Wuthrick, E.; Gregory, K. M.; Freedman-Cass, D. A. NCCN Guidelines Insights: Colon Cancer, Version 2.2018. *J. Natl. Compr. Canc. Netw.* **2018**, *16* (4), 359–369. https://doi.org/10.6004/jnccn.2018.0021.
(80) Shafiei, M.; Beale, P.; Blinman, P. Utilisation of Adjuvant Chemotherapy and 5-Year Survival Analysis of Prospectively Recorded Cohort Data for Older Adults Versus Younger Adults with Resected Primary Colon Cancer. *J. Gastrointest. Cancer* **2019**. https://doi.org/10.1007/s12029-019-00343-5.
(81) André, T.; de Gramont, A.; Vernerey, D.; Chibaudel, B.; Bonnetain, F.; Tijeras-Raballand, A.; Scriva, A.; Hickish, T.; Tabernero, J.; Van Laethem, J. L.; Banzi, M.; Maartense, E.; Shmueli, E.; Carlsson, G. U.; Scheithauer, W.; Papamichael, D.; Möehler, M.; Landolfi, S.; Demetter, P.; Colote, S.; Tournigand, C.; Louvet, C.; Duval, A.; Fléjou, J.-F.; de Gramont, A. Adjuvant Fluorouracil, Leucovorin, and Oxaliplatin in Stage II to III Colon Cancer: Updated 10-Year Survival and Outcomes According to BRAF Mutation and Mismatch Repair Status of the MOSAIC Study. *J. Clin. Oncol.* **2015**, *33* (35), 4176–4187. https://doi.org/10.1200/JCO.2015.63.4238.
(82) Siegel, R. L.; Miller, K. D.; Jemal, A. Cancer Statistics, 2019. *CA. Cancer J. Clin.* **2019**, *69* (1), 7–34. https://doi.org/10.3322/caac.21551.
(83) Kusumoto, T.; Ishiguro, M.; Nakatani, E.; Yoshida, M.; Inoue, T.; Nakamoto, Y.; Shiomi, A.; Takagane, A.; Sunami, E.; Shinozaki, H.; Takii, Y.; Maeda, A.; Ojima, H.; Hashida, H.; Mukaiya, M.; Yokoyama, T.; Nakamura, M.; Munemoto, Y.; Sugihara, K. Updated 5-Year Survival and Exploratory T x N Subset Analyses of ACTS-CC Trial: A Randomised Controlled Trial of S-1 versus Tegafur-Uracil/Leucovorin as Adjuvant Chemotherapy for Stage III Colon Cancer. *ESMO Open* **2018**, *3* (6). https://doi.org/10.1136/esmoopen-2018-000428.
(84) Babcock, B. D.; Aljehani, M. A.; Jabo, B.; Choi, A. H.; Morgan, J. W.; Selleck, M. J.; Luca, F.; Raskin, E.; Reeves, M. E.; Garberoglio, C. A.; Lum, S. S.; Senthil, M. High-Risk Stage II Colon Cancer: Not All Risks Are Created Equal. *Ann. Surg. Oncol.* **2018**, *25* (7), 1980–1985. https://doi.org/10.1245/s10434-018-6484-8.
(85) Xu, Z.; Becerra, A. Z.; Fleming, F. J.; Aquina, C. T.; Dolan, J. G.; Monson, J. R.; Temple, L. K.; Jusko, T. A. Treatments for Stage IV Colon Cancer and Overall Survival. *J. Surg. Res.* **2019**, *242*, 47–54. https://doi.org/10.1016/j.jss.2019.04.034.
(86) Radhakrishnan, H.; Walther, W.; Zincke, F.; Kobelt, D.; Imbastari, F.; Erdem, M.; Kortüm, B.; Dahlmann, M.; Stein, U. MACC1—the First Decade of a Key Metastasis Molecule from Gene Discovery to Clinical Translation. *Cancer Metastasis Rev.* **2018**, *37* (4), 805–820. https://doi.org/10.1007/s10555-018-9771-8.
(87) Stein, U.; Dahlmann, M.; Walther, W. MACC1 — More than Metastasis? Facts and Predictions about a Novel Gene. *J. Mol. Med.* **2010**, *88* (1), 11–18. https://doi.org/10.1007/s00109-009-0537-1.

(88) Zhang, R.; Shi, H.; Ren, F.; Liu, Z.; Ji, P.; Zhang, W.; Wang, W. Down-Regulation of MiR-338-3p and Up-Regulation of MACC1 Indicated Poor Prognosis of Epithelial Ovarian Cancer Patients. *J. Cancer* **2019**, *10* (6), 1385–1392. https://doi.org/10.7150/jca.29502.
(89) Jin, Y.; Zhou, K.; Zhao, W.; Han, R.; Huo, X.; Yang, F.; Chen, J. Clinicopathological and Prognostic Significance of Metastasis-Associated in Colon Cancer-1 in Gastric Cancer: A Meta-Analysis: *Int. J. Biol. Markers* **2019**. https://doi.org/10.1177/1724600818813634.
(90) Söyleyici, N. A.; Aslan, F.; Avcýkurt, A. S.; Akgün, G. A. Importance of MACC1 Expression in Breast Cancer and Its Relationship with Pathological Prognostic Markers. *Indian J. Pathol. Microbiol.* **2020**, *63* (1), 19. https://doi.org/10.4103/IJPM.IJPM_658_19.
(91) Kopczyńska, E. K. The Potential Therapeutic Applications and Prognostic Significance of Metastasis-Associated in Colon Cancer-1 (MACC1) in Cancers. *Contemp. Oncol.* **2016**, *20* (4), 273–280. https://doi.org/10.5114/wo.2016.61846.
(92) Stein, U.; Burock, S.; Herrmann, P.; Wendler, I.; Niederstrasser, M.; Wernecke, K.-D.; Schlag, P. M. Circulating MACC1 Transcripts in Colorectal Cancer Patient Plasma Predict Metastasis and Prognosis. *PLOS ONE* **2012**, *7* (11), e49249. https://doi.org/10.1371/journal.pone.0049249.
(93) Isella, C.; Mellano, A.; Galimi, F.; Petti, C.; Capussotti, L.; Simone, M. D.; Bertotti, A.; Medico, E.; Muratore, A. MACC1 MRNA Levels Predict Cancer Recurrence After Resection of Colorectal Cancer Liver Metastases. *Ann. Surg.* **2013**, *257* (6), 1089–1095. https://doi.org/10.1097/SLA.0b013e31828f96bc.
(94) Dong, G.; Wang, M.; Gu, G.; Li, S.; Sun, X.; Li, Z.; Cai, H.; Zhu, Z. MACC1 and HGF Are Associated with Survival in Patients with Gastric Cancer. *Oncol. Lett.* **2018**, *15* (3), 3207–3213. https://doi.org/10.3892/ol.2017.7710.
(95) Wang, C.; Wen, Z.; Xie, J.; Zhao, Y.; Zhao, L.; Zhang, S.; Liu, Y.; Xue, Y.; Shi, M. MACC1 Mediates Chemotherapy Sensitivity of 5-FU and Cisplatin via Regulating MCT1 Expression in Gastric Cancer. *Biochem. Biophys. Res. Commun.* **2017**, *485* (3), 665–671. https://doi.org/10.1016/j.bbrc.2017.02.096.
(96) Ashktorab, H.; Hermann, P.; Nouraie, M.; Shokrani, B.; Lee, E.; Haidary, T.; Brim, H.; Stein, U. Increased MACC1 Levels in Tissues and Blood Identify Colon Adenoma Patients at High Risk. *J. Transl. Med.* **2016**, *14* (1), 215. https://doi.org/10.1186/s12967-016-0971-0.
(97) Ren, B.; Zakharov, V.; Yang, Q.; McMahon, L.; Yu, J.; Cao, W. MACC1 Is Related to Colorectal Cancer Initiation and Early-Stage Invasive Growth. *Am. J. Clin. Pathol.* **2013**, *140* (5), 701–707. https://doi.org/10.1309/AJCPRH1H5RWWSXRB.
(98) Lemos, C.; Hardt, M. S.; Juneja, M.; Voss, C.; Förster, S.; Jerchow, B.; Haider, W.; Bläker, H.; Stein, U. MACC1 Induces Tumor Progression in Transgenic Mice and Colorectal Cancer Patients via Increased Pluripotency Markers Nanog and Oct4. *Clin. Cancer Res. Off. J. Am. Assoc. Cancer Res.* **2016**, *22* (11), 2812–2824. https://doi.org/10.1158/1078-0432.CCR-15-1425.
(99) Wang, L.; Zhou, R.; Zhao, Y.; Dong, S.; Zhang, J.; Luo, Y.; Huang, N.; Shi, M.; Bin, J.; Liao, Y.; Liao, W. MACC-1 Promotes Endothelium-Dependent Angiogenesis in Gastric Cancer by Activating TWIST1/VEGF-A Signal Pathway. *PLOS ONE* **2016**, *11* (6), e0157137. https://doi.org/10.1371/journal.pone.0157137.
(100) Stein, U.; Smith, J.; Walther, W.; Arlt, F. MACC1 Controls Met: What a Difference an Sp1 Site Makes. *Cell Cycle* **2009**, *8* (15), 2467–2469. https://doi.org/10.4161/cc.8.15.9018.
(101) Pachmayr, E.; Treese, C.; Stein, U. Underlying Mechanisms for Distant Metastasis - Molecular Biology. *Visc. Med.* **2017**, *33* (1), 11–20. https://doi.org/10.1159/000454696.
(102) Hua, F.-F.; Liu, S.-S.; Zhu, L.-H.; Wang, Y.-H.; Liang, X.; Ma, N.; Shi, H.-R. MiRNA-338-3p Regulates Cervical Cancer Cells Proliferation by Targeting MACC1 through MAPK Signaling Pathway. *Eur. Rev. Med. Pharmacol. Sci.* **2017**, *21* (23), 5342–5352. https://doi.org/10.26355/eurrev_201712_13919.
(103) Wang, L.; Lin, L.; Chen, X.; Sun, L.; Liao, Y.; Huang, N.; Liao, W. Metastasis-Associated in Colon Cancer-1 Promotes Vasculogenic Mimicry in Gastric Cancer by Upregulating TWIST1/2. *Oncotarget* **2015**, *6* (13), 11492–11506. https://doi.org/10.18632/oncotarget.3416.

(104) Juneja, M.; Ilm, K.; Schlag, P. M.; Stein, U. Promoter Identification and Transcriptional Regulation of the Metastasis Gene MACC1 in Colorectal Cancer. *Mol. Oncol.* **2013**, *7* (5), 929–943. https://doi.org/10.1016/j.molonc.2013.05.003.

(105) Zerbino, D. R.; Achuthan, P.; Akanni, W.; Amode, M. R.; Barrell, D.; Bhai, J.; Billis, K.; Cummins, C.; Gall, A.; Girón, C. G.; Gil, L.; Gordon, L.; Haggerty, L.; Haskell, E.; Hourlier, T.; Izuogu, O. G.; Janacek, S. H.; Juettemann, T.; To, J. K.; Laird, M. R.; Lavidas, I.; Liu, Z.; Loveland, J. E.; Maurel, T.; McLaren, W.; Moore, B.; Mudge, J.; Murphy, D. N.; Newman, V.; Nuhn, M.; Ogeh, D.; Ong, C. K.; Parker, A.; Patricio, M.; Riat, H. S.; Schuilenburg, H.; Sheppard, D.; Sparrow, H.; Taylor, K.; Thormann, A.; Vullo, A.; Walts, B.; Zadissa, A.; Frankish, A.; Hunt, S. E.; Kostadima, M.; Langridge, N.; Martin, F. J.; Muffato, M.; Perry, E.; Ruffier, M.; Staines, D. M.; Trevanion, S. J.; Aken, B. L.; Cunningham, F.; Yates, A.; Flicek, P. Ensembl 2018. *Nucleic Acids Res.* **2018**, *46* (D1), D754–D761. https://doi.org/10.1093/nar/gkx1098.

(106) Li, H.; Zhang, H.; Zhao, S.; Shi, Y.; Yao, J.; Zhang, Y.; Guo, H.; Liu, X. Overexpression of MACC1 and the Association with Hepatocyte Growth Factor/c-Met in Epithelial Ovarian Cancer. *Oncol. Lett.* **2015**, *9* (5), 1989–1996. https://doi.org/10.3892/ol.2015.2984.

(107) Li, S.; Zhu, J.; Li, J.; Li, S.; Li, B. MicroRNA-141 Inhibits Proliferation of Gastric Cardia Adenocarcinoma by Targeting MACC1. *Arch. Med. Sci. AMS* **2018**, *14* (3), 588–596. https://doi.org/10.5114/aoms.2017.68757.

(108) Li, M.; Wang, Q.; Xue, F.; Wu, Y. LncRNA-CYTOR Works as an Oncogene Through the CYTOR/MiR-3679-5p/MACC1 Axis in Colorectal Cancer. *DNA Cell Biol.* **2019**, *38* (6), 572–582. https://doi.org/10.1089/dna.2018.4548.

(109) Wei, C. J.; Zhang, Z. W.; Lu, J. H.; Mao, Y. M. MiR-638 Regulates Gastric Cardia Adenocarcinoma Cell Proliferation, Apoptosis, Migration and Invasion by Targeting MACC1. *Neoplasma* **2020**. https://doi.org/10.4149/neo_2020_190719N651.

(110) Yang, F.; Lei, Y.; Zhou, M.; Yao, Q.; Han, Y.; Wu, X.; Zhong, W.; Zhu, C.; Xu, W.; Tao, R.; Chen, X.; Lin, D.; Rahman, K.; Tyagi, R.; Habib, Z.; Xiao, S.; Wang, D.; Yu, Y.; Chen, H.; Fu, Z.; Cao, G. Development and Application of a Recombination-Based Library versus Library High- Throughput Yeast Two-Hybrid (RLL-Y2H) Screening System. *Nucleic Acids Res.* **2018**, *46* (3), e17. https://doi.org/10.1093/nar/gkx1173.

(111) Fellmann, C.; Gowen, B. G.; Lin, P.-C.; Doudna, J. A.; Corn, J. E. Cornerstones of CRISPR-Cas in Drug Discovery and Therapy. *Nat. Rev. Drug Discov.* **2017**, *16* (2), 89–100. https://doi.org/10.1038/nrd.2016.238.

(112) Zielonka, J.; Zielonka, M.; Cheng, G.; Hardy, M.; Kalyanaraman, B. High-Throughput Screening of NOX Inhibitors. *Methods Mol. Biol. Clifton NJ* **2019**, *1982*, 429–446. https://doi.org/10.1007/978-1-4939-9424-3_25.

(113) Shaabani, S.; Huizinga, H. P. S.; Butera, R.; Kouchi, A.; Guzik, K.; Magiera-Mularz, K.; Holak, T. A.; Dömling, A. A Patent Review on PD-1/PD-L1 Antagonists: Small Molecules, Peptides, and Macrocycles (2015-2018). *Expert Opin. Ther. Pat.* **2018**, *28* (9), 665–678. https://doi.org/10.1080/13543776.2018.1512706.

(114) Huang, L.; Wang, X.; Huang, X.; Gui, H.; Li, Y.; Chen, Q.; Liu, D.; Liu, L. Diagnostic Significance of CK19, Galectin-3, CD56, TPO and Ki67 Expression and BRAF Mutation in Papillary Thyroid Carcinoma. *Oncol. Lett.* **2018**, *15* (4), 4269–4277. https://doi.org/10.3892/ol.2018.7873.

(115) Sack, U.; Walther, W.; Scudiero, D.; Selby, M.; Kobelt, D.; Lemm, M.; Fichtner, I.; Schlag, P. M.; Shoemaker, R. H.; Stein, U. Novel Effect of Antihelminthic Niclosamide on S100A4-Mediated Metastatic Progression in Colon Cancer. *J. Natl. Cancer Inst.* **2011**, *103* (13), 1018–1036. https://doi.org/10.1093/jnci/djr190.

(116) Ray, M. A.; Johnston, N. A.; Verhulst, S.; Trammell, R. A.; Toth, L. A. Identification of Markers for Imminent Death in Mice Used in Longevity and Aging Research. *J. Am. Assoc. Lab. Anim. Sci. JAALAS* **2010**, *49* (3), 282–288.

(117) Markossian, S.; Ang, K. K.; Wilson, C. G.; Arkin, M. R. Small-Molecule Screening for Genetic Diseases. *Annu. Rev. Genomics Hum. Genet.* **2018**, *19* (1), 263–288. https://doi.org/10.1146/annurev-genom-083117-021452.

(118) Kim, H. J.; Moon, S. J.; Kim, S.-H.; Heo, K.; Kim, J. H. DBC1 Regulates Wnt/β-Catenin-Mediated Expression of MACC1, a Key Regulator of Cancer Progression, in Colon Cancer. *Cell Death Dis.* **2018**, *9* (8), 831. https://doi.org/10.1038/s41419-018-0899-9.
(119) Mathijssen, R. H. J.; Sparreboom, A.; Verweij, J. Determining the Optimal Dose in the Development of Anticancer Agents. *Nat. Rev. Clin. Oncol.* **2014**, *11* (5), 272–281. https://doi.org/10.1038/nrclinonc.2014.40.
(120) Man, S.; Munoz, R.; Kerbel, R. S. On the Development of Models in Mice of Advanced Visceral Metastatic Disease for Anti-Cancer Drug Testing. *Cancer Metastasis Rev.* **2007**, *26* (3–4), 737–747. https://doi.org/10.1007/s10555-007-9087-6.
(121) Gómez-Cuadrado, L.; Tracey, N.; Ma, R.; Qian, B.; Brunton, V. G. Mouse Models of Metastasis: Progress and Prospects. *Dis. Model. Mech.* **2017**, *10* (9), 1061–1074. https://doi.org/10.1242/dmm.030403.
(122) Céspedes, M. V.; Espina, C.; García-Cabezas, M. A.; Trias, M.; Boluda, A.; Gómez del Pulgar, M. T.; Sancho, F. J.; Nistal, M.; Lacal, J. C.; Mangues, R. Orthotopic Microinjection of Human Colon Cancer Cells in Nude Mice Induces Tumor Foci in All Clinically Relevant Metastatic Sites. *Am. J. Pathol.* **2007**, *170* (3), 1077–1085. https://doi.org/10.2353/ajpath.2007.060773.
(123) Heijstek, M. W.; Kranenburg, O.; Rinkes, I. H. M. B. Mouse Models of Colorectal Cancer and Liver Metastases. *Dig. Surg.* **2005**, *22* (1–2), 16–25. https://doi.org/10.1159/000085342.
(124) Sugarbaker, P. H.; Hoskins, E. R. Splenic Metastases – Hematogenous Disease or Invasive Peritoneal Implants? Case Reports of Two Patients. *Int. J. Surg. Case Rep.* **2020**, *72*, 266–270. https://doi.org/10.1016/j.ijscr.2020.05.086.
(125) Zinn, K. R.; Chaudhuri, T. R.; Szafran, A. A.; O'Quinn, D.; Weaver, C.; Dugger, K.; Lamar, D.; Kesterson, R. A.; Wang, X.; Frank, S. J. Noninvasive Bioluminescence Imaging in Small Animals. *ILAR J.* **2008**, *49* (1), 103–115. https://doi.org/10.1093/ilar.49.1.103.
(126) Jain, R.; Fischer, S.; Serra, S.; Chetty, R. The Use of Cytokeratin 19 (CK19) Immunohistochemistry in Lesions of the Pancreas, Gastrointestinal Tract, and Liver. *Appl. Immunohistochem. Mol. Morphol.* **2010**, *18* (1), 9–15. https://doi.org/10.1097/PAI.0b013e3181ad36ea.
(127) Zhuo, J.-Y.; Lu, D.; Tan, W.-Y.; Zheng, S.-S.; Shen, Y.-Q.; Xu, X. CK19-Positive Hepatocellular Carcinoma Is a Characteristic Subtype. *J. Cancer* **2020**, *11* (17), 5069–5077. https://doi.org/10.7150/jca.44697.
(128) CD34, PCNA and CK19 Expressions in AFP– Hepatocellular Carcinoma. *European Review*, 2018.
(129) Khera, N.; Rajput, S. Therapeutic Potential of Small Molecule Inhibitors. *J. Cell. Biochem.* **2017**, *118* (5), 959–961. https://doi.org/10.1002/jcb.25782.
(130) Kobelt, D.; Dahlmann, M.; Dumbani, M.; Güllü, N.; Kortüm, B.; Vílchez, M. E. A.; Stein, U.; Walther, W. Small Ones to Fight a Big Problem—Intervention of Cancer Metastasis by Small Molecules. *Cancers* **2020**, *12* (6). https://doi.org/10.3390/cancers12061454.
(131) Winkler, G. C.; Barle, E. L.; Galati, G.; Kluwe, W. M. Functional Differentiation of Cytotoxic Cancer Drugs and Targeted Cancer Therapeutics. *Regul. Toxicol. Pharmacol.* **2014**, *70* (1), 46–53. https://doi.org/10.1016/j.yrtph.2014.06.012.

Statutory Declaration

"I, Shixian Yan, by personally signing this document in lieu of an oath, hereby affirm that I prepared the submitted dissertation on the topic: ***Identification of novel compounds for targeted therapy of MACC1 driven metastasis (Identifizierung neuer Substanzen für die zielgerichtete Behandlung der MACC1-vermittelten Metastasierung)*** independently and without the support of third parties, and that I used no other sources and aids than those stated.
All parts which are based on the publications or presentations of other authors, either in letter or in spirit, are specified as such in accordance with the citing guidelines. The sections on methodology (in particular regarding practical work, laboratory regulations, statistical processing) and results (in particular regarding figures, charts and tables) are exclusively my responsibility.

Furthermore, I declare that I have correctly marked all of the data, the analyses, and the conclusions generated from data obtained in collaboration with other persons, and that I have correctly marked my own contribution and the contributions of other persons (cf. declaration of contribution). I have correctly marked all texts or parts of texts that were generated in collaboration with other persons.

My contributions to any publications to this dissertation correspond to those stated in the below joint declaration made together with the supervisor. All publications created within the scope of the dissertation comply with the guidelines of the ICMJE (International Committee of Medical Journal Editors; www.icmje.org) on authorship. In addition, I declare that I shall comply with the regulations of Charité – Universitätsmedizin Berlin on ensuring good scientific practice.

I declare that I have not yet submitted this dissertation in identical or similar form to another Faculty.

The significance of this statutory declaration and the consequences of a false statutory declaration under criminal law (Sections 156, 161 of the German Criminal Code) are known to me."

Date Signature

My curriculum vitae does not appear in the electronic version of my paper for reasons of data protection.

My curriculum vitae does not appear in the electronic version of my paper for reasons of data protection.

Publications

1. **Shixian Yan**, Daguang Wang, Yujia Chen, Hengchang Liu, Yuechao Xu. Expression of Eph A2 and Ephrin A1 in gastric cancer tissues with helicobacter pylori infection and its relationship with distant metastasis. [J] Medicine & Philosophy (B). 2016, 37(04): 63-66. (Chinese Journal)

2. **Shixian Yan**, Weihua Tong, Yujia Chen, Hengchang Liu, Yuechao Xu. Effect of obesity on perioperative status in patients with total gastrectomy for gastric cancer. [J] Chinese Journal of Gastroenterology. 2016, 21(7): 409-413. (Chinese Journal)

3. **Shixian Yan**, Daguang Wang, Na Liu, Wei Li, Liguo Feng, Miao Li, Yuchao Xu. Expressions of Survivin and p53 in colorectal cancer and the effect on prognosis. [J] Chinese Journal of Gastroenterology and Hepatology. 2017, 26(4): 423-427. (Chinese Journal)

4. Zheyu Song, Daguang Wang, Tengfei Li, **Shixian Yan**, Jian Suo. Clinical features and prognosis of familial and sporadic gastric cancer. [J] Chinese Journal of Gerontology, 2016, 36(2): 360-362. (Chinese Journal)

Acknowledgment

First of all, I am very grateful to my supervisor Prof. Dr. Ulrike Stein for giving me this opportunity to study and live abroad, and for providing me with all the help I needed to research in the field of metastasis formation in colorectal cancer. Without her patience, endurance and scientific advice my project would not have been possible. At the same time, it is a great honor to work in such an excellent team for 3 years. Meanwhile, I would like to thank PD Dr. Robert Preißner for his co-supervision.

Many thanks to Prof. Dr. Wolfgang Walther and Dr. Dennis Kobelt, who have been very patient from the beginning of my project to the end in answering various questions I encountered. Their scientific support and helpful comments made my experiment go smoothly. Thanks to our collaborator Dr. Marc Nazare and his team for their great help in the process of the compound screening. Many thanks to Pia Herrmann, Margarita Mokrizkij and Janice Smith for helping me with the experimental skills at the beginning and sharing their experience, so that I can be more careful and conscientious in the experiment process and get more accurate results. At the same time, I would like to thank Dr. Mathias Dahlmann, Dr. Fabian Zincke, Dr. Chenyu Zhang, my brilliant colleagues PhD student Benedikt Kortüm, Nazil Güllü, Malti Dumbani, MD student Yukai Sun and Miguel.Alberto for solving the problems and making the research life more colorful.

Thanks to the China scholarship council (CSC), Spark Berlin and Berlin Institute of Health (BIH) for the funding, which provides a guarantee for my life and scientific research.

Finally, I would like to thank my friends and family for their support, especially my parents and wife, who have been standing behind me silently and gave me tremendous support. This is the motivation for me to keep moving forward.